Developing tools for inter-site transport of brain tissue models in tissue engineering research

BUSHRA KABIRI

A THESIS SUBMITTED FOR THE DEGREE OF:

MASTER OF PHILOSOPHY IN NEUROSCIENCE

NEURAL TISSUE ENGINEERING KEELE (NTEK)

JULY 2022

KEELE UNIVERSITY

Senate award: October 2022

Abstract

Collaborators: Sonia Morlando, Stuart Iain Jenkins, Divya Maitreyi Chari

Penetrating traumatic brain injury (pTBI) remains one of the leading causes of death in the younger population in the UK, as no clinical regenerative therapies are available. Experimental therapies currently being screened for efficacy are wide ranging and complex (such as biomaterial implantation, nanotherapies and electrostimulation) which require effective multi-disciplinary collaboration between biological and physical scientists, such as engineers, chemists and physicists. Generating complex and pathomimetic models of pTBI requires costly equipment, expert training and access to animal facilities, making them logistically inaccessible to the majority of physical scientists, representing a bottleneck in neurotherapy development.

Developing the capacity for inter-site transport of complex brain injury models would significantly ease this logistical barrier. Specifically, complex primary models of pTBI can be transported to sites remote from the site of biological model production for testing, promoting multi-disciplinary collaboration and efficiency in cross-disciplinary research.

Our laboratory recently developed two multicellular and *in vitro* primary cortical models of pTBI (a glial and neuronal model) which offer significant advantages as facile but complex, injury simulating and pathomimetic models of pTBI. The objective of this study was to establish if Hibernate™, a commercially available neural tissue storage medium, could be used safely for storage and transport of these model at room temperature (RT) (removing the need for cold chain transport), without detriment to neural cell viability, maturation or reactivity.

Findings indicate there is no effect of Hibernate™ storage at RT for four hours on neural cell culture confluency, overall cell viability or proportions of each cell type. Moreover, neurons and oligodendrocytes show no significant decrease in maturation after storage, nor do astrocytes and microglia show any significant increase in reactivity. This indicates transportation of primary neural

models is feasible and could facilitate multi-site transport of complex brain tissue models for neuroregenerative research.

Table of Contents

List of tables

List of figures

List of abbreviations

ATLS	Advanced trauma life support
BBB	Blood brain barrier
BDNF	Brain derived neurotrophic factor
BoC	Brain-on-a-chip
Calcein-AM	Calcein acetoxymethyl
CES	Cortical electrical stimulation
CNS	Central nervous system
CO_2	Carbon dioxide
CSF	Cerebrospinal fluid
CT	Computed tomography
Cy3	Cyanine 3
Cy5	Cyanine 5
DAPI	4',6-diamidino-2-phenylindole (also known as Hoechst stain)
ddH_2O	Double distilled water
DIV	Days *in vitro*
DMEM	Dulbecco's modified Eagle medium
DNA	Deoxyribonucleic acid
EEG	Electroencephalography
ES	Electrostimulation
ESC	Embryonic stem cell
FBS	Foetal bovine serum
FGF-2	Fibroblast growth factor-2
FITC	Fluorescein isothiocyanate
GABA	Gamma amino-butyric acid
GCS	Glasgow coma scale
GFAP	Glial fibrillary acidic protein
HEPES	4-(2-hydroxyethyl)-1-piperazineethanesulfonic acid
ICP	Intracranial pressure

Iba1	Ionised calcium binding adapter molecular-1
ICC	Immunocytochemistry
IPA	Isopropyl alcohol
LTD	Long-term depression
LTP	Long-term potentiation
MBP	Myelin basic protein
MSC	Mesenchymal stem cell
MOPS	3-N-morpholino-propanesulfonic acid
NDS	Normal donkey serum
NMDA	N-methyl-D-aspartate
NSC	Neural stem cell
NTEK	Neural tissue engineering group at Keele University
OPC	Oligodendrocyte precursor cell
PBS	Phosphate buffered saline
PDL	Poly-d-lysine
PFA	Paraformaldehyde
pTBI	Penetrating traumatic brain injury
rpm	Revolutions per minute
RT	Room temperature
rTMS	Repetitive transcranial magnetic stimulation
TBI	Traumatic brain injury
TMS	Transcranial magnetic stimulation
Tuj1	Purified anti-neuron-specific class III beta-tubulin
VEGF	Vascular endothelial growth factor
UV	Ultraviolet

Acknowledgements

I am extremely grateful to have had the opportunity to complete this study. I would like to first and foremost mention my supervisor Professor Divya Chari. Her expert guidance was a welcome light in the dark times of this degree. Despite the troubles, Professor Chari was able to focus my energy and limited ability toward success where I would otherwise have ended up in the laboratory research equivalent of a car crash. I would also like to thank her patience through many missed "soft" deadlines and early, unintelligible drafts of this thesis.

I would also like to thank Dr Stuart Jenkins for my early introduction into the world of neuroscience research. His continued support throughout this study has been unwavering, no question was too stupid, no mistake unforgiveable. Along with Dr Jenkins was Dr Christopher Adams who was kind enough to lend much of his limited time and expert resources to helping me succeed, for which I am forever grateful. Thank you to the whole Neural Tissue Engineering group at Keele (NTEK), particularly Sonia and Anthea, for being not just excellent colleagues but also wonderful friends.

Thank you also to Sonia Morlando, research technician at NTEK, for producing three primary mixed cortical neuronal cultures that I was able to use for experimentation.

This project was also made possible by the Association of Clinical Pathologists, who I am incredibly grateful for. Their contribution has given me new opportunities this past year, improving many of my personal and profession skills and my overall development as a neuroscientist.

I am also incredibly lucky to have such amazing friends, Charlotte, MJ, Frances, and particularly Keenan who have stuck by me since before I knew what a neuron was. Lastly, I would like to thank my family who are an immense source of comfort and support. My wonderful, annoying and brilliant siblings, Asma, Emad, and Safia, and my beloved parents are my role models.

Chapter 1: General Introduction

In this introduction, several discreet and separate topics will be discussed. To start, the context within which this study was undertaken, penetrating traumatic brain injury, will be explained. Its epidemiology, pathophysiology and current management will be elucidated. To follow, the emerging clinical neurotherapies that are being trialled in this area will be explained, for instance biomaterial implantation, stem cell therapy, nanotherapeutics and electrostimulation. Available models of pTBI that are currently used in experimental research for these therapies will also be discussed and the limitations to the way in which experimental research is currently undertaken will be addressed.

Following on from this, the availability of *in vitro* models of pTBI and current methods of storage and transport of biological tissue, with specific examples of neural tissue, will be considered. To conclude, Hibernate™ will be introduced as a method for transport of neural tissue.

1.1 Penetrating traumatic brain injury:

1.1.1 Epidemiology

Penetrating traumatic brain injuries (pTBI) represents a significant socioeconomic burden on our population. They are a subset of all traumatic brain injuries, which are the commonest cause of death in the UK in population under 40 years [1]. While pTBI represents a minority (4-5% [2]) of all head injury cases, they carry the worst prognosis, with the higher mortality and morbidity rates [1]. Generally, the majority of patients die before reaching a hospital [3].

1.1.2 Mechanisms of injury

All traumatic brain injuries can be broadly into contact or acceleration-deceleration injuries. Contact injuries with foreign objects include blunt or penetrating objects, within which pTBI is classified [4]. Gunshot wounds are contact, penetrating injuries more common in the USA than in the UK but are

still to be considered for their particularly poor outcomes [5] [6]. In the UK, the majority of severe pTBIs are caused by motor vehicle collisions, motor vehicle collisions, sports-related injuries or abuse/assault [6] [7].

1.1.3 Pathophysiology

Similar to mild TBIs, after an injury, the soft tissue hits the hard intracranial surface of the brain [8]. The severity of the impact, as well as the depth, course and velocity of the penetrating object will have a significant impact on clinical course and prognosis [9]. Any penetration will cause mechanical tearing of neurons and shear axons to disrupt the circuitry at that level [10]. Any disruption to the surrounding vasculature will allow movement of erythrocytes, leukocytes and serum (and all its associated serum proteins) into the parenchyma and neurons and glia not normally exposed to these factors. The direct impact of the penetrating object causes crush injury and necrosis of cells and at the lesional edge, apoptosis in the surrounding perilesional vicinity and a local inflammatory response begins. This mobilises microglia and astrocytes to the primary location of injury resulting in further oedema and inflammation. Astrocytes begin the process of 'palisading' processes into the lesional site which over time forms a glial scar preventing axonal outgrowth into the lesion which is a substantial barrier for neuronal regeneration in pTBI [11]. This phase of immediate injury is associated with gliosis, demyelination and continued apoptosis [12]. The energy of the penetrating object also causes the surrounding tissue to expand and contract due to shock waves from a high energy impact, forming a temporary cavity which settles and creates a greater cavity [10]. The repeated expansion and contraction due to impact also causes repeated stress and damage to the tissue [13]. Entry of a foreign object into the cranium, usually kept sterile, is a significant risk for infection which is a common complication. Disruption of the dura causes CSF leakage which increases the risk of infection and frequently requires surgical repair. pTBI runs some of the most

significant long-term risks of disability, due to the loss of the neuronal circuitry at the injury and irreversible long-term effects of the associated neuroinflammation, demyelination and gliosis.

Primary and secondary injury

The pathophysiology can be separated into primary and secondary injuries. The primary injury is the direct or indirect result of the foreign object/blast, and varies depending on the object, the nature of the trauma and (if penetrating) its course through the brain. This includes shearing, rotation, compressing, laceration and ricocheting injuries that can result in haematoma formation, contusions, microvascular injuries and axonal shearing [14].

Secondary injuries are the sequelae of non-mechanical damage due to the biochemical cascades caused by membrane disruption and occur over a longer time span of hours to days post-insult. The neuronal death results in the release of excitatory neurotransmitters, namely glutamate and aspartate. This impacts other cells in the vicinity resulting in excitotoxicity and mitochondrial dysfunction. The release of free radicals and caspase enzyme activation from the damage causes further dysregulation of cerebral blood flow (CBF) and ischaemia, all setting the stage for a pro-inflammatory state. After immediate insult, the restoration of CBF can cause reperfusion injury, causing further stress to neurons and glia. This complex inflammatory biochemical cascade is secondary injury and translates clinically to parenchymal oedema, cerebral vasospasm, decreased CBF and elevated intracranial pressure (ICP) [8] [9].

This distinction between primary and secondary injuries in pTBI is important as their incidences can be reduced in separate ways. Primary injuries can be reduced by implementing preventative measures in the community, preventing the injury from occurring in the first place, as once they occur, the initial damage is usually irreversible. Secondary injuries, however, can be mitigated with the appropriate supportive care. Here, medical intervention with neuroprotective agents in a time-critical window after the initial injury can interrupt secondary cell death and the biochemical

cascades causing secondary injuries can be delayed or prevented. Research in the field is focused on neuroprotective therapies that can be administered at this stage but this has yet to be realised in the clinical setting [5] [15].

1.1.4 Current management

Acute initial management

As elaborated earlier, primary injury as the direct result of the trauma cannot be undone once occurred. However, there are known systemic parameters that can be altered to offset the secondary injury that occurs. Hypotension, hypoxia, and hypercapnia are all known factors that contribute to mortality in early severe pTBI, thus acute management focuses on maintaining blood pressure, systemic blood oxygen and carbon dioxide levels [2]. Preventing these from becoming deranged is thought to prevent the decrease in CBF that promotes ischaemia and worsened brain inflammation. Interestingly, prehospital intubation by paramedics is known to increase mortality in severe TBIs, thought to be due to the transient hypoxia, excessive overventilation and hypocarbia occurring due to prehospital intubation resulting in the vasoconstriction that ultimately impairs CBF [16]. This implies that there is a need for more rapid transfer to definitive care by focussing on more basic initial airway management in the interim between injury and hospital presentation.

Acute hospital management

At this point, advanced trauma life support (ATLS) principles of management can commence with rapid clinical examination. The airway can be definitively secured, and induction agents can be used with tight management of systemic blood pressure, oxygenation and carbon dioxide levels to prevent cerebral vasospasms [17]. Imaging to include a CT scan (at minimum), to assess presence of

other injuries and risk stratify severe patients should also be undertaken within 4 hours of presentation [18].

Presence of mass lesions, Glasgow coma scale (GCS) score (criteria for scoring and associated mortality shown in **Table 1.1**) of <9, presence of epidural haematomas, midline shift of >5 mm, or any focal neurological defects should all merit surgical evaluation [19]. Evidence of parenchymal lesions with progressive decline, mass effect, GCS of 6-8 with frontal/temporal contusions, compression of cisterns or a lesion volume of over 50 cm^3 should be considered for decompression (such as with a decompressive craniotomy). Early operative intervention has been shown to have a mortality benefit in these cases [20].

Criteria	Subcategory	Score
Eyes	No eye opening	1
	Opens to pain	2
	Opens to voice	3
	Spontaneous opening	4
Voice	No response	1
	Incoherent sounds	2
	Incoherent words	3
	Confused	4
	Normal speech	5
Motor	No movement	1
	Abnormal extension	2
	Abnormal flexion	3
	Flexion withdrawal	4
	Localises pain	5
	Obeys commands	6

Table 1.1 Glasgow Coma Scale used in all head injury cases to classify and stratify patients into severity

Novel medical interventions

Accordingly, the initial focus on patients with TBI is mainly supportive and in some cases surgical, helping to repair the anatomical effects of the trauma, and provide decompression where appropriate. The following are medical interventions that are used in some cases however are not all evidence backed or widespread [2] [5]:

A) Head elevation is thought to reduce ICP by gravity, CSF physically moving downwards as well as helping to promote venous outflow [2].

B) Hyperosmolar therapy (use of hypertonic saline or mannitol) has been shown to reduce blood viscosity, improve microcirculation and decreased ICP, however there is still insufficient evidence on clinical outcomes to support its widespread use [21].

C) Barbiturates are pharmacological gamma amino-butyric acid (GABA) receptor modulators that have been trialled in patients without mass lesions and refractory ICP >20 mmHg, who are not suitable for surgery. Pentobarbital, for instance, is used to initiate a barbiturate coma and can improve cerebral perfusion pressure however also inadvertently causes hypotension as a significant side effect which prevents its widespread use. When used, electroencephalography (EEG) monitoring is required ensure dose dependent cerebral activity suppression as well as continuous blood pressure monitoring to prevent hypotension [22]. Benzodiazepines such as midazolam have also been shown to work similarly.

D) Hyperventilation can also reduce intraarterial CO_2 partial pressure which results in vasoconstriction, theoretically reducing cerebral volume, preventing a rise in ICP. This is to be carefully monitored and only to be used in cases of severe TBI for brief periods [23].

E) Therapeutic cooling (hypothermia) is another clinical therapy being explored. Randomised controlled trials have shown their associated reduced mortality and improvements in neurological function in patients with diffuse TBI [24]. However, its role, in not only pTBI but a range of other neurological emergencies, such as stroke or intracranial haemorrhages, with similar pathophysiologies, is yet to be further investigated and validated [25].

1.2 Emerging experimental therapies

1.2.1 Pharmacological therapy development for penetrating traumatic brain injury

The need for drug development is clear however there are many aspects and properties a drug must possess, to not only be effective in countering the pro-inflammatory, excitotoxic biochemical cascades that occur in the aftermath of injury, but also in order to target the site of therapeutic action would be. The body is quick to clear foreign substances, with kidneys that clear molecules smaller than 10 µm, and the liver metabolising agents before they reach the systemic circulation to reach the brain [26]. Any surface charges can cause a drug molecule to interact with various circulating serum proteins or cell membranes, or to be digested by resident macrophages [27]. They may also be susceptible to various proteases, hydrolysis, the pH of various body components, all causing unfavourable binding. When finally reaching the CNS, the blood brain barrier (BBB) is notorious for inhibiting the passage of many macro- and micro-molecules. Once in the brain parenchyma, a drug must be able to navigate to reach the diseased area to reach the effector site, which may be intracellular, so must also have the surface properties for cell-specific uptake [28].

Nanotherapeutics used with pharmacological agents

Nanoparticles (NPs) have shown promise in this field. They have the ability to maintain stability, overcome the BBB as well as can be formulated to include various components, including polymeric nanoparticles, liposomes, hydrogels etc. Depending on its structure, it can control drug release, targeting specific sites, and prolong drug action through its protection from proteases. Their size, shape and flexibility can be altered to overcome non-specific binding to alter their pharmacokinetics and improve brain accumulation. They can also be decorated with cell specific surface ligands or

surfactants to further maximise therapeutic delivery [29]. Certain nanoparticles can also act as biomarkers for diseases and this an exciting area which is being tested further [30].

1.2.2 Stem cell transplantation

Another promising area of research is the transplantation of stem cells into the sites of injury. The adult brain usually has a limited capacity for self-repair compared to other organs, due to mature neurons' inability to undergo mitosis, so promoting regeneration would require replacement of lost cells [27], promotion of neurotrophic factors , removal of any growth inhibition, and a system to guide axons, all with the appropriate intracellular signalling pathways [31]. The use of endogenous stem cells that exist in the adult brain was already shown to have limited capability of regenerating new, functional neurons, so exogenous transplantation of stem cells is favoured. Some successful experimental stroke [32] and Parkinson's disease models using stem cell transplant therapies [32] are evidence of the ability to regenerate neuronal function via cell implantation and was thus trialled for pTBI [34].

Enhancing neurogenesis, angiogenesis and immunoregulation by secreting chemokine and growth factors are all important for functional recovery induced by stem cells/progenitor cells. While many studies have demonstrated beneficial effect, there is also a need to address logistical issues such as administration routes, doses, time window for transplantation, for this therapy to become mainstream or widespread [35].

Mesenchymal stem cells (MSCs) have been explored for implantation. These cells are isolated from bone marrow, umbilical cord and adipose tissue and are able to differentiate terminally into various bone, muscular, connective and neural tissues [36]. They can be injected into the lateral ventricles or intravenously. Neurorestoration is thought to be the likely mechanism via which mesenchymal stem cell induced TBI recovery rather than neuroreplacement. This is because the MSCs release a mixture

of growth factors (FGF-2, VEGF, BDNF) which all promote neurogenesis, angiogenesis and synaptogenesis, making them attractive options for transplantation and neural regeneration [37] [37].

Neural stem cells (NSCs) are another viable option frequently used in TBI experimental studies [38]. These cells reside in the mammalian brain at the ependymal lining, subventricular zone and hippocampus. Promoting their proliferation and differentiation has been shown to stabilise the microenvironment and enhance post-TBI recovery [40]. Exogenous transplantation promotes neuroprotection, hippocampal neurogenesis and improves overall functional outcomes. NSCs, unlike MSCs, are able to differentiate into functional neurons for neuroreplacement. NSCs are also shown to interact with the endogenous immune system, enhancing their endogenous regenerative responses and promoting NSC functional integration into their new environment [41]. The main downside to their use when compared with MSCs is ethical sourcing.

Transplantation of embryonic stem cells has also been studied, showing similar post-traumatic inflammatory response inhibition and improved neurological outcomes however this had an increased risk of tumorigenesis when compared to NSCs or MSCs and is thus a less likely candidate for transplantation [35].

1.2.3 Biomaterial implantation

While transplanted neural or mesenchymal stem or progenitor cells have shown promise, studies have shown a graft material that could act as a scaffold or matrix for the implanted cells vastly improves outcomes. After a pTBI, there is a drastic loss of living cells, with lots of dead cells and debris. There is also a loss of the natural extracellular matrix, made up of connective tissue, within which neurons were endogenously supported. Replacing this with an exogenous biomaterial graft has been shown to vastly improve outcomes when transplanting neural or mesenchymal

stem/progenitor cells as the graft material acts as a scaffold or matrix to guide cells attachment and axonal regeneration.

In order to create a suitable matrix or scaffold for cell transplantation, a biomaterial would need to have certain properties. This includes it being non-toxic and biocompatible, not adversely affecting cell function, for neither the transplantable cells but also any host cells still surviving. The material should not be carcinogenic or toxic in the short or long term, nor should its constituent products be toxic or carcinogenic. It should be robust enough that it lasts long enough for transplanted cells to establish, but biodegradable enough that it can slowly be broken down and replaced with the host's own extracellular matrix, all while preventing further rises in intracranial pressure, inflammation or triggering fibrous encapsulation by the host. It would be ideal for the biomaterial to be injectable, as injuries can vary drastically in size and shape, and creating a graft that can mould to its surroundings would prevent costs in having to create size-specific grafts for each injury. If a graft were to be tailored to fit the injury in each case, it must be created quickly enough to allow for implantation to meet the time-specific window after injury, which would be difficult as patients may already be late to hospital presentation after injury. The graft must also be highly porous, to allow for infiltration of host or transplanted cells. It would also be ideal for the graft material to be adaptable to carrying trophic factors or pharmacological agents that can support endogenous or exogenous cells through growth promotion or anti-inflammatory effects. Of the materials that are able to fulfil those requirements, Hydrogel systems or microspheres or nanoparticle systems are the two main candidates supported in the literature.

Hydrogels

These are water soluble polymer chain networks. As the name implies, they are gels made up of 99% water, and can be used to incorporate nutrients or oxygen allowing for cell survival if used as a scaffold. They can also be modified to include proteins, glycosaminoglycans, cytokines or other drugs

to stimulate cell adhesion or growth. Their physical properties make them a good candidate as they are liquid at room temperature but stiffen into a gel like structure at warmer temperatures, making them ideal for liquid injection directly into a CNS wound where they would only form a 3D matrix once exposed to 37°C body temperature, to suit the injured space. The difficulty preventing widespread use is their lack of mechanical structure which prevents cellular migration and outgrowth. Neuronal outgrowth particularly is known to need a stiff and rigid structure for the neuronal growth cones to pull on in order to process effectively. Cells placed into softer structures are often round and maintain very short processes. As they are, hydrogels are too soft to create a suitable environment for glial or neuronal cells that need to extend their processes for long distances in order to regenerate in a wound. Furthermore, their biodegradability is difficult to control, making their use for pTBI implantation unlikely.

Microspheres and nanoparticles

These, unlike hydrogels, possess a rigid surface structure, and can support the tension that neuronal processing and growth requires. Furthermore, they can be implanted easily via injection when suspended in a liquid or gel that can be moulded to an injury site. Like hydrogels, they can be modified to deliver a variety of trophic growth factors or anti-inflammatory pharmacological agents that can aid engraftment and survival of transplantable or endogenous cells. The downsides to their use that they need to be suspended in a further material for their use, which would also need to be tested for implantation, to ensure microspheres can establish transplantable cells within them. Furthermore, elasticity of a material has been shown to be important for neuronal stem cell differentiation. Microspheres have weak elasticity, which while good for neuronal outgrowth, may also decrease the differentiation of stem cells, which is a significant concern when the therapeutic mechanism of stem cells relay on their capability to differentiate and grow into the injury site.

1.2.4 Electrical neurostimulation

Electrical stimulation (ES) is another exciting area of neurotherapeutics. This involves the ability to stimulate a certain area of the brain or can act on the peripheral nervous system where stimulation usually occurs over the skin with nerves directly underneath. In relation to TBI, there is evidence that ES can help mitigate short- and long-term clinical sequelae [28] though questions still remain as to the logistics, of when, where and how electrical stimulation would be administered.

There are different theories as to how electrical stimulation is beneficial. If given acutely after a TBI, there is evidence that neurostimulation can decrease cortical hyperexcitability, helping to mitigate secondary injury. If given later on after injury, ES can help to modulate synaptic plasticity. In the long term, when combined with physical and behavioural therapy, ES can facilitate cortical reorganisation and help to consolidate specific neural networks. These all can help to decrease the long-term disabilities associated with pTBI.

A few methods developed include repetitive transcranial magnetic stimulation (rTMS) or cortical electrical stimulation (CES). rTMS is based on Faraday's principle of electromagnetic induction. Passing a brief and large electrical current through a coil held over the scalp creates a rapidly changing magnetic field that penetrates through the scalp and induces a current. This current can then depolarise cortical neurons which can simultaneously activate many different populations of neurons in the neocortex resulting in varying effects in the area of direct stimulation and related brain regions through synaptic spread. Different neuronal populations have different baseline activations and thresholds for stimulation resulting in a degree of selectivity when stimulating depending on the parameters used. Conversely, using lower frequencies of alternating magnetic current can decrease cortical excitability due to preferential stimulation of GABAergic neurons. Interestingly, rTMS can also be used to induce changes in regional CBF, likely reflecting changes in cortical excitability and resulting oxygen demand.

In the long term, rTMS of several sessions varying 10-15 minutes each shows a greater magnitude by inducing an environment for neuroplasticity. Even though the precise mechanism is yet to be fully elucidated, NMDA glutamatergic receptor modulation is theorised to be responsible due to a process comparable to long term potentiation (LTP)/long term depression (LTD). Low frequency rTMS can induce LTD and high frequency TMS induce LTP. rTMS can also be done on a smaller scale to target specific functionally or anatomically remote brain regions for stimulation, showing a degree of adaptability for focus on specific regions.

Alternatively, CES involves direct stimulation of the cortex after surgical exposure. This can be beneficial as it allows for more specific stimulation of brain regions. It was originally developed as a method for the treatment of neuropathic or intractable central pain. When experimented with in a wider variety of neuropathologies, it was also shown to improve motor and sensory functions in stroke patients. Animal studies show it can modulate motor cortical excitability via plasticity-like mechanisms. When coupled with traditional rehabilitative training, CES promotes synaptic plasticity and improves motor function after ischaemic stroke. This can be translated to pTBI patients who suffer similar pathophysiological neuronal loss, albeit via a different mechanism. The only downside when compared to rTMS is in its prerequisite for surgical exposure, exposing the patient to all the additional risks of surgery (time, cost, expense, side effects of sedative drugs, infection risks etc.).

The main clinical downside to the widespread use of electrical stimulation, particularly early on after injury, is the risk of inducing seizures and issues with skull conductance (in rTMS). There is also a longer-term increased risk of post-TBI personality changes. Identifying patients which are at increased risk of this complication may be a way to screen and exclude patients from this procedure, while still eliciting benefit in patients who have had injury but who would not experience this side effect [29]

1.3 Experimental models of pTBI

The need to develop therapies that can translate into clinical trials is apparent. While many upcoming experimental therapies are being researched, accurate, high throughput, convenient models of pTBI are logistically difficult to set up and maintain. There are a range of live animal or cell models available to mimic pTBI for experimental purposes. Live animal experiments have some of the most compelling and clinically applicable evidence however there are significant logistical drawbacks and ethical concerns. Meanwhile cell-based models, of which there are wide range and variety are much cheaper and accessible, however can fail to accurately mimic *in vivo* conditions such that findings based on these need to be taken cautiously.

1.3.1 *In vivo* models

Of the *in vivo* options available, live animal experimentation can be done using large mammals or small rodents. An injury can be induced into the head of a monkey or sheep and pTBI pathology can be studied post-mortem or therapeutic interventions can be delivered and effects can be studied. These models are the most accurate to human neuropathology and any new knowledge procured as a result of these studies are highly applicable. However significant concerns prevent their widespread use. They are typically very costly, requiring access to large cattle, and with many ethical concerns, resulting in these studied being very rare. Smaller rodents, such as rats or mice, are favoured for *in vivo* experimentation due to their being easier to handle, more cost effective, and generally having a wider availability. However ethical concerns are still present, despite these being considered 'less sentient' animals frequently used for experimentation. For experimental validity, several animals are required, with long experimental processes, and animal training and surgical expertise for handling and inducing injury or administering therapeutics, and further logistical problems making these models low throughput. Due to ethical concerns surrounding the use of

animals in research, stringent regulations are set in place to standardise and prevent their misuse. There is also a push to limit the role of animals, including small rodents, in scientific research, with focuses on the 3Rs (replacement, reduction and refinement), to promote removal of animals altogether, to reduce the number of animals needed, or to limit the suffering or distress of any animals if involved.

1.3.2 *In vitro* models

Immortalised single cell type monocultures:

Monocultures of single cell types can be commercially bought and are frequently used in pTBI research. Individual cell lines can be used as they are incredibly convenient in ways that live animal experiments are not. Cell lines themselves usually procured from cancerous biopsies (e.g., rat phaeochromocytoma cells [44]) or from cells that are immortalised, effectively inducing cancer. This gives the added advantage of being much less ethically questionable. They are easy to set up, maintain, are highly replicable, require minimal training, and are much more cost-effective [45]. The main downside to this approach is their over-simplistic, reductionist nature. At best they only represent the behaviour of one cell line, of which there are many in the CNS. They are resistant to death under stress, which while useful for creating viable cultures, raises concerns over their ability to accurately depict the normal behaviour of their *in vivo* counterparts. They are highly neoplastic and thus have high variability in their genetic makeup, expression and can exhibit abnormal variability in their physiological responses. Moreover, it has been proven there is frequent cellular cross-contamination with cell lines being procured from various sources and not always being validated [44]. Thus, findings from studies based on these lines may have limited therapeutic applicability.

Organotypic slices

Organotypic slices represent an interface between *in vivo* conditions that can be most accurately replicated *in vitro*. Donor tissue from various mammals, not limited to small rodents but also including rabbits, pigs, dogs and even humans, can be dissected and sliced into thin pieces that can be maintained in a controlled *in vitro* environment [47] [47]. The slices can be thick enough to maintain the three-dimensional environment of the tissue. Replicating the natural cytoarchitecture and extracellular environment allows for any normal *in vivo* neuronal necrosis or regeneration to occur, as well as mimicking the reactive gliosis and mobilisation of microglia and astrocytes to injury. Altogether this demonstrates the neuroplasticity which can be studied after injury, this process may be hindered in other over-simplistic or reductionist models [44]. The disadvantage is that these slices, while providing extremely valuable information, can be still technically challenging to set up and maintain, making them medium throughput at best. Typically, there is difficulty in actually separating slices and culturing in a way where cellular behaviours can be studied, giving a low output of cultures suitable for experimentation, and thus requiring more animals to generate enough data from which meaningful conclusions can be drawn.

3D organoids

3D organoids are another option that has been used for testing. Primary stem cells (or induced pluripotent stem cells) can be harvested, from animal, embryonic or adult human sources, that can be cultured to replicate smaller versions of the organs they go on to develop. These cultures develop into three dimensional systems, where the cells proliferate and organise into small organoids only micrometres long [30]. Pluripotent adult stem cells were proven to have the intrinsic ability to organise themselves into smaller, biologically simulative organoids through processes called self-patterning and morphogenetic rearrangements [31] [32], resulting in a system with the appropriate cytoarchitecture and extracellular matrix for testing. This occurs through many positive and negative

feedback loops through a variety of endogenous and exogenous signalling pathways that encourage the differentiation and organisation of a homogenous population of stem cells into functionally separate cell populations that represents an immature microcosm of their mature, *in vivo* counterpart [30]. This has the added advantage in the ability to forego the use of animals, and can be derived from adult human stem cells, making them more ethically sound. The literature exhibits many examples of a variety of different tissue types in which 3D organoids have been used to simulate *in vivo* organs for experimental testing, including and not limited to intestines (small and large) [33] [34], pancreas [35], liver [36], lung tissue [37], thyroid [38], kidneys [39], and neural tissue [40] [41] [42]. When used for neuroscience research, and specifically pTBI research, they have logistical disadvantages [58]. These organoids typically take longer time periods to culture, can be difficult to study at a cellular level where multiple individual cell types can be difficult to identify when all the cells are cultured together, and only cells on the outer surface of organoids are visible. They lack an immune component as neurons and glial cells typically develop separately. As organoids grow and develop, cells at the centres of spheroids may have difficulty accessing nutrient and oxygen from the culturing medium due to the increased radii, causing an unwanted response to hypoxia, compromising the ability to attribute these pathophysiological responses to a controlled injury. Mechanically, if looking to induce a laceration type injury, it can be difficult to induce injury to simulate pTBI as spheroids are usually free floating, and even if this is somehow managed, it can be difficult to see the specific responses of individual cells to that injury. These limitations make 3D neural organoids a less preferable option.

Brain-on-a-chip (BoC)

There are also examples of highly specialised, engineered platforms to grow neurons such as brain-on-a-chip (BoC). This technique was originally developed by bioengineers, using soft lithography techniques (where various materials including ‘soft’ polydimethylsiloxane (PDMS)) are used to

create microchannels for the study of microfluids [43]. These microchannels can become controlled microenvironments for the growth of neurons. Controlling the height and depth of the channels can sort neuronal somas from axons, allowing the guided processing of axonal outgrowths. This allows for axons to be studied directly, as real time growth and myelination can be viewed. The network of microchannels can allow for continuous perfusion of individual cells, more accurately mimicking the continuous supply of oxygen and nutrients neurons naturally bathe in. This model has obvious advantages for the specific study of axonal growth, injury, degeneration or regeneration. Myelination is implicated in the pathophysiological mechanism for many autoimmune/myelination disorders, such as multiple sclerosis, Guillain Barre syndrome, and chronic inflammatory demyelination polyradiculoneuropathy to name a few. This system is highly specialised, and can be used in drug development or testing, can be adapted to include multiple material interfaces for an additional 3D component, and can be adapted to include a cellular barrier through which the drug enters, mimicking a BBB. This model is highly specific, and while it can be used to study axonal responses to injury [60], its single celled nature lacks the individual responses of glia or the immune component to injury thus excluding cell-cell interactions and any effect this may have on neuronal function, plasticity or regeneration, which is integral to the pathophysiology of pTBI. Moreover, to set these cultures up, expensive materials, techniques and engineering expertise is required, negating the purposes of creating a simple, inexpensive but biologically simulative model of pTBI. While the BoC model has its place for the specific study of neuronal axonal and myelination, it is an ultimately incomplete model of pTBI and logistically not suitable for the purposes of this study.

Neural stem cell cultures

Neural stem cell cultures are also frequently used in the field of neuroscience. These can be primary neural stem cells (NSCs) or induced pluripotent stem cells (iPSCs) where adult cells can be genetically modified to be pluripotent and proliferative. Primary neural stem cells are usually harvested from

embryonic rodents from regions of the brain with naturally occurring stem cells (such as the subventricular zone), where they can be dissociated (enzymatically or mechanically) and seeded into flasks or culture plates, onto plastic or glass, in a specialised medium and cultured [44]. The stem cells proliferate into neurons and glia and establish into a 2D multicellular culture. Advantages to these cultures include their multicellular nature, including the immune component, the glial and neuron cell-cell interactions thus exhibiting the host of pathophysiological responses to injury. iPSCs can be harvested directly from the adult animal or human, dissociated before being cultured in a specialised medium including a chemical that induces a genetic reprogramming of the cell, allowing it to become proliferative and grow in a similar mechanism to neural stem cells. There is the obvious ethical advantage of being able to take adult human cells, but this can also allow for patient specific cultures that theoretically can be used for later transplantation, allowing for a degree of genetic homogeneity with the patient. This is an important advantage for clinical outcomes after transplantation where rejection due to MHC incompatibility is a significant risk. The cultures can be propagated for an indefinite amount of time, and the process of harvesting, dissociating and culturing make these models logistically simple with easy maintenance, while avoiding the neoplastic disadvantages of commercially available cancerous cell lines. Injury can also be induced with signs of cell death as a result [62]. There are some negatives to their use, however. Their two-dimensional nature is a significant difference than the three-dimensional environment the cells would naturally grow in, which has been proven to be paramount for normal neuronal growth, regeneration and glial growth and reactivity. Moreover, as with all indefinitely propagating cells, there is still the risk of malignant transformation into neoplastic cells where cells become too genetically diverse and deviate from the expected behaviour of healthy primary cells, limiting its applicability.

Primary neural cultures

Primary neural cultures are another option for a CNS model for neuropathology. Postnatal animals are used, neural tissue dissected out and dissociated either mechanically or enzymatically, before being cultured as a monolayer. Once a mature culture is established, an injury can be created, using a scratch needle injury, requiring less animal and surgical expertise and training than in live animal models. The cells procured for culture are derived directly from animals, are not immortalised and cancerous and are mixed populations all normally found *in vivo*, thus a mixed cell population, all interacting and modulating each other's behaviours, represents a better CNS model than individual commercially available cell lines. Mixed glial cultures are frequently used, forming a culture with astrocytes, oligodendrocyte precursor cells (OPCs), oligodendrocytes, and microglia. When subjected to a scratch needle injury, palisading astrocytes forming a 'brush border' is evident as astrocytes infiltrate and 'wall off' the injury site, exhibiting early signs of gliosis, thus proving the model exhibits the natural pathophysiological response to injury [63]. Microglial mobilisation and infiltration into the lesion site have also been shown, proving the normal physiological reaction to injury of the immune component of the multicellular culture, a clear advantage over single population cultures [63]. The lack of neurons in mixed glial cultures is a significant disadvantage however, as neuronal behaviours and responses to injury are not shown, neuroplasticity cannot be studied. Hence mixed neuronal cultures were developed at our lab which involves a simple medium switch to a medium shown to support the growth of neurons and glia, creating a multicellular mixed neuronal model that can be grown and maintained as a monolayer. Details of this are included below (Chapter 3: Evaluating the feasibility of storing primary mixed cultures in Hibernate^{TM}).

Table 1.2 includes a summary of *in vitro* models of pTBI, included sources of their use, and a few models that have not been discussed in depth thus far (modified from unpublished data, Basit et al, June 2022)

Model	Description	Advantages	Disadvantages
Immortalised single cell lines	Pure cells (NSCs/ESCs)	- Indefinite propagation - Low technical difficulty - Useful for specific cell response studies - Cells can be of human origin - Facile injury induction	- Genetically and phenotypically differ from endogenous counterparts - High risk of mycoplasma contamination - Resistant to cell death - Frequent cross-cellular contamination - Lacks immune component
3D Organotypic slices	Ex vivo brain tissue slices	- Retain *in vivo* cytoarchitecture - Retain major brain cell types - Moderate difficulty inducing injury - Biomaterial interface - Display complex injury responses - Adaptable for excitotoxicity/hypoxia studies	- Moderate throughput - Can be technically difficult isolating and maintaining slices - Requires more animals than other *in vitro* models
Organoids	Stem cell derived self-organising spheroids (iPSC origin)	- Cytoarchitecture recapitulates developing tissues - Can be human/patient specific - Closes simulates *in vivo* cell behaviour and communication - Adaptable for excitotoxicity/hypoxia studies	- Moderate throughput - Little uniformity between aggregates - Largely immature cellular development - Long culturing periods - Few injury systems are reported - Lack immune component - Difficult mechanical injury induction due to free-floating nature - Larger spheroids can become hypoxic - Difficult cellular analysis
Brain-on-a-chip	Microfluidic culture systems of iPSC derived cultures	- Tissue-like physiology - Physiological-like perfusion system of 3D tissue - Adaptable for disease/toxicity mechanisms - Axonal strain injury attempted	- Low throughput - Scalability limitations - Lack immune component - Largely immature cellular component - Difficult mechanical injury induction
Neural stem cell cultures	Cultures of primary, differentiated stem cells	- High throughput - Low technical difficulty - Multicellular cultures - Facile injury induction - Simple maintenance and analysis - Facile biomaterial interfacing	- Lack immune component - Moderate length differentiation protocols - Mostly 2D cultures - Preferential differentiation to astrocytes
Induced pluripotent stem cells (iPSCs)	Stem cell genetically reprogrammed from adult cells	- Indefinite propagation - Ethical, human origin - Patient specific (retains genetic homogeneity with patient for transplantation) - Patient specific disease modelling	- Long differentiation protocol (moderate throughput) - Differ genetically/phenotypically from endogeneous cell counterparts - Heterogeneity of cells - Resistant to cell death (teratogenicity risk) - Lack immune component - Risk of mycoplasma contamination
2D primary pure cell cultures	Primary cultures from brain dissociates purified using media components or shaking	- High throughput - Low technical difficulty - Useful for specific cell response studies - Facile injury induction	- Over-simplistic, reductionist model - Unicellular, lacks complex multicellular cell-cell interactions - Lacks immune component
2D primary multicellular neural cultures	Complex multicellular cultures of brain dissociates	- Encompasses all major brain cell types (including immune cells) - Facile injury induction - High throughput - Low technical difficulty (simple set up and maintenance) - Facile cellular analysis - Adaptable to multiple injury mechanisms - Amenable for biomaterial, pharmaceutical, stem cell transplantation, nanotherapeutic studies	- 2D environment (may have abnormal cell responses to flat, stiff surface that cultures are established onto)

Table 1.2 Showing each* in vitro *model of pTBI, with its associated advantages/disadvantages

1.3.3 Limitations to novel therapy experimentation for pTBI

From the above it is clear there are many avenues of research to develop potential new therapies for pTBI. The variety of proposed interventions (particularly with nanoparticles, biomaterials, electrostimulation etc.) require the input of many different disciplines, including but not limited to biomaterial scientists, engineers, physicists, chemists, and mathematicians. The current limitations that stand in the way for more convenient but accurate models of pTBI to these disciplines are the costs, training, equipment and expertise. For instance, in order to set up a live animal experiment, there need to be ethical permissions, facilities that enable frequent and ready access to animals within the appropriate age range for experimentation, expertise in animal handling, surgical expertise in inducing injury and any dissections, equipment for each stage of the process and expertise in handling the equipment to list a few. These are resources that may not be available to research teams outside of the purely biological domain and present key logistical challenges preventing high throughput but accurate experimentation for these research teams.

To facilitate reliable modelling of the CNS across non-specialist laboratories, it would be ideal to have an *in vitro* culture system which is medium/high throughput, technically simple but produces a complex, multicellular model, in serum-free conditions, of cells that behave accurately and predictably. It would also be ideal for access for culture systems like these to not be limited to sites with direct access to animal facilities. **A method for transportation of pTBI models would be beneficial here, as it would allow for non-expert laboratories access to primary neuronal cells.** Animal tissues can be dissected, dissociated and prepared into a confluent, mature and complex culture at a specialist site, before being transported for up to several hours without specialised infrastructure, to multiple other sites for experimental use. This removes the limitations of ethics, cost, expertise and inconvenience for non-specialist laboratories, as only one site is set up to create the cultures that can then be shared. The applications of easier transportation of neural cells would

ease the bottleneck in research for not only pTBI but for all areas of regenerative neurological research requiring multidisciplinary collaboration, (which is arguably all of regenerative neuroscientific/neurological research).

1.4 Maintaining cells during storage/transport is becoming possible

The successful storage of many different cells, tissues and organs is already known. One of the most common types of tissues that are stored are blood products, such as red blood cells and platelets, being the most common form of clinical transplantation[6]. RBC units are received from donors, then centrifuged to remove plasma before being leuco-filtered. Cell viability and shelf life is increased by adding acid citrate dextrose to allow for storage for up to 3 weeks [45]. Most European banks, however, use preservatives that contain saline-adenine-dextrose-mannitol which have extended shelf life of RBCs for up to 6 weeks (and potentially longer [46]) at 1-6 °C [45].

A wide range of other tissues have been successfully and routinely stored including bone grafts, tissue biopsies, eye transplants, tendons, hepatocytes, epidermal cells and heart valves at various temperatures. National Health Service (NHS) tissue and eye service guidelines advocate for transplants and grafts to be kept either freeze dried, frozen or cryopreserved depending on the tissue [47]. Once kept at extremely low temperatures, shelf life of some tissues, such as bone or tendons, be up to 3 months if frozen or 5 years if cryopreserved or freeze dried [47].

1.4.1 Current neural storage methods and transports

There is evidence of the ability to store neural tissue, mostly of intact neural tissue and mainly at cryogenic or hypothermic temperatures [48]. For the purposes outlined above, cryopreservation or freezing, that has been proven to allow for survival of tissue for up to several months, would be a

poor method of routine transport, as additional specialised infrastructure, such cryogenic freezers not suitable for transport, would be needed to maintain tissues at low temperatures while being transported. Currently, dissociated neuronal tissue can only be kept at ambient CO_2 concentrations for only short periods of time, and only if cells are kept in hypothermic temperatures, again requiring infrastructure such as portable fridges to maintain a cold transport chain, preventing too much mechanical damage while being moved, and only for limited periods of time. These are limiting factors for long distance transport.

Types of storage media

Of the media available to store these cells, HypoThermosol and Hibernate™ medium are mentioned in the literature and are available commercially for the storage of neural tissue. HypoThermosol is marketed as a hypothermic preservation medium that can store cells and tissues at temperatures of 2-8°C. It is proven to store a wide variety of tissue including epidermal cells[9], hepatocytes and liver tissue[10], coronary vessel tissue[11], adipose tissue, mesenchymal stromal cells etc. for no more than a week.

Hibernate™ medium is a commercially available medium originally formulated from Neurobasal-A medium (a serum-free medium created for the growth and maintenance of neurons) except with a few key distinctions related to pH control. Hibernate™ medium has a greatly decreased bicarbonate ion concentration compared to Neurobasal-A medium and alternatively uses MOPS (3-N-morpholino-propanesulfonic acid) instead of HEPES (4-2-hydroxyethyl-1-piperazine ethane sulfonic acid) as an acidity buffer which allows it to tolerate the lower ambient CO2 concentrations and prevent the increase in pH seen in Neurobasal-A when exposed to ambient CO2, preventing cellular death due to alkaline conditions. There are a variety of alternative formulations of ‘Hibernate’ that are quoted in the literature, however the name Hibernate™ is now a trademark for the formulation

produced by ThermoFisher Scientific. The differences in composition of these various media are shown in **Table 1.3**.

The advantage of Hibernate™ medium over HypoThermosol was its proven ability to store specifically neuronal cells without loss of viability for up to several days, while HypoThermosol is a generalised media for most cell types and is ideally used for hypothermic storage. There is one case reported in the literature of HypoThermosol and Hibernate™ medium being directly compared for hypothermic storage of Engineered neural tissue (Schwann cells in collagen gels) that found Hibernate™ performed better [49]. There was no increase in cell deaths after storage where HypoThermosol caused significantly increased cell deaths during storage, this difference increased incrementally with longer storage times [49].

	Original Hibernate medium [50] [51] [52]	Hibernate-alternative/newer formulation [53]	Neurobasal-A
pH	6.8-7.4		
KCl (mM)	30-70	5.36	5.3
Na+ (mM)	10-30	76	78
PO_4^{2-} (mM)	5-50	0.9	0.9
Lactic acid (mM)	20	0	0
Glucose (mM)	5	25	25
Ca^{2+} (mM)	<0.1 mM	1.8	1.8
Sorbitol	164.7	0	0
Pyruvate (mM)	0	0.23	0.23
$Fe(NO_3)_3$ (mM)	0	0.0002	0.000258
Amino acids	/	/	/
Vitamins	/	/	/
$MgCl_2$ (mM)	0.24	0.812	0.814
$NaHCO_3$ (mM)		0.88	26.2
Buffer	/	MOPS	HEPES
Osmolality (mOsm/L)		230-240	

Table 1.3: Composition of various 'Hibernate' media identified in the literature, comparison with Neurobasal-A

Table 1.4 shows details on cases of successful storage of neural and neuronal tissue in Hibernate™ medium. These were mainly at hypothermic or freezing temperatures. Tissues were mainly stored as opposed to transported, identifying another gap in the literature, and would be valuable proof of concept. Hibernate™ medium has also been proven useful as a dissection medium [55] [56] [57] [58].

	Cell type Source Species	**Temperature (degrees Celsius)**	**Additives**	**Time in storage**	**Experimental conditions**	**Results**
1986 Kawamoto [50]	E15-16 cerebellar tissue Rat	0°C, 3°C, 8°C, 15°C, 23°C, 35°C	Various	Up to 8 days	Intact tissue kept in various ionic compositions, acidic metabolites, osmolality, pH, glucose etc.	Optimised long-term survival in Hibernate medium at 3-8°C.
1995 Nikkah [51]	Foetal VM tissue Rat	4°C, 21°C	None	Up to 8-12 days (12 days for intact tissue, 8 days for cell suspension)	Intact tissue stored for up to 12 days Cell suspension stored for up to 8 days	Tissue remains viable after 8-12 days with limited loss of neural tissue
1996 Brewer [53]	E18 hippocampal neurons Rat	37°C (ambient CO2 and O2)	B27	Up to 3 days	Cultured, mature cells kept in storage	Viability maintained for at least 2 days in B27/Hib (cultured neurons)
		8°C (ambient CO2 and O2)		1 days, 4 days	Whole hippocampi tissue in storage then mechanically dissociated, then cultured	Low viability of cells by 4 days
		8°C (ambient CO2 and O2)		Up to 4 weeks	Whole hippocampi tissue in storage – recovered and cultured in neurobasal	About 50% survival after 1 month storage
1998 Apostolides [59]	E14 VM tissue Rat	4°C (ambient CO2 and O2)	Control, GDNF	6 days	Whole VMs kept in storage before dissociated into cell suspensions and implanted into adult rats with induced Parkinson's disease	Cell suspensions showed 98% cell viability across all groups
2000 Castilho [52]	E14 VM tissue Rat	4°C	Control, FK506,	7 days	Intact VM tissue kept in storage	79% viability of cells immediately

			cyclosporin A			after storage compared to non-storage
2000 Hurelbrink [60]	E66-88 striatal tissue Human	4°C	None	24 hours	Whole human foetal striatal tissue stored before grafts implanted into rats with induced Huntington's disease	No significant difference between graft stored tissue volumes vs non stored control tissue
2000 Peterson [61]	Embryonic VM tissue Rat	4°C	Tirilazad mesylate, GDNF	8 days	Whole tissue in Hibernate™, 70% change at 3 days	No statistically significant difference in grafted dopamine neurons despite downward trend of approx. 50% reduced cell survival
2002 Hebb [62]	Embryonic VM tissue Rat	4°C	GDNF (vs control with none)	6, 9, 12, 15 days	Whole tissue kept in Hibernate™ storage then dissociated and seeded in DMEM/F12/B27/Penstrep, standard culturing conditions for 48 hrs	Dopaminergic neurons retained significant viability until 15 days, improved viability with GDNF
2017 Day [49]	Schwann cells in collagen hydrogels (engineered neural tissue)	4°C (+cryogenic)	None	2, 7, 14 days	Whole EngNT kept in hypothermic and cryogenic storage in various media (inc. HypoThermosol)	No significant difference in cell deaths after 2 days storage compared to non-storage controls Significantly decreased cell deaths compared to other storage media
2021 Woods [54]	P0-2 OPCs Mouse	RT, 4°C (ambient CO2 and O2)	None	3 days	OPCs kept in storage as cell suspension	No significant loss of cell viability between storage and non-storage controls, or RT and 4 C

Table 1.4: Cases of Hibernate™ used for the storage of neural tissue

There is also one case of transport, as opposed to storage, of neural tissue in Hibernate™ that was successful [63]. E18 and P1 rat derived hippocampal neurons were dissociated and cultured in standard culturing conditions before being placed in cold Hibernate™ medium with B27 supplement. Cultures were maintained in standard conditions for 2 days *in vitro* (DIV) packaged in 4°C cooled gel packs into shipping containers before being transported. Once received, they were replaced with their original growth medium Neurobasal, and allowed to recover for 7 DIV in standard culturing conditions. Results showed no indications of a decreased viability after transport, however when the experiment was repeated with cultures shipped at 5 DIV, there was a noticeable decrease in viability [63]. The reason for this is not mentioned, however this is evidence of the ability of Hibernate™ to keep cells viable during actual transport as opposed to only storage. Limitations to this study are in the use of hippocampal neurons, which would be a poor model of pTBI. The monocellular culture, composed of only neurons, would fail to simulate the complexity of cell-cell interactions, including glial responses, to injury. There is little detail in the study on the actual mode of transport, distance, and time in transit, and how this may have influenced culture viability in transport. Moreover, the effect of cooled Hibernate™ and gel-packs to ensure cultures were kept at hypothermic temperatures can introduce further logistical problems. An ideal method of transport would ideally be at room temperature, with no additional equipment required.

In summary, there are many available forms of transport of a variety of different tissues and cell suspensions. There is evidence in the use of Hibernate™ as an optimised neural storage medium however, to date **the storage and transport of an established complex multicellular culture has not been evaluated and represents the goal of this thesis**. This study prioritised storage of cultured neural tissue in place of transport to deliver only proof of concept at this stage that Hibernate™ does not detrimentally affect cultured neural tissue, although the possibility of transport of neural tissue is also discussed later in Chapter 4: Discussion.

Chapter 2: Materials and Methods

2.1. Materials

All materials with source company and product code are listed in **table 2.1.**

2.1.1 Culturing materials

Cultures were grown in plastic 24 well plates. 13 mm round glass coverslips were added to each well of the plates and cultures were established on these. These were treated with either Poly-D-lysine (PDL), or Poly-ornithine and laminin. Enzymes used during the dissociation process included 0.25% Trypsin EDTA and DNAse. 0.4% Trypan blue stain was used after the dissociation procedure. Media used included, Neurobasal-A medium, Dulbecco's minimum essential medium (DMEM), and Hibernate-A^{TM}. Media additives included HEPES, B27, PenStrep, GlutaMAX, Foetal bovine serum (FBS), and sodium pyruvate. Postnatal day 0-3 mice were used and supplied from Keele University animal housing facilities (UK).

2.1.2 Fixation and immunocytochemistry preparation materials

All materials 4% paraformaldehyde in PBS (PFA), was used to fix cultures prior to staining. Normal donkey serum (NDS) and Triton X-100 in phosphate buffered saline (PBS) was used to make up the antibody solutions (0.3% v/v Triton X-100 and 5% v/v NDS in PBS).

2.1.3 Assay materials

Calcein acetoxymethyl (Calcein-AM) and ethidium homodimer-1 was used as a commercially available live/dead assay. Primary antibodies used to stain cell specific markers included mouse anti-beta tubulin III (Tuj1), rabbit glial fibrillary acidic protein (GFAP), goat ionised calcium binding adapter molecule (Iba1) and rat myelin basic protein (MBP). Secondary antibodies included donkey

anti-mouse fluorescein isothiocyanate (FITC), donkey anti-rat cyanine 3 (Cy3), donkey anti-rabbit cyanine 5 (Cy5) and donkey anti-goat fluorescein isothiocyanate (FITC).

2.1.4 Imaging materials

VECTASHIELD mounting medium with Hoechst stain (DAPI) was used to mount coverslips onto glass slides. EVOS^{TM} XL Core imaging system phase microscope was used to image cells throughout it's culturing period. ZEISS AXIO Observer Z.1 fluoroscopic microscope was used after ICC staining to obtain fluorescent images for analysis.

	Material	Product name	Company	Product Code
Materials used in preparation prior to culturing	24 well plates	24 well plates, not treated	Merck	CLS3738-100EA
	Glass coverslips	Epredia x1000 round coverslips	Fisher Scientific	15737602
	Poly-ornithine	Poly-ornithine	Merck	P4957
	Laminin	Laminin from Engelbreth-Holm-Swarm murine sarcoma basement membrane	Merck	L2020
	Poly-D-lysine (PDL)	Poly-D-lysine hydrobromide	Merck	P6407
Media	DMEM	Gibco™ DMEM, high glucose, pyruvate	Fisher Scientific	11594486
	Neurobasal-A	Gibco™ Neurobasal-A Medium	Fisher Scientific	10888022
Media additives	B-27	Gibco™ B-27™ Supplement (50X), serum free	Fisher Scientific	11530536
	GlutaMAX	GlutaMAX™ Supplement	Fisher Scientific	11574466
	Sodium pyruvate	Sodium pyruvate solution	Merck	S8636-100ML
	PenStrep	Gibco™ Penicillin-Streptomycin (5,000 U/mL)	Fisher-Scientific	11528876
	Foetal Bovine Serum	Gibco™ Fetal Bovine Serum, qualified	Fisher Scientific	11573397
Cortical dissociation step materials	0.25% Trypsin EDTA	Gibco™ Trypsin-EDTA (0.25%), phenol red	Fisher Scientific	11560626
	DNase	Roche DNase	Merck	10104159001
	0.4% Trypan blue	Gibco™ Trypan Blue Solution, 0.4%	Fisher Scientific	15250061
Live/dead assay materials	Calcein AM	Calcein-AM 4 mM in anhydrous DMSO fluorescent dye, for histology	VWR International	89139-470
	Ethidium homodimer-1	Ethidium homodimer I solution	Merck	E1903-.5ML
ICC preparation materials	Phosphate buffered saline (PBS)	Phosphate buffered saline tablets	Merck	P4417-100TAB
	4% Paraformaldehyde (PFA)	Paraformaldehyde Solution, 4% in PBS, Thermo Scientific™	Fisher Scientific	15670799
	Normal donkey serum (NDS)	Donkey serum	Merck	17000121
	Triton X-100	Triton™ X-100 solution	Merck	93443
Imaging tools	Mounting medium with DAPI	VECTASHIELD[R] Antifade Mounting Medium with DAPI	2B Scientific	H-1200-10
	Phase microscope (EVOS)	EVOS™ XL Core Imaging System	Thermo Fisher Scientific	AMEX1000
	ICC microscope (ZEISS)	ZEISS AXIO Observer Z.1	ZEISS	

Table 2.1. Materials used at each stage of experimentation, the source company and the product code

2.2 Methods

2.2.1 Preparation of Primary rodent mixed neuronal and glial cultures

Preparation of culturing materials- coating of coverslips

Prior to establishing cultures, glass coverslips were set into two 24 well plates. 70% isopropyl alcohol (IPA) was then added to each well and plates were left under UV light for 15 minutes to sterilise. From this point onwards, all conditions were kept sterile. The IPA was removed and double distilled water (ddH_2O) then added and removed to wash each well.

From here, one of two coating protocols were used. 300 µL of PDL (0.1 mg/mL) in ddH_2O was added to each well for at least one hour at RT before being removed. PBS was then added into each well, left for five minutes and then removed. This wash with PBS was repeated two further times. Coverslips were then left to dry completely at room temperature (RT) with lids removed from the plate in sterile conditions.

Alternatively, 300 µL of poly-ornithine (0.1 mg/mL) in ddH_2O was added into each well for at least one hour at 37°C. After it was removed, three washes with ddH_2O was performed, each lasting five minutes. Laminin was then diluted in ddH_2O (5-10 µg/mL) and 300 µL of this was then added to each well and left for at least one hour at 37°C. After three further five-minute washes with ddH_2O, the coverslips were left to dry completely at RT with lids removed from the plate in sterile conditions.

Dissection medium and mixed neuronal and glial culture growth media

PBS was used as a dissection medium throughout the dissection process. This was kept cool on ice prior to and throughout the dissection. The culturing medium for the mixed neuronal cultures was a complete Neurobasal-A medium. This was made up of Neurobasal-A medium with additive B27 (2% v/v), GlutaMAX (1% v/v) and PenStrep (1% v/v). The mixed glial cultures grew in D10 medium which

was made up of DMEM with added FBS (10% v/v), PenStrep (1% v/v), GlutaMAX (1% v/v) and sodium pyruvate (1% v/v).

Preparation of mixed cortical neuronal cultures

Animal use in this study was approved by the local ethical committee. This was a Schedule 1 procedure in accordance with the Animals and Scientific Procedures Act (1986).

Tissue was sourced from litters of 5-12 P0-2 CD1 mice from Keele University. They were euthanised with a lethal overdose of 0.04 ml Pentobarbitone via intraperitoneal injection at the animal housing facility. After collection to our laboratory, they were then decapitation under sterile conditions. The method for obtaining the cortices are shown in **figure 2.1**. A sagittal cut was then made in the skin from occiput to snout to expose the skull. A coronal cut was made between the eye sockets to split the skull from the snout. The skull was then cut sagittally from the cut edge of the head towards the snout to expose the soft brain tissue which was then carefully lifted out and collected into PBS kept cool on ice. Once the brain tissue was collected from all pups, each brain was carefully rolled onto prior prepared autoclaved tissue to remove meninges and blood vessels. To obtain only the cortex, the brain was set onto the tissue with dorsum facing upwards before cutting away the hindbrain and the olfactory bulbs to leave the midbrain and forebrain. This was then bisected sagittally and each half rolled over to expose the midbrain, which was then removed. Each cortex was then placed in a new petri of fresh, cool PBS. Once all cortices were obtained, they were lifted out of the PBS and placed into a dry, sterile, flat glass petri. A curved scalpel was used to mince all the cortices until pieces were smaller than one millimetre.

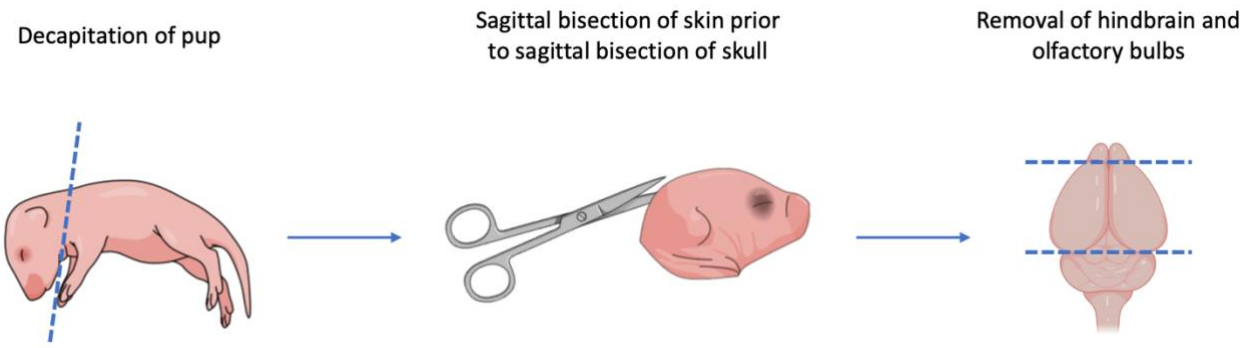

Figure 2.1. Dissection of mouse pups to obtain cortices

Here, the dissociation process was split into either mechanical or enzymatic dissociation.

Mechanical dissociation entailed triturating the minced brain tissue in the dissection medium, 20 times with a plastic Pasteur pipette, 10 times with a P1000 pipette set to 900 µL and 10 times with a P200 pipette set to 190 µL. The solution was then centrifuged at 1200 rpm for four minutes and resuspended in two to four millilitres of complete neurobasal medium.

Alternatively, enzymatic dissociation entailed centrifuging the tissue at 1200 rpm for four minutes, removing the PBS and resuspending in 0.25% Trypsin EDTA (100 µL per brain) and 20 µg/mL DNase (50 µL per brain). The solution was then slowly triturated two times with a Pasteur pipette to mix. This was then placed onto a shaker at 90 rpm and 37 °C for five minutes, then triturated slowly with a Pasteur pipette four times, before being placed onto the shaker for a further two minutes. In order to halt the enzymatic dissociation process, two to three millilitres of FBS and two to three millilitres of complete neurobasal medium was added before the whole solution was triturated slowly with a Pasteur pipette 10 times. The solution was then centrifuged again at 1200 rpm for four minutes before being resuspended in two to four millilitres of complete neurobasal medium.

Whether mechanically or enzymatically dissociated, the solution was now filtered, once through a 70 µm filter then through a 40 µm filter.

Here, the 0.4% Trypan blue stain and a Neubauer cell counter haemocytometer was used to establish the cell density. When viewed under a phase microscope, the haemocytometer allows for the identification of viable cells, distinguished from non-viable cells that take up the Trypan stain. Complete neurobasal medium was added to create a solution at $2x10^6$ cells/mL. This solution was then seeded onto the prepared, dry coverslips, 300 µL of the cell solution into each well.

Cells were seeded into two separate 24 well plates, one to be later used as a test plate while the other a control plate. Once seeded, the cultures were allowed to establish in sterile standard culturing conditions of 37°C and 5% CO_2, humidified air. Within 24 hours, 100% of the culturing medium was removed to clear any cellular debris and 500 µL of fresh, pre-warmed culturing medium added. Thereafter only 50% of medium was exchanged every 2-3 days.

Preparation of mixed cortical glial cultures

For the preparation of a mixed glial culture, the protocol was identical except in the use of D10 medium in place of complete neurobasal medium. This medium is able to support the growth of glial cells instead of complete neurobasal medium which was used to support the growth of neurons in a mixed neuronal culture.

If using enzymatic dissociation, cells were washed in D10 medium, and after their removal from PBS, D10 medium was added instead of complete neurobasal medium. If using mechanical dissociation, cells were triturated in PBS before being centrifuged and resuspended in D10 instead of complete neurobasal medium. Cells were also seeded and cultured in standard culture conditions in D10.

2.2.2 Method for monolayer storage experiments

Once the culture became mature and confluent, (10-14d *in vitro*), the culturing medium in one of the 24 well plates, the 'test' plate, was removed and replaced with 300 µL of Hibernate-A™ medium. This plate was then kept at RT in a dry, dark cupboard for four hours. Four hours was chosen as the timepoint for storage testing, as it was feasible within a day of culture work and represents a significant travelable distance within the UK, which is elaborated upon in Chapter 4: Discussion. After four hours, the medium was again replaced with 300 µL of the appropriate culturing medium (complete neurobasal medium for mixed neuronal cultures and D10 medium for mixed glial cultures) and returned to standard culturing conditions. At this point, 100% of the culturing medium from the control plate was also replaced with fresh medium to mimic the 'stress' of medium replacements in the control cells. Both plates were then allowed to recover for 24 hours in standard culturing conditions.

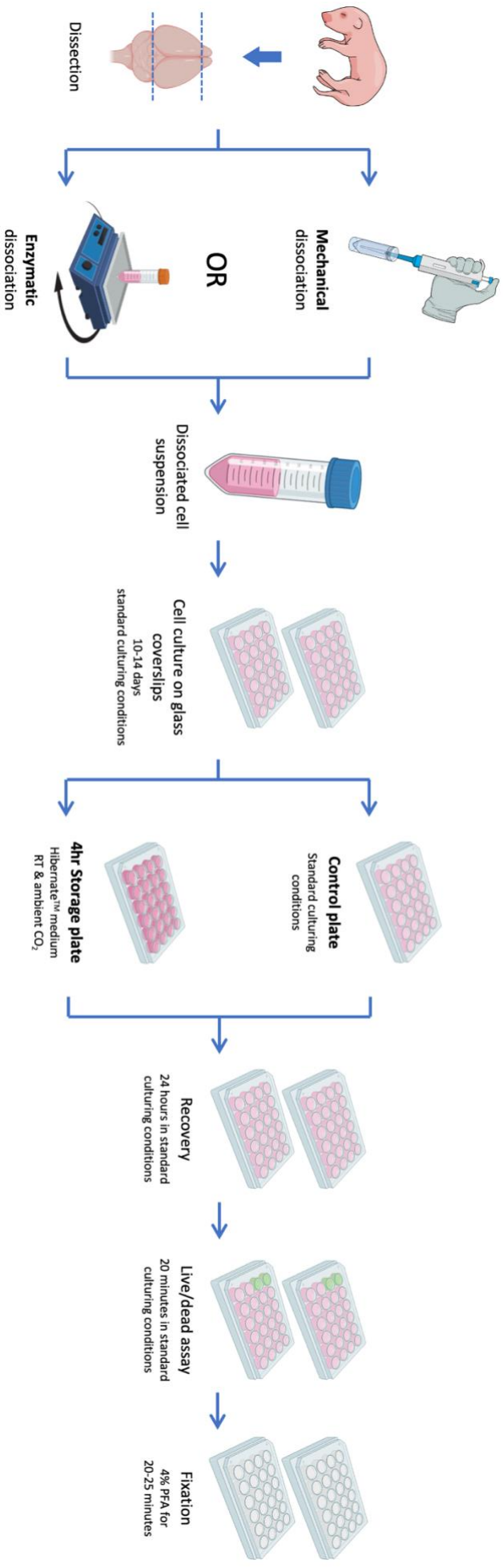

Figure 2.2. Whole experimental protocol

2.2.3 Assays

Calcein AM and Ethidium homodimer-1 (Live/dead) assays

To perform the live/dead assay, calcein-AM and ethidium homodimer-1 was used. Calcein-AM is a substrate that passively crosses the membranes of cells and is hydrolysed by the enzyme esterase to a polar green fluorescent product that is retained within cells with an intact membrane. This makes it useful as an assessment of viable cells with intact membranes, as well as for the function of esterases. Ethidium homodimer-1 is a 'dead' stain, it is membrane impermeable so only enters cells without intact membranes. It naturally binds to DNA so dead cell nuclear fragments can be viewed or counted under any fluorescence microscope.

When assessing for live and dead cells, two wells from each 24 well plate were assayed by adding 3 µL/mL of calcein-AM and 6 µL/mL of Ethidium homodimer-1 to 300 µL of the culturing medium in each well. This was left to incubate in standard culturing conditions for at least 30 minutes before being imaged.

Immunocytochemistry staining

After performing the live/dead assay and imaging, all growth medium was removed. PBS was then added and removed to remove debris. 4% PFA in PBS was added and left for 20-25 minutes at RT. PFA works as a fixing agent by cross-linking proteins (primarily lysine). After fixing, cultures were washed in PBS, leaving each wash for five minutes, a further three times.

A blocking solution was made up of 5% v/v of NDS and 0.3% v/v of Triton X-100 in PBS. Triton X-100 is a commonly used non-ionic surfactant for lysing cells and extracting proteins for staining. It is used to permeabilise the cell membranes of cells that are already fixed. This allows for better entry of antibodies to bind to intracellular target antigens. This was used as the solution to make up primary (**table 2.2**) and secondary antibody (**table 2.3**) solutions for staining.

Cell type	Primary antibody	Species of primary antibody	Company	Product code	Dilution in blocking solution
Neurons	Anti-beta tubulin III (TUJ1)	Mouse	BioLegend	801202	1/500
Astrocytes	Anti-glial fibrillary acidic protein (GFAP)	Rabbit	Agilent	Z033429-2	1/500
Microglia	Anti-ionised calcium binding adapter molecule (Iba1)	Goat	Abcam	ab5076	1/200
Oligodendrocytes	Anti-myelin basic protein (MBP)	Rat	Bio-Rad Laboratories, Inc.	MCA409S	1/200

Table 2.2: Primary antibody used to identify each cell type, the native species of origin for each antibody and their dilution factors within the blocking solution

Primary antibody	Corresponding secondary antibody	Company	Product code	Dilution factor in blocking solution	Excitation wavelength	Emission wavelength
Tuj1	Donkey anti-mouse FITC	Stratech Scientific Ltd.	715-095-151	1/200	495 nm	519 nm
GFAP	Donkey anti-Rabbit Cy5	Stratech Scientific Ltd.	711-175-152-JIR	1/200	651 nm	670 nm
Iba1	Donkey anti-Goat FITC	Stratech Scientific Ltd.	705-095-003	1/200	495 nm	519 nm
MBP	Donkey anti-Rat Cy3	Stratech Scientific Ltd.	712-165-153	1/200	555 nm	596 nm

Table 2.3: Secondary, fluorescent antibodies used to bind primary antibodies and their associated properties

Once the primary antibodies were added, the solution was left overnight at 4-8°C in the dark. After 24 hours, the antibody solution was removed and three PBS washes, each for five minutes, was performed. The secondary antibody solutions were then prepared in the blocking solution according to the appropriate dilution ratios. When added, after removing the last PBS wash, the solution was left at RT for 2 hours in the dark. Three further washes with PBS were performed, each wash left for

five minutes before removing. After the washes, each coverslip was removed from the well with a needle and paddle forceps. A droplet of VECTASHIELD mounting medium with DAPI staining was added onto a glass slide onto which the coverslip, with the culture grown on one side, was mounted. Clear varnish was used to seal the edges of the coverslip to prevent it drying. Glass slides were clearly labelled and kept in cool, dark conditions before being imaged and analysed.

2.2.4 Imaging and morphological/statistical analysis

Imaging

Phase images were taken throughout culturing to establish if the culture was developing normally and if any cell detachment took place post storage, as an early sign of cell stress. This was done with an EVOS™ XL Core Imaging System.

After live/dead staining with calcein-AM and ethidium homodimer-1, one drop of mounting medium with DAPI staining was added to the medium to stain for nuclei before imaging. For each coverslip, areas of viable staining were imaged, with four to five images taken of each coverslip. A live/dead proportion was then obtained by counting every nucleus in each image and counting each as stained green (calcein, alive) or stained red (ethidium homodimer-1, dead). The total number of nuclei in each image varied from 30 to 250. This was repeated for every coverslip (across both control and storage wells) that was assayed.

After ICC staining and mounting of coverslips, all slides were imaged with the ZEISS AXIO Observer Z.1 fluoroscopic microscope (details above). For each slide, the appropriate secondary antibody was excited with the appropriate emission wavelength light filtered from the microscope.

Summary of analyses

Table 2.4 shows a summary of all the analyses that were done for each cell type. The method for each analysis is elaborated below.

Cell type	**Morphological and quantitative analyses**
Neuron	Cell proportion
	Neurite length
Astrocyte	Cell proportion
	Area (cell hypertrophy)
	Optical density
Oligodendrocytes	Cell proportion
	Cell area
	Stages of maturation
Microglia	Cell proportion
	Cell area
	Circle value
	Roundedness Index
	Ramified vs Amoeboid

Table 2.4: Summary of analyses done for each cell type; *a cell proportion was established for each cell type. Morphological analyses done for each cell type indicates either its maturation or reactivity*

Assessment of cellular proportions for each cell type

For each cell type's antibody stain, the ZEISS ZEN Pro 3.3 microscope software was used to simultaneously image the DAPI staining of the same field excited by UV light. Each coverslip was imaged four to five times, with areas of clear and even staining chosen for imaging. The ZEISS ZEN Pro 3.3 software was able to superimpose images of the antibody stain with the DAPI stained nuclei of the same field. From these images, all visible nuclei were counted using the cell counter function on ImageJ (FIJI plugin) software. Of the nuclei counted, some were marked as being stained by the

secondary antibody used to stain for each cell type. From all imaged fields and coverslips for each condition, a total number of nuclei was obtained, and a total number of nuclei stained by each antibody. By dividing the total number of nuclei stained by each antibody with the total number of nuclei visible, a percentage was obtained for each antibody stain and its associated cell type.

Neuronal analysis

a) Assessment of neuronal proportion:

As elaborated above, the total number of DAPI stained nuclei was counted in each image. Of the visible, some were marked as TUJ1 positive. These numbers were totalled across several fields and coverslips for each condition. By dividing the total number of TUJ1 positive-stained cells by the total number of visible nuclei, the percentage of neuronal cells was obtained.

b) Neuronal morphological assessment: Assessment of neurite length

In addition to assessing the proportion of DAPI stained nuclei that were also Tuj1 positive, each clearly visible Tuj1 positively neuron was also measured from its soma to its longest process to assess neuronal process length. Neurites extended beyond the image boundary were excluded. This was done using ImageJ software (FIJI plugin), to draw and measure each process length (**figure 2.3**). The images' brightness and contrast values were increased to visualise punctate staining of any fine or delicate processes. Right-clicking on the drawn line would allow for 'measure' to be selected, where the software displays the scaled length of the line. The results were all collated and statistical analysis performed (detailed below).

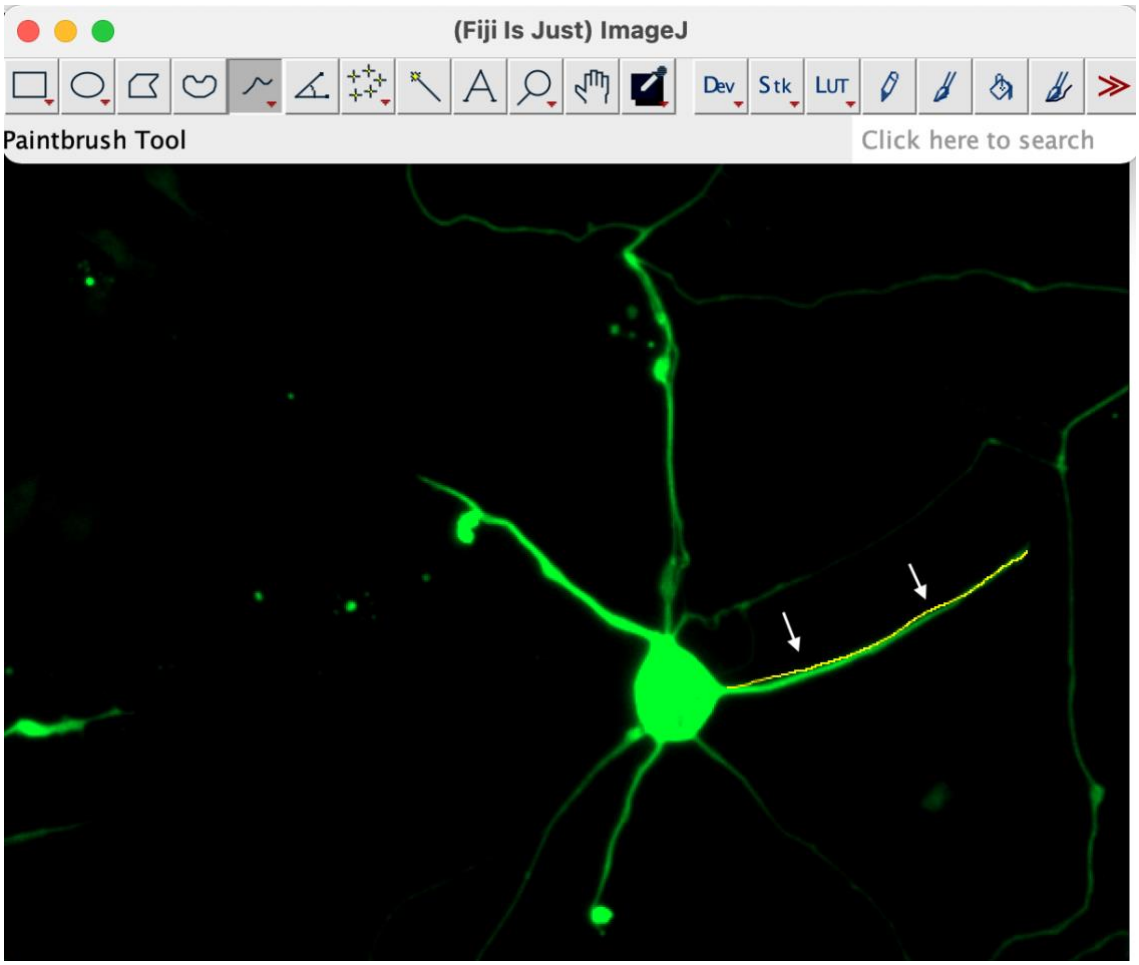

Figure 2.3: 'Freehand line' tool used to draw processes of each clearly visible neuron*, yellow 'drawn' line indicated by white arrows*

Astrocyte analysis

a) Assessment of astrocyte cell proportion:

As elaborated above, the total number of DAPI stained nuclei was counted in each image. Of the visible, some were marked as GFAP positive. These numbers were totalled across several fields and coverslips for each condition. By dividing the total number of GFAP positive-stained cells by the total number of visible nuclei, the percentage of astrocytes was obtained.

b) Astrocyte reactivity analysis:

Reactivity of astrocytes can be analysed by differences in the uptake of GFAP staining (the more reactive the population of astrocytes, the more GFAP staining, the brighter the emitted light by the sample), and by the hypertrophy of the cells, (as astrocytes become larger when more reactive). When imaging for astrocytes, care was taken to ensure image exposure (1000ms) and light intensity (30% of the maximum intensity of the microscope) was kept consistent across all images taken.

(i) Assessment of astrocyte area:

Patches of clearly visible individual astrocytes were chosen for analysis. The brightness and contrast of each image was increased to identify any areas of staining not immediately visible. The 'freehand selections' tool of ImageJ software (plugin FIJI) was chosen to draw around the periphery of astrocytes, and 'measure' selected to give a quantified area value of that selected portion (**figure 2.4**).

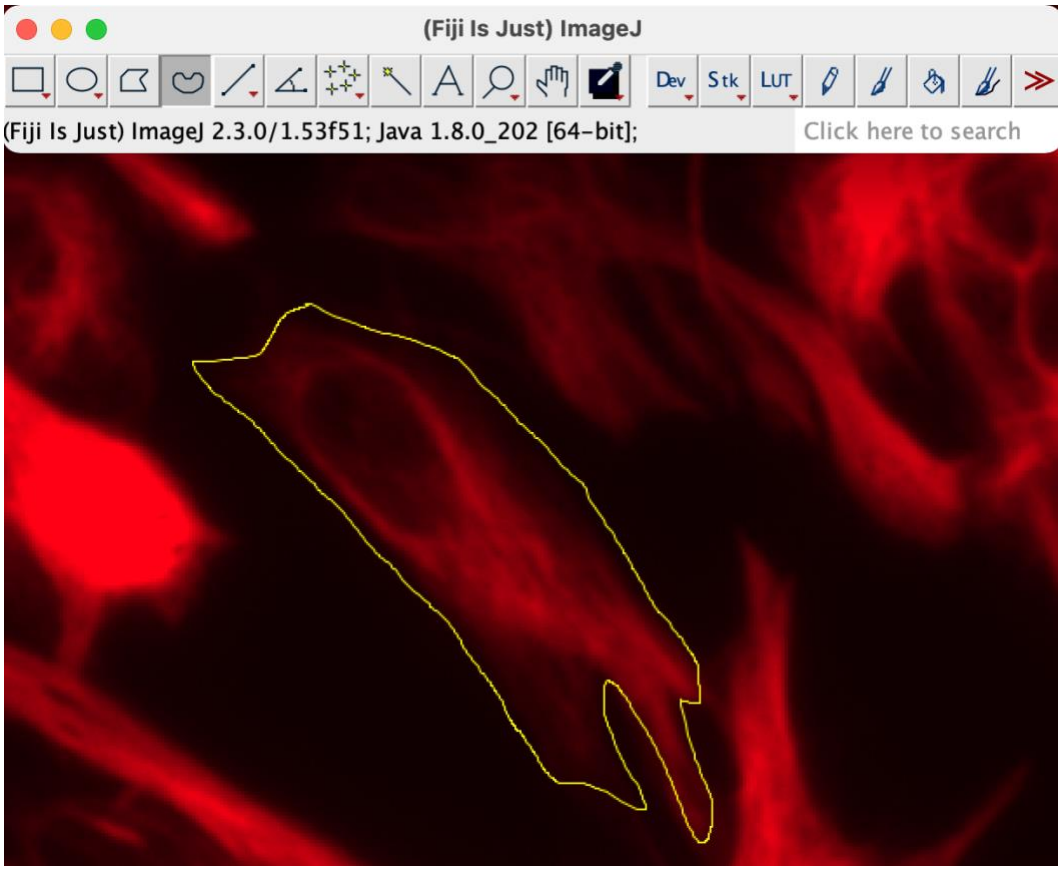

Figure 2.4: 'Freehand selection' tool used to draw around clearly visible astrocytes

(ii) Assessment of astrocyte optical density:

In addition to assessing the cell proportions and astrocytic area, the intensity of the stain was also quantified to identify differences in astrocyte reactivity, which would increase stain intensity as astrocytes became more reactive. Images of only Cy5 staining (without the DAPI nuclei image) was used. The median gray value of each image, not choosing individual cells, and without altering the brightness or contrast, was taken using the same ImageJ software (plugin FIJI). By selecting the image and right-clicking 'measure' on the image, a median gray value is then displayed. The median gray values of each image was then averaged across all images and coverslips from the same experimental repeat, giving an average median gray value for a control and storage condition for each experimental repeat. A maximum possible gray value was obtained by using the same feature on a pure white image of the same format, yielding a 'maximum intensity value' of 4095 (this number may vary according to the format of the image on ImageJ, where different RGB or gray value formulas are used). All median gray values were divided by this maximum value (which in this case was 4095) to obtain a ratio of intensity. The logarithm to the base 10 of the ratio of stain intensity was then obtained using the following equation to work out the optical density, with an increasingly lower number indicating an increased stain intensity and reactivity of the astrocytes:

$$OD = -log_{10}\left(\frac{Avg\ median\ gray\ value}{maximum\ intensity\ value}\right)$$

OD: optical density

Oligodendrocyte analysis

a) Assessment of oligodendrocyte cell proportion:

As elaborated above, the total number of DAPI stained nuclei was counted in each image. Of the visible, some were marked as MBP positive. These numbers were totalled across several fields and

coverslips for each condition. By dividing the total number of MBP positive-stained cells by the total number of visible nuclei, the percentage of oligodendrocytes was obtained.

b) Oligodendrocyte morphological analysis:

Oligodendrocytes exhibit clear signs of maturation during culture. This begins with processing, with immature oligodendrocytes exhibiting a bipolar morphology. As the cells mature, more processing in multiple directions occurs, increasing the area of the oligodendrocyte, with the cell starting to show a 'spider-web' morphology. As cells become more developed, increasing primary and secondary processes become finer and start to resemble 'fried-egg' morphology, with increasing amounts of fine processes resembling 'netting'. To assess this development, a quantitative measurement of area was done, and a qualitative measure of development was also done, comparing cells to known stages of oligodendrocyte development. A qualitative measure ensures that oligodendrocytes with similar areas but with different levels of maturation in their processing (for instance the presence of 'netting', which would not show an increase in area) are also differentiated between.

(i) Assessment of oligodendrocyte area:

In addition to assessing cell proportions, each MBP positively stained cell was also drawn around and the ImageJ software (plugin FIJI) used to quantify the cellular area (**figure 2.5**). Each image was increased to its maximum brightness and contrast to visualise punctate staining of delicate processing/branching. The 'freehand selections' tool was used to draw around the circumference of each oligodendrocyte, right-clicking and selecting 'measure' would then allow the software to generate an area value. The units of measurement were then scaled and results were collated and statistical analysis performed (detailed below).

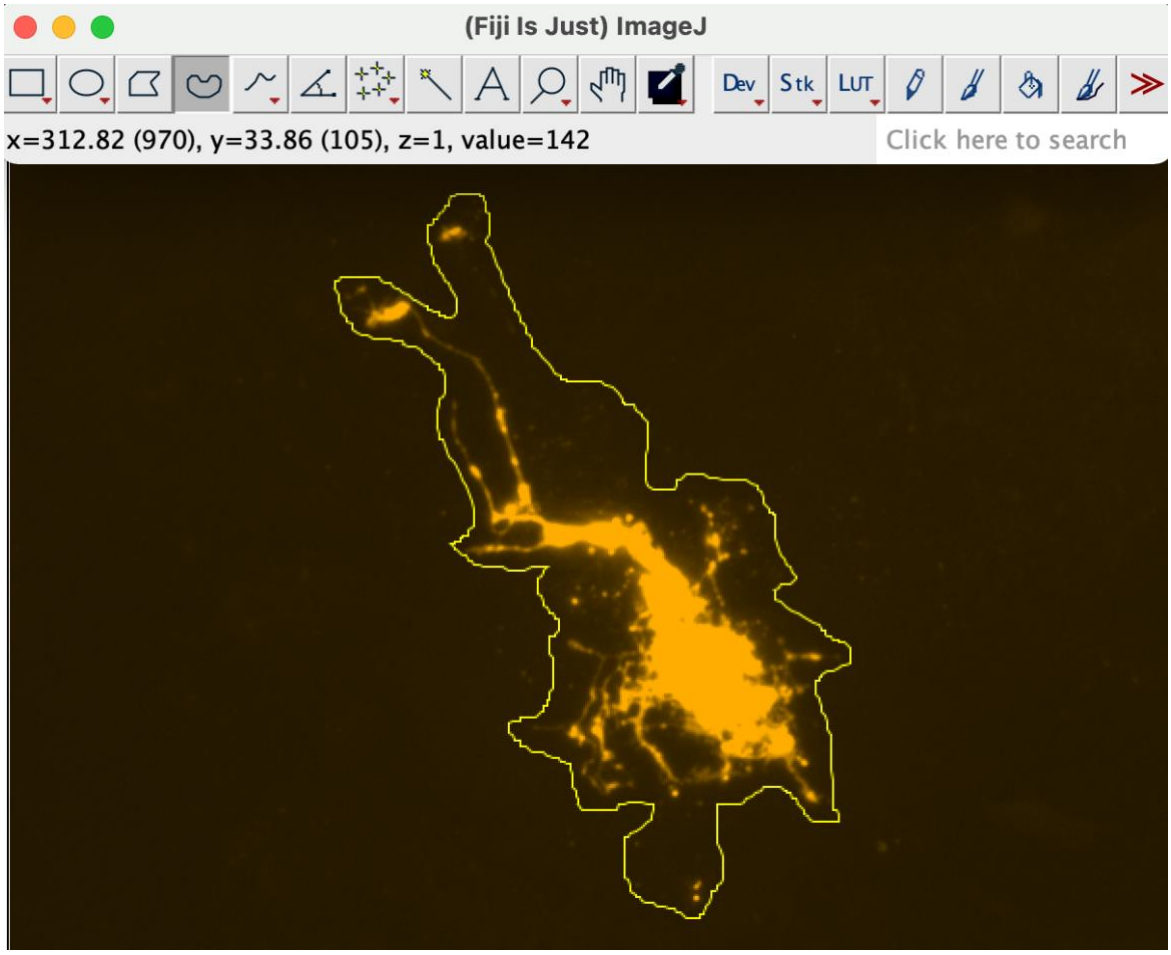

Figure 2.5: 'Freehand selections' tool used to draw around the perimeter of each oligodendrocyte

(ii) Assessment of stages of oligodendrocyte maturation

Figure 2.6 depicts the stages of oligodendrocyte maturation that all oligodendrocytes images were classified into. The number of oligodendrocytes in each stage was divided by the total number of oligodendrocytes that were analysed and a percentage was derived. An overall percentage for each stage, each condition and each experimental repeat was obtained, and statistical analyses were performed (see below) between control and storage conditions within each stage and experimental repeat.

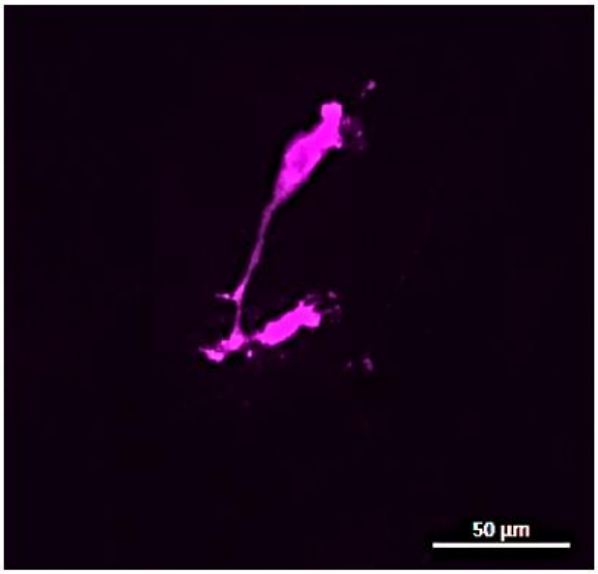

Immature

Small, minimal processing, bipolar cell, 1 or 2 long processes

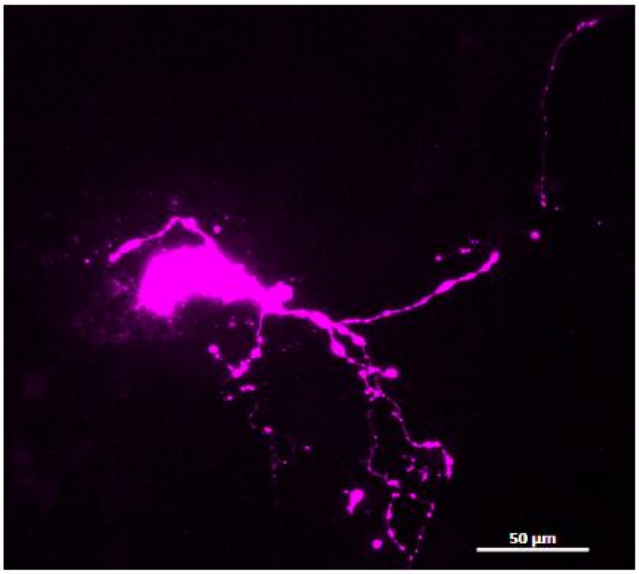

Intermediate-1

Bipolar cell with at least 1 long process outside of the longest axis of the cell

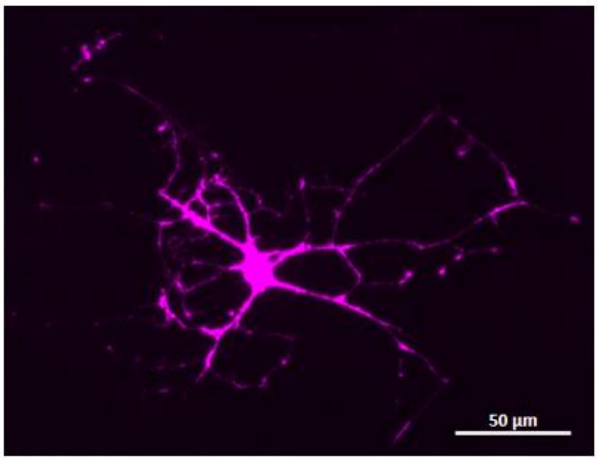

Intermediate-2

'Spider-web' morphology with multiple long processes (2/+) outside of the longest axis of the cell

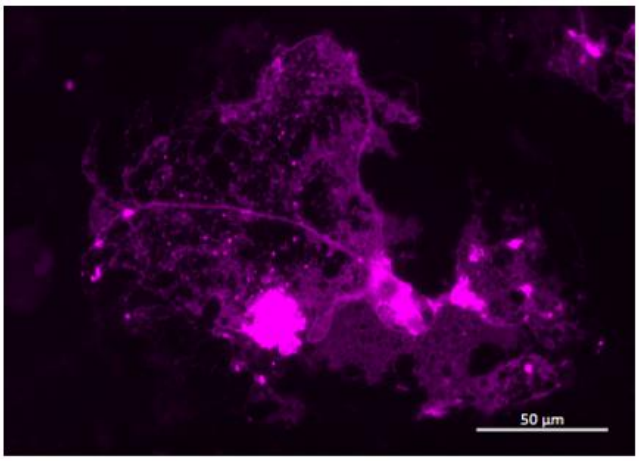

Mature

'Fried-egg' morphology
Round cell with presence of fine 'netting'

Figure 2.6. Shows the different stages of oligodendrocyte maturation evident in their cellular morphology

Microglial analysis

a) Assessment of microglial cell proportion

As elaborated above, the total number of DAPI stained nuclei was counted in each image. Of the visible, some were marked as Iba1 positive. These numbers were totalled across several fields and coverslips for each condition. By dividing the total number of Iba1 positive-stained cells by the total number of visible nuclei, the percentage of microglia was obtained.

b) Microglial reactivity analysis

Microglia, as immune cells of the brain, have the ability to respond and react to molecular signals in their surroundings, and part of that reactivity is displayed in their altered morphology, going from small ramified, processed cells (ramified microglia) that survey their environment, to large, reactive, circular cells (amoeboid microglia) focusing on phagocytosis and release of cytokines as part of the inflammatory response.

(i) Microglial area, circle value and roundedness:

A few ways to measure this objectively is through increases in the cellular area, the higher circle value, and the higher roundedness. A circle value is a ratio of a shape's area to its perimeter, which decreases as a cell becomes more processed without increasing its area. The roundedness index is a ratio between the area of the shape and the area of a perfect circle of the same diameter, showing how much of that perfect circle is 'filled up' by the shape. Both values increase as the cells become more circular or round, indicating their increasing reactivity.

Derivation of circle value:

$$CV = \frac{4\pi \mathrm{A}}{P^2}$$

CV: circle value; A: area; P: perimeter

Derivation of roundedness index:

$$RI = \frac{4A}{\pi(Feret's\ diameter)^2}$$

RI: roundedness index; A: Area; Feret's diameter: longest diameter of the shape

The 'freehand selection' tool (**figure 2.7**) was used to draw around each clear and visible microglia from each image, right clicking on this allowed for 'measure' to be selected, where the software then displays the area and other shape descriptors including circle value and roundedness index.

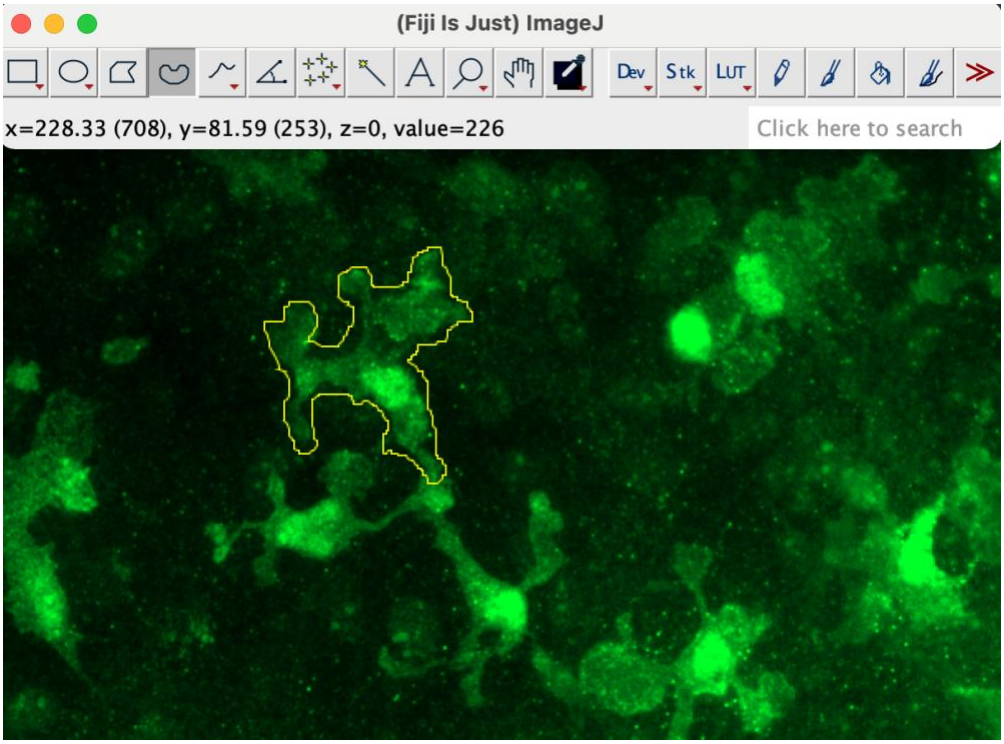

Figure 2.7: 'Freehand selection' tool used to draw around clearly visible microglia

(ii) Microglial ramified vs. amoeboid analysis:

In addition to shape descriptors of microglial cells, cells were also categorised into resting 'ramified' microglia and reactive 'amoeboid' microglia. All available microglia from each image used for analysis was classified into either category according to their shape. Ramified microglia include cells

that were processed, subjectively smaller, with the perimeter of the cell close to the nucleus. Amoeboid microglia were cells that were subjectively larger, circular and with limited processing. Examples of both cell type morphologies are shown in **figure 2.8**. The number of microglia exhibiting each morphology was divided by the total number of microglia analysed to give a proportion of ramified vs amoeboid for each condition and experimental repeat. This number was then collated and statistically evaluated (detailed below).

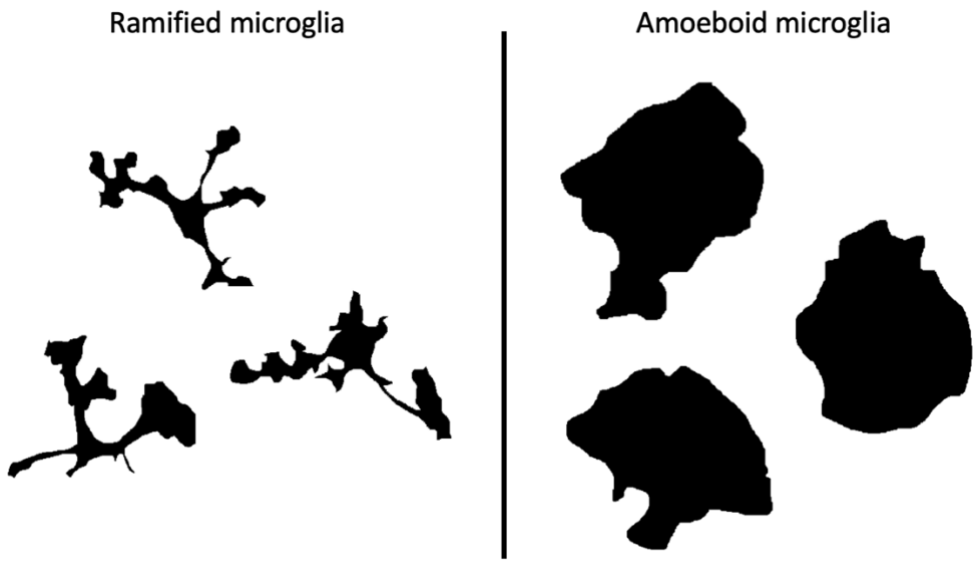

Figure 2.8: Examples of shapes of ramified and amoeboid microglia

Statistical analysis

When all images were taken and image analysis performed, an average of each quantitative parameter was calculated for each experimental repeat, one value for the control cells and one for the experimental cells. From this, one value from each experimental repeat was entered into GraphPad Prism (Version 9.3.1) software that generated graphs for each parameter measured. When all values were inputted, a 'Group Comparison' was performed. From here, an unpaired parametric t-test, assuming 'normal' Gaussian distribution, was selected (Welch's t-test), giving a P

value (an indication of statistical significance). If the P value was below 0.05 this was considered statistically significant.

Chapter 3: Evaluating the feasibility of storing primary mixed cultures in Hibernate™

3.1 Introduction

The primary mixed cortical glial culture system is well established and used widely for pharmacological, biochemical and molecular studies [64] [65]. It was originally developed by McCarthy and de Vellis for the bulk production of primary glial cells that could then be separated into individual astrocyte and oligodendrocyte populations [64]. These cultures are shown to have high purity, with little cross-cellular contamination. The protocol uses primary cortices that are dissociated and plated into large plastic flasks and cultured for seven to nine days. Throughout this period, there is a characteristic stratification of cells, where astrocytes form a confluent bed layer and oligodendrocytes, OPCs and microglia develop overlying this bed layer. This stratification enables selective detachment of microglia then oligodendrocytes, at specific time points, which can be collected, leaving behind the astrocytic bed layer [64]. During establishment, cultures modulate the proportions of different cell populations, with the majority of cells being astrocytes (82.6 ± 5.2%), followed by microglia (9.3 ± 3.6%) and OPCs/oligodendrocytes (6.7 ± 2.1%) [66]. Our laboratory recently adapted this protocol to create multicellular mini-cultures on glass coverslips in smaller 24 well plates, for potential high-throughput applications. Growth of the cells as a confluent monolayer allows for an easily induced injury into each coverslip with a needle or pipette tip [66]. Subsequent pathological responses can then be detected and assessed using routine image analysis techniques.

Without intervention, the cultures establish into primary, multicellular monolayer cultures which offer a significant advantage as CNS models in their ability to accurately simulate *in vivo* cellular behaviours. This model allows for specific modelling of astrocyte, OPC/oligodendrocyte and microglial cellular responses to injury. Cell-cell interactions are integral to the pathophysiology of pTBI and include both immunocompetent cell types, the astrocytes and microglia. These cells are responsible for the inflammation, astrocytosis and glial scarring which contribute to early and late mitigating factors for neuroregeneration that directly translate to clinical symptom severity. This

model has already been proven by the NTEK group to exhibit the pathophysiological cell responses to injury such as microglial invasion and hypertrophic, palisading astrocytes, with GFAP upregulation and a 'brush border' forming at the injury edge [66]. It has already proven its use as a pTBI model for experimental biomaterial implantation, with our laboratory successfully implanting DuraGen Plus™, a bovine collagen scaffold material originally formulated as a dural graft material, into the lesion [66]. Part of the success of biomaterial implantation depends on the microglial and astrocytic response to the material, as they can remodel and degrade the material through cell fibrillary contractions, allowing neuronal outgrowth into the material [67]. The microglia and astrocytes in the model have been shown to behave in the expected way, infiltrating into implanted DuraGen Plus™ [66]. Further studies into the biodegradability and toxicity of biomaterials would also be feasible with this model, as cell behaviours are directly observable.

The model also has also key logistical advantages. As described earlier, the cortices of postnatal animals can be easily surgically dissected and removed, dissociated and plated onto glass coverslips. Maintenance of the culture is also facile, requiring only a medium change every few days. The ability to produce injury and implant a biomaterial is also a simple process, as proved by the NTEK research group [66], and with the high throughput nature of the model, it would be feasible to quickly screen multiple biomaterial types, to optimise various qualities including (but not limited to) stiffness, biodegradability and porosity to reduce pathological cellular responses to injury. Additionally, it is feasible to introduce multiple injury types, instead of the scratch needle injury established by our group, with a view to simulating other types of TBI. The technically facile, high throughput but complex, pathomimetic nature of the model makes its applicability in pTBI research widespread. Another advantage is its alignment with the principles of ethical animal use in research through reduction and refinement, limiting the number of animals used while limiting pain and suffering, as few animals are required to obtain many experiments.

However, a core limitation to the mixed glial model is the absence of viable neurons. Trying to address this limitation of the model, the NTEK group modified the glial model protocol and recently established a new primary mixed cortical neuronal culture model (PhD thesis J Wiseman, submitted June 2022, unpublished data). This modification of the primary mixed cortical glial culture allows for the growth of neurons in addition to glial cells. The model has been characterised in previous studies by our laboratory, with cell proportions varying depending on the type of dissociation protocol that was used (enzymatic vs mechanical). Neurons were present in substantial numbers (enzymatic: 45.8 ± 2.1% vs mechanical: 21.9 ± 1.8%), followed by astrocytes (enzymatic: 35.3 ± 0.2% vs mechanical: 62.7 ± 2.6%), OPCs (enzymatic: 11.2 ± 0.3% mechanical: 13.0 ± 1.8%), microglia (enzymatic: 10.4 ± 3.9% mechanical: 11.3 ± 0.5%) and oligodendrocytes (enzymatic: 2.7 ± 0.2% mechanical: 4.0 ± 0.3%) (PhD thesis J Wiseman, submitted June 2022, unpublished data). For the intended purposes of using this model as a potential model of pTBI, further validation would be required, to check cell viability and ensure the presence of all cell types in expected numbers and morphologies.

As a model of pTBI, the additional neuronal population makes a significant improvement on the mixed glial model's ability to simulate complex neural cell responses to injury and therapy. While a mixed glial model is beneficial for obtaining specific cell types to study specific glial responses to injury, the additional neuronal population allows for more pathomimetic cell-cell interactions. Neuronal behaviour, as influenced by surrounding glial cells and vice versa can also be modelled. While this is an obvious advantage over purely glial cultures, it is also an advantage over purely neuronal cultures. Neuroregenerative studies using only purely neuronal (or neural stem cell) cultures are ultimately limited as models of pTBI due to the lack of immunocompetent, glial cell populations.

The protocol which determines the additional growth of neurons is a simple switch in chemical supporting cell medium. No additional steps are required in the protocol (over the mixed glial model) meaning there are no additional logistical barriers to the growth of neurons compared to the

glial model, whilst offering the same logistical advantages in facile set up and maintenance. The ease with which injury is induced is also as simple and quick, with no changes to the protocol used previously for the primary glial model. The high throughput nature of the model with the additional neuronal component means assessing accurate *in vivo* neuronal behaviour for neuronal regeneration studies is much more accessible. All the logistical advantages of the primary mixed cortical glial model with the added advantages of the neuronal component make this model more simulative and pathomimetic (**Figure 3.1**). It would also be equally feasible to introduce pharmacological agents or nanoparticles into an injury made in this model, or even into a biomaterial which can be implanted into an injury, combining multiple complex therapies with a view to not only passively promote cellular infiltration by introducing a cellular scaffold into the injury site, but to directly impact the associated inflammatory process. Screening of biomaterials, nanotherapeutics and pharmaceutical agents designed to alter neuronal behaviour which would previously use purely neuronal cultures, are now just as facile as with this multicellular glial model, ***making the neuronal model ultimately a more attractive option with no increase in costs, logistical difficulties or any increase in expertise requirements.***

For these reasons, both cell culture models were chosen as test models to establish if their transportation was feasible. As elaborated earlier (Chapter 1: 1.5.1: Types of storage media) Hibernate™ is a neural tissue storage medium originally formulated for the hypothermic storage of intact neural tissue. Since its formulation, it has been proven with a range of neural tissues and suspensions, however its use as a RT storage medium for an intact, established 2D *in vitro* culture for the purposes of transportation have not yet been trialled.

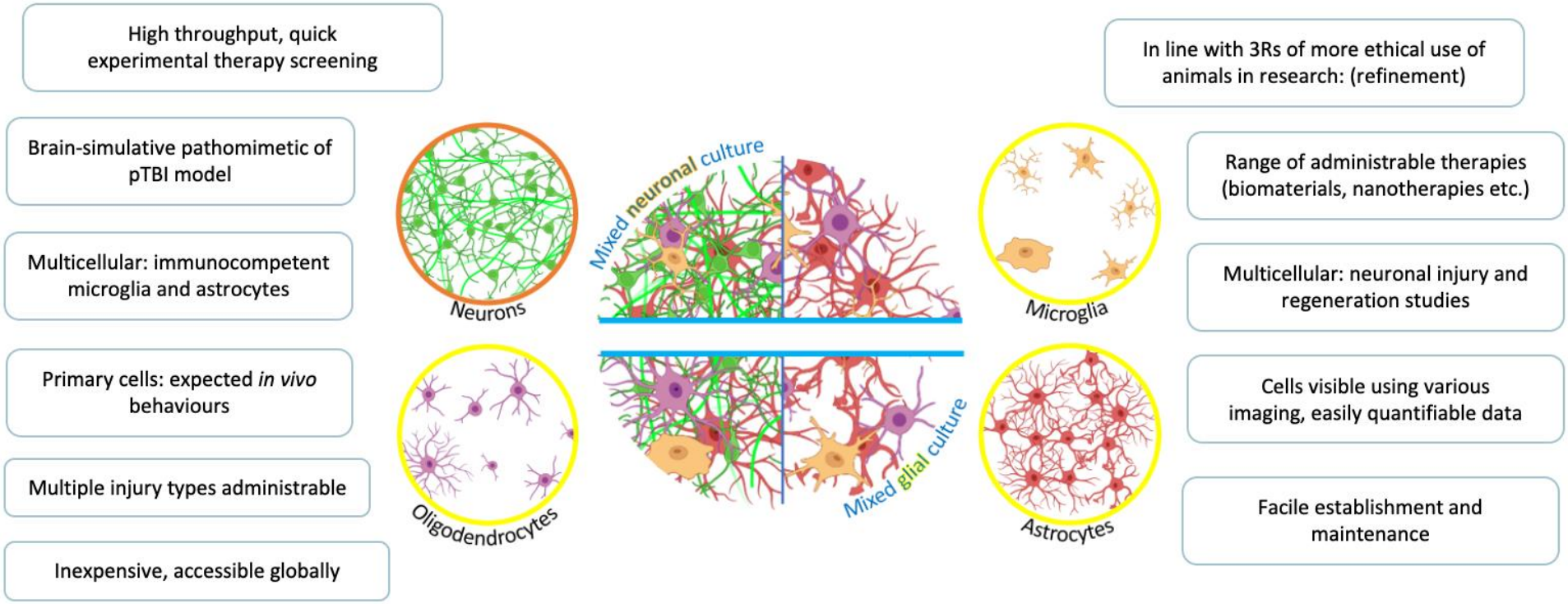

Figure 3.1: Features of primary mixed cortical neuronal cultures. *Model shows scratch-needle model of pTBI with all major primary cell types included (green cells=neurons present in mixed neuronal cultures, purple cells=oligodendrocytes present in both neuronal and glial cultures, yellow cells=microglia present in neuronal and glial cultures, red cells=astrocytes present in neuronal and glial cultures)*

3.2 Hypotheses

1) Storage of primary mixed (neuronal and glial) cortical cultures in Hibernate™ for 4 hours at RT will not affect culture confluency and adherence.

2) Storage of primary mixed cortical (neuronal and glial) cultures in Hibernate™ for 4 hours at RT will not alter cell viability (as measured by calcein-AM and ethidium homodimer-1 staining).

3) Storage of primary mixed cortical (neuronal and glial) cultures in Hibernate™ for 4 hours at RT will not alter astrocyte viability or reactivity (as measured by astrocyte cell proportion, astrocyte area and optical density).

4) Storage of primary mixed cortical (neuronal and glial) cultures in Hibernate™ for 4 hours at RT will not alter oligodendrocyte viability or maturation, (as measured by oligodendrocyte cell proportion, area and stages of maturation).

5) Storage of primary mixed cortical (neuronal and glial) cultures in Hibernate™ for 4 hours at RT will not alter microglial viability or reactivity, (as measured by microglial cell proportion, microglial area, circle value, roundedness and ramified vs. amoeboid proportions).

6) Finally, storage of primary mixed cortical (neuronal) cultures in Hibernate™ for 4 hours at RT will not alter neuronal viability or maturation, (as measured by neuronal cell proportion and neurite length).

3.3A: Evaluating the feasibility of storing primary mixed glial cultures in Hibernate™

3.3A.1 Normal establishment of primary mixed glial cultures

Primary mixed glial cultures showed defined changes in their maturation status and progressive appearance and development of individual glial cell types which is shown in **figure 3.2**.

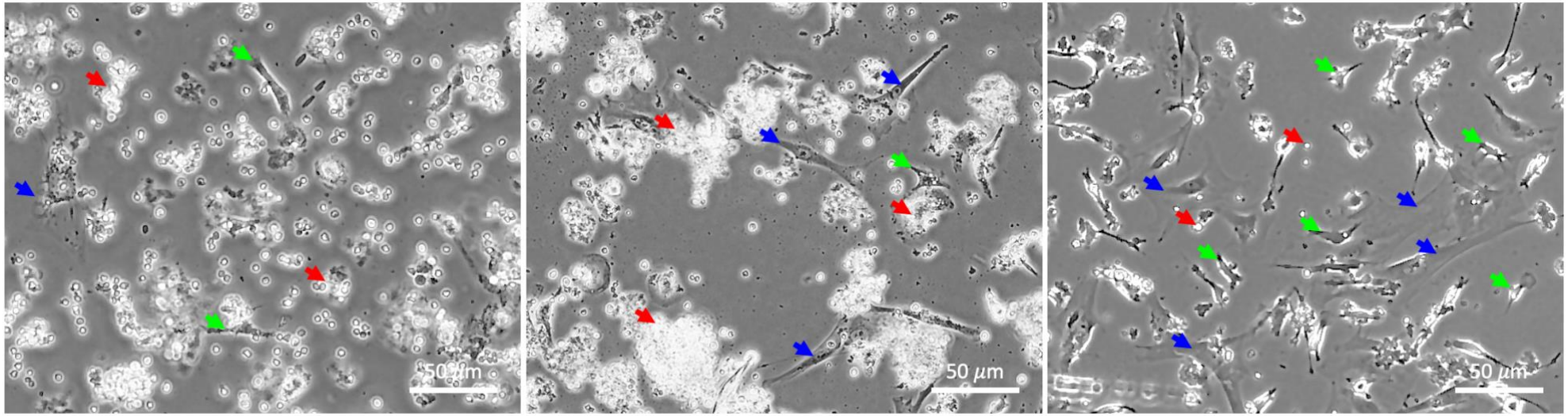

Day 1

Presence of many small bright round dots that are dead cell nuclei, some grouped in clusters (red arrows)

Some small cells with short, thick processes, likely microglia, attached (green arrows)
Evidence of larger, 'thin' cells also attached, likely astrocytes (blue arrows)

Day 3

Still many large clusters of small bright round dots that are dead cell nuclei (red arrows)

Increased number of large cells with long thick processes, astrocytes (blue arrows)

Smaller cells with short, thick processes, sometimes small white circles inside them, (vesicles) are microglia (green arrows)

Day 5

Increased number of large cells with long thick processes, astrocytes (blue arrows), trying to establish into a confluent layer

Many small cells with short, thick processes, varying morphologies, likely microglia (green arrows)

Still few small bright round dots, dead cells, present (green

Figure 3.2 Features of normal establishment of a primary mixed cortical glial culture

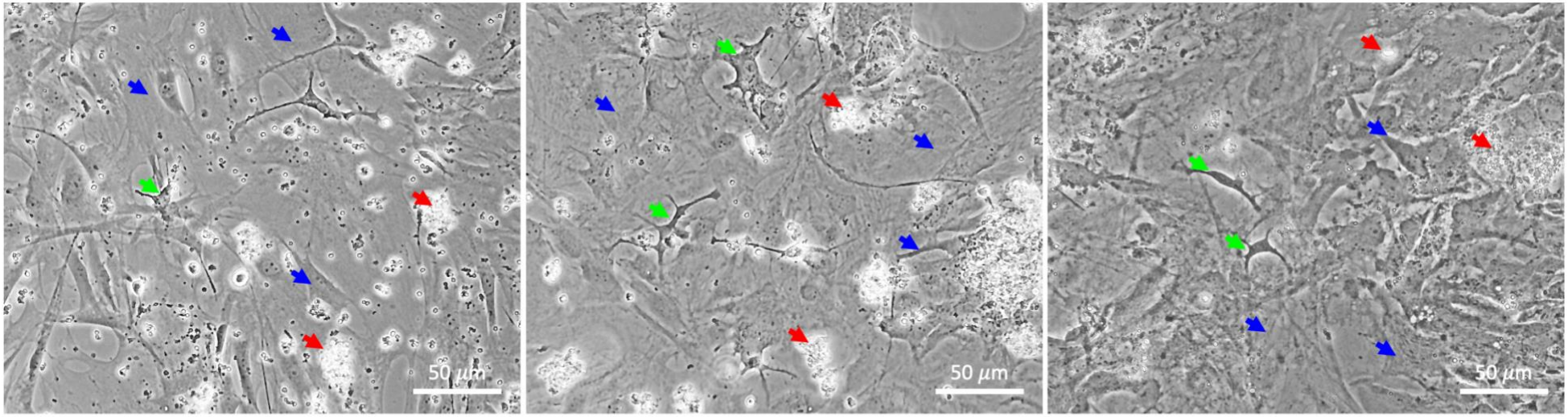

Day 8

Large, 'thin' astrocytes mostly confluent (blue arrow)

Smaller cells with multiple short, thick processes overlying confluent astrocyte layer (green arrow)

Smaller clusters of dead cells and debris still present (red arrow)

Day 10

Confluent astrocyte layer becoming 'thicker' (darker), as increased cells proliferating

Smaller cells with multiple short, thick processes overlying confluent astrocyte layer (green arrow)

Smaller clusters of dead cells and debris still present (red arrow)

Day 13

Confluent astrocyte layer even darker as cells proliferate and astrocyte layer becomes thicker

Smaller cells with multiple short, thick processes overlying confluent astrocyte layer (green arrow)

Minimal clusters of dead cells and debris present (red arrow)

Figure 3.2 Features of normal establishment of a primary mixed cortical glial culture cont.

3.3A.2 Confluency and adherence of established primary mixed cortical glial cultures were similar between control and 4hr storage in Hibernate™ at RT conditions

After 24 hours recovery post 4 hr Hibernate™ storage, phase images were taken to identify any early and outwardly visible signs of cell stress as cell shrinking/detachment. As indicated in **figure 3.3**, astrocytes that had established an 'astrocyte pavement' remained in this state after storage, with no sign of disruption of astrocytes. There were clearly identifiable microglia, small, dark cell with short thick processes, that were still identifiable after storage. There are also small bright white dots, nuclear fragments from dead cells, that decrease throughout normal culture establishment (**figure 3.2**) that did not noticeably increase in number after storage compared to storage. This indicates that there was no disruption in culture confluency or adherence of cells after storage.

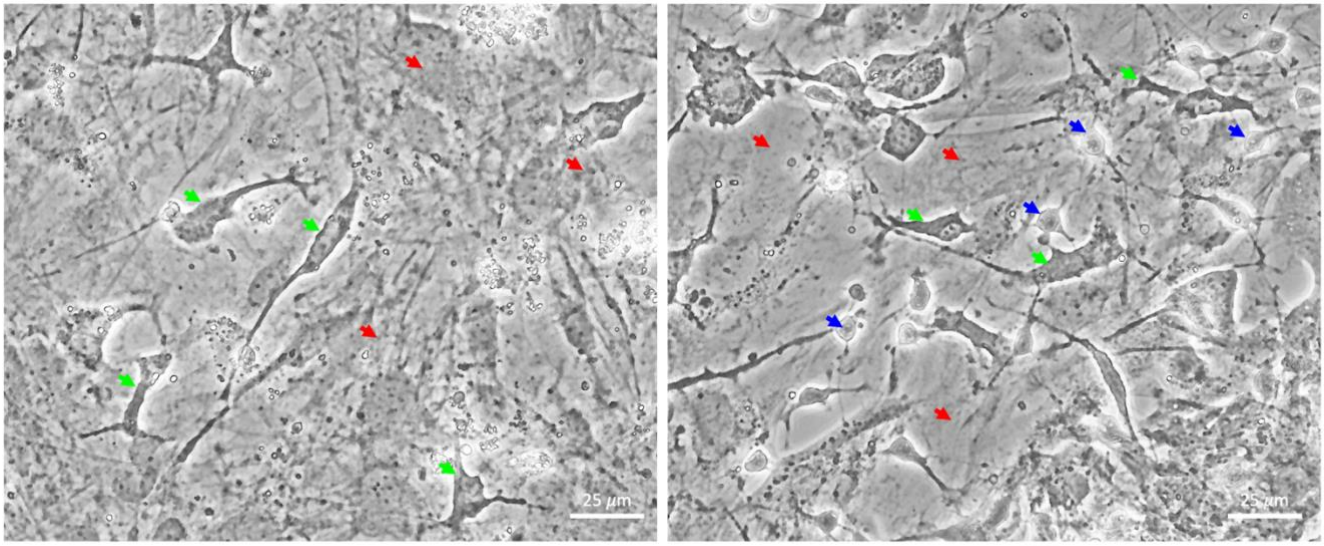

Figure 3.3 High magnification phase images showing a range of morphologies of different cell types in control and 4hr Hibernate™ storage conditions. *Red arrows point to patches of confluent astrocytes forming an 'astrocyte pavement'. Green arrows point to small, dark cells with short, thick processes, likely microglia, overlying the astrocyte pavement. Blue arrows show small, bright round*

cell bodies with short, fine processing, most exhibiting a bipolar morphology, likely OPCs which were also present in glial cultures.

3.3A.3 Primary mixed cortical glial cultures do not show changes in cell viability after storage in Hibernate™ medium for 4 hours at RT

The majority of cells stained with calcein-AM and ethidium homodimer-1 took up the green, calcein stain indicating a high cell viability. There were sparse nuclear fragments of dead cells that took up the ethidium homodimer-1 stain (**figure 3.4 and figure 3.5 (A)).** When quantifying the number of live cells as a percentage of the total number of DAPI stained nuclei, compared to dead cells, there was no significant change in cell viability (**figure 3.5 (B)**, n=4: control: 77.5 ± 6.4% vs. storage: 85.6 ± 5.1%, Welch's t-test **P=0.2588**), showing that Hibernate™ storage does not negatively impact cell viability.

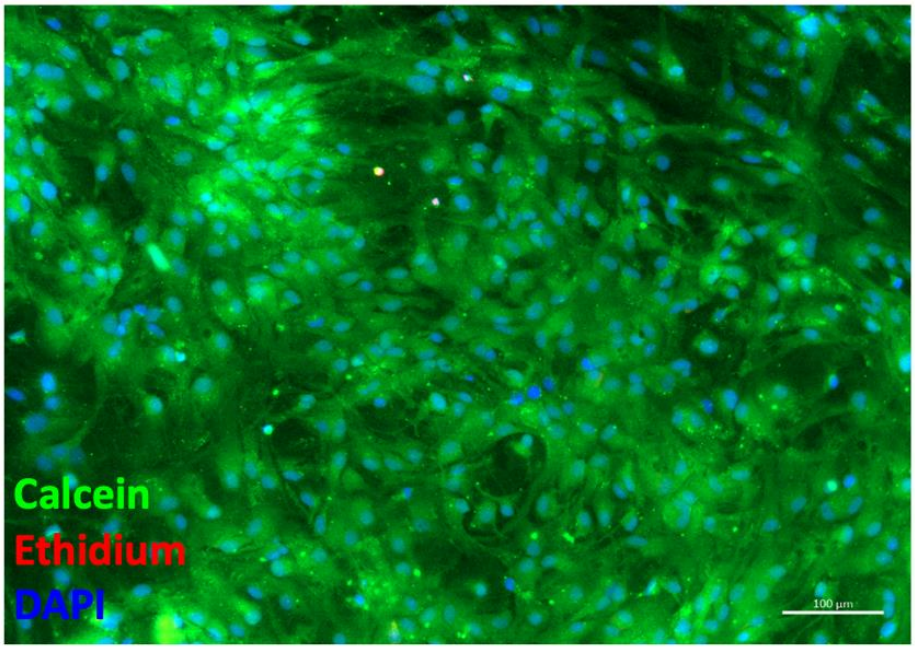

Control

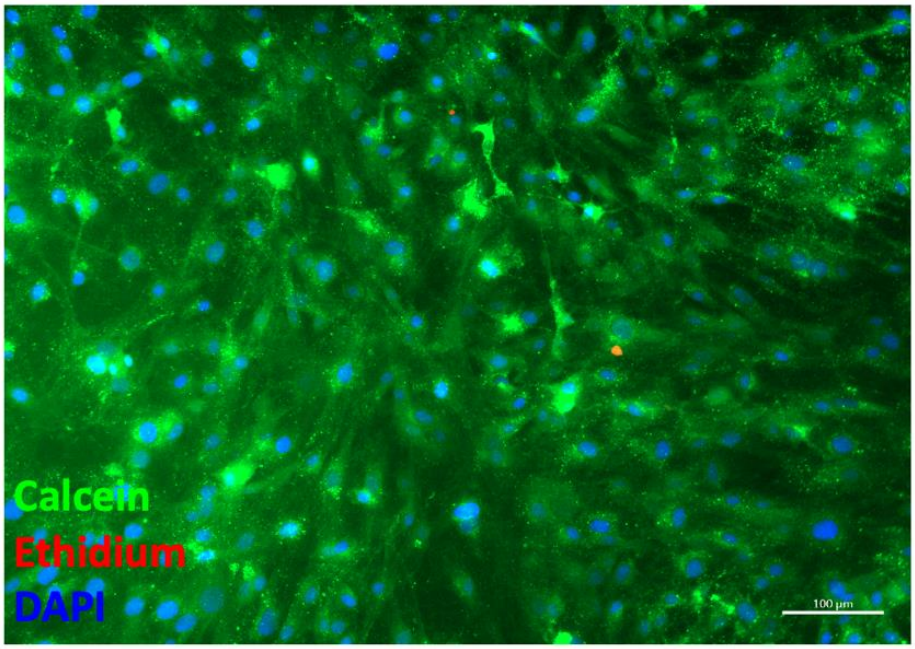

4hr Hibernate™ storage

Figure 3.4 Low magnification fluorescence images of calcein-AM, ethidium homodimer and DAPI staining showing high proportion of live cells. *The majority of cells were stained with calcein showing a high cell viability with few red 'dots', nuclear fragments of dead cells stained with ethidium, present in control (**top**) versus 4hr Hibernate™ storage cultures (**bottom**).*

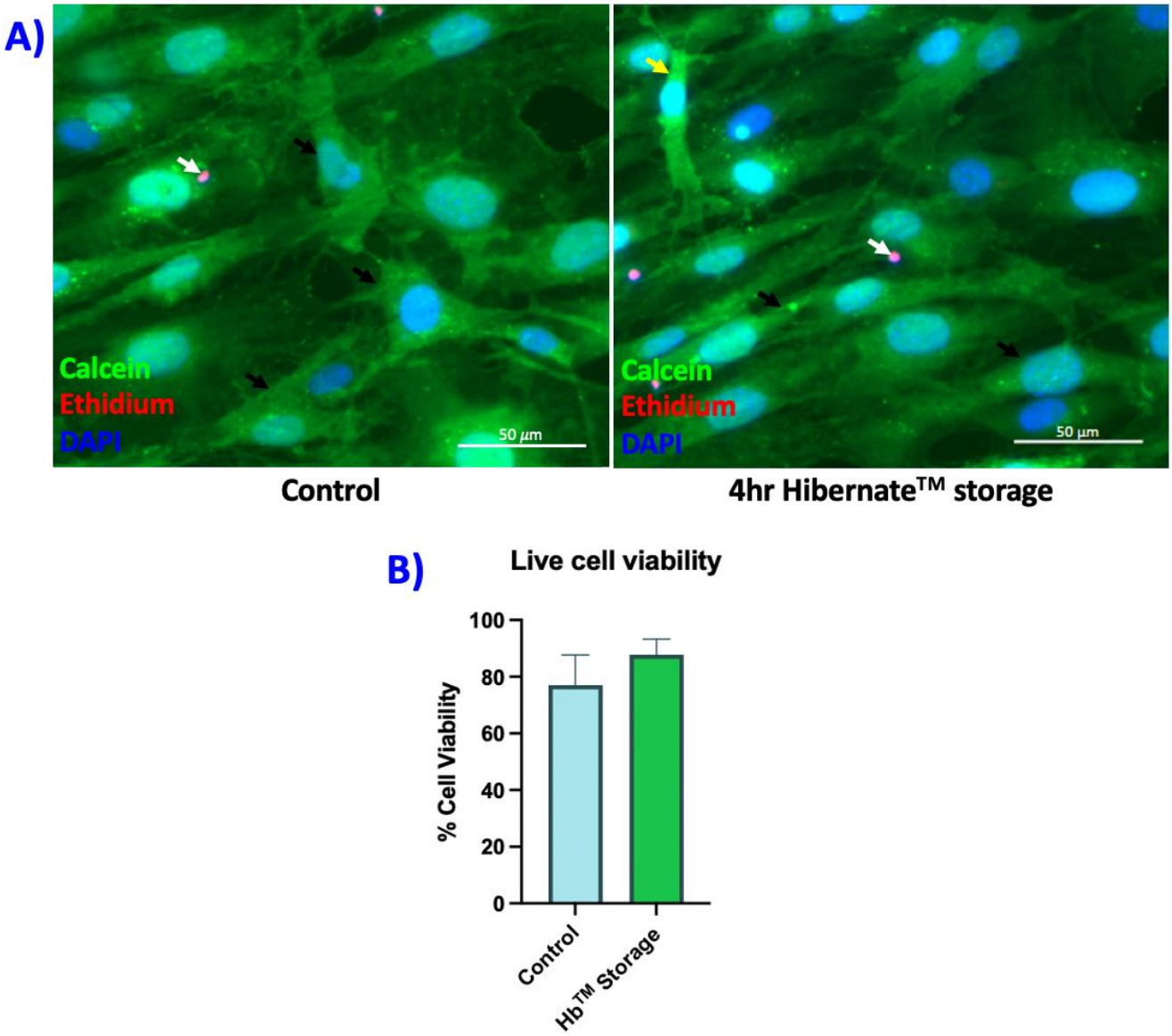

Figure 3.5 High magnification fluorescence images of calcein-AM, ethidium homodimer and DAPI staining showing live and dead proportion. *The majority of cells were stained with calcein, showing a high cell viability with few red 'dots' (**white arrows**) which were nuclear fragments of dead cells stained with ethidium, present in control (**A, left**) versus 4hr Hibernate™ storage cultures (**A, right**). Using high magnification imaging, morphologies of individual cells were clear, with astrocytes (**black arrows**) and microglia (**yellow arrow**) visible. The percentage cell viability is shown (**B**) (n=4, mean ± SEM)*

3.3A.4 All major neural types were identified in primary cortical glial cultures in control and 4hr Hibernate™ storage conditions

All three major glial cell types, astrocytes, oligodendrocytes and microglia (depicted later) were all identified by immunocytochemistry staining after storage (**figure 3.6**). The normal bed layer of astrocytes showed no signs of disruption post storage, with a similar high confluency of astrocytes in all areas of coverslips present in stored cultures and the majority of cells being astrocytes when analysed (**figure 3.6**). Oligodendrocytes were comparatively rarer but identifiable in sparse and high-density patches, showing various morphologies from small, bipolar cells with short processes, to larger, multipolar cells with long thick and fine processing. Microglia were also stained clearly and evenly and identified in stored cultures in similar numbers to control cultures (microglia staining to be shown below).

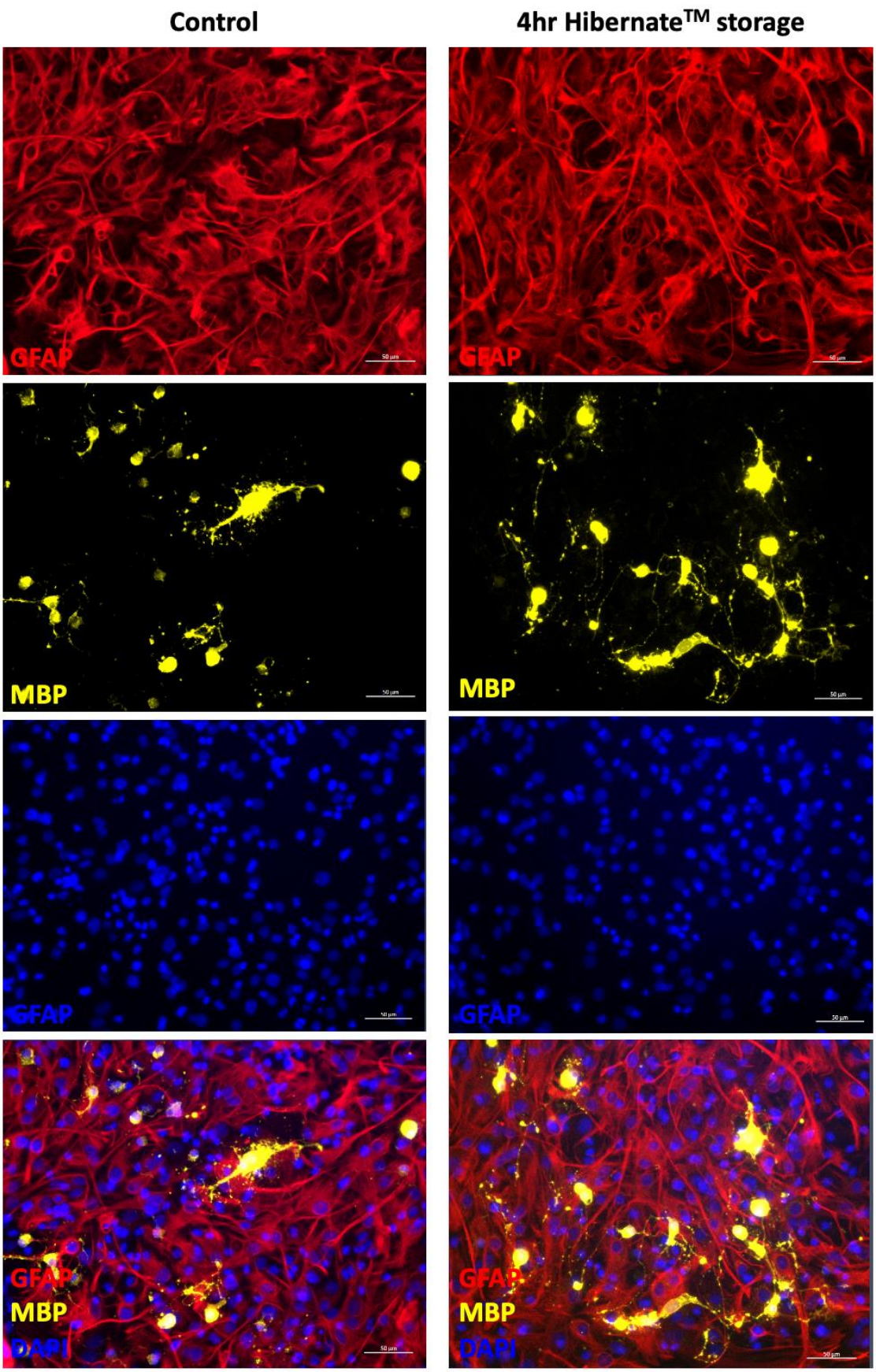

Figure 3.6 Low magnification fluorescence images of astrocytes, oligodendrocytes and nuclei staining showing cell proportions. *There was a high proportion of astrocytes (GFAP) in a confluent*

*layer, with patches of oligodendrocytes (MBP) showing various morphologies (images of microglia are shown further below). There were no obvious differences in the number of astrocytes and oligodendrocytes in both control (**left panel**) and 4hr Hibernate™ storage cultures (**right panel**).*

3.3A.6 Hibernate™ storage of established primary mixed cortical glial cultures does not adversely alter astrocyte cell proportion or reactivity

Analysing astrocyte cell proportions and morphology for measures of cell reactivity did not yield any significant differences indicating Hibernate™ storage has any significant impact on astrocyte proportion or reactivity. Cell counts showed a marginal increase in astrocyte cell proportion (**figure 3.7 (B)**, n=4: control: 77.0 ± 11.0% vs. storage: 80.9 ± 9.8%, Welch's t-test **P=0.7557**), showing no evidence of increased astrocyte cell detachment or death compared to other cells. When assessing reactivity, there was no indication of cell hypertrophy, a sign of astrocyte reactivity as cells become larger. There was a marginal decrease in astrocyte cell area (**figure 3.8 (B)**, n=4: control: 1824 ± 96 μm^2 vs storage: 1610 ± 222 μm^2, Welch's t-test **P=0.1897**). GFAP upregulation in more reactive astrocytes increases the brightness of the stain, which causes a decrease in optical density. There was a small increase in optical density (**figure 3.8 (C)**, n=4: control: 1.473 ± 0.251 vs storage: 1.629 ± 0.156, Welch's t-test **P= 0.9651**) indicating non-significant decrease in reactivity. Both differences are statistically non-significant indicating there is no evidence that Hibernate™ increases astrocyte reactivity.

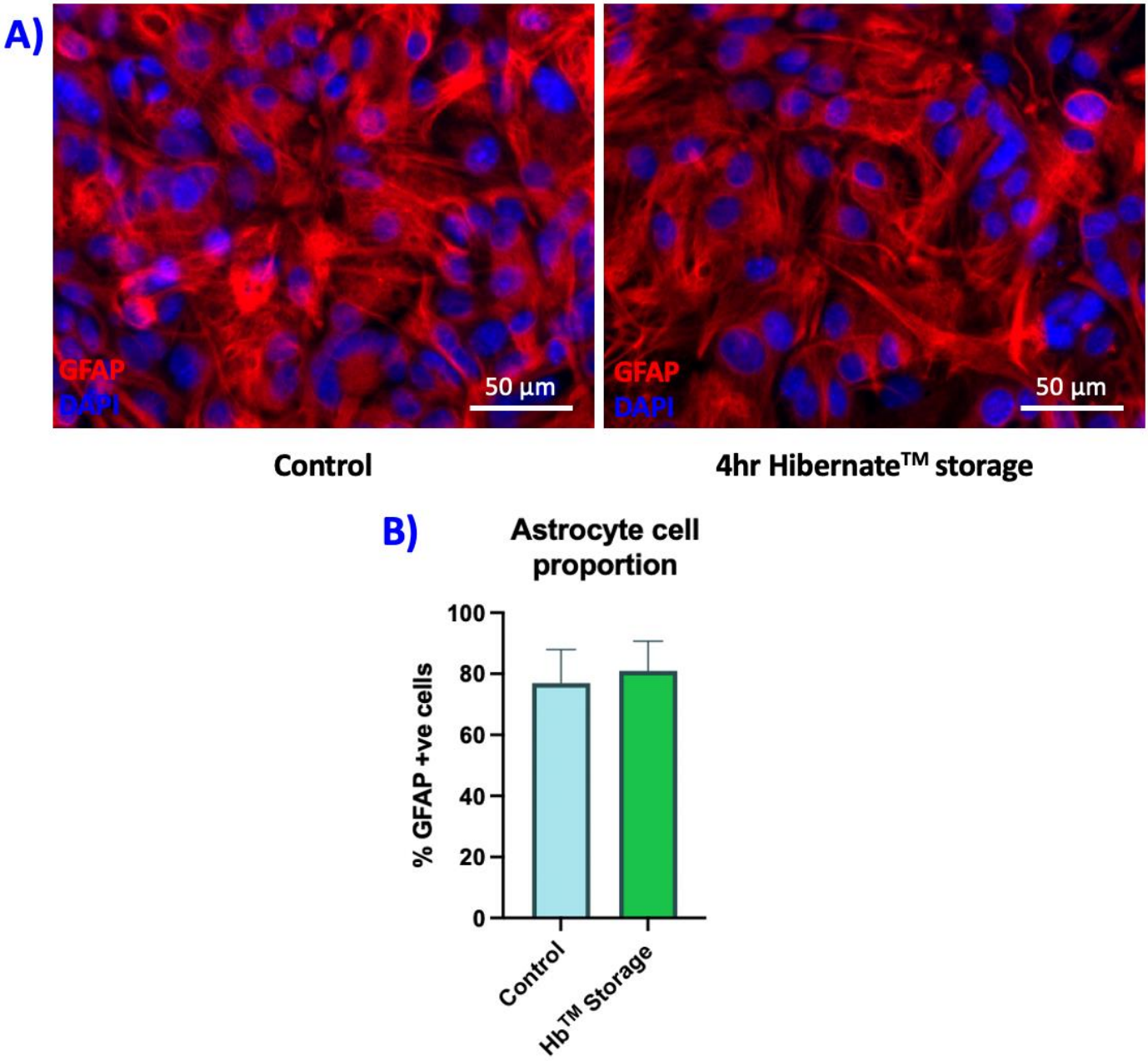

Figure 3.7 Low magnification fluorescence images of GFAP and DAPI staining showing astrocyte cell proportion. *There was a high proportion of astrocytes in a confluent layer with no immediately obvious differences visible in control (**A, left**) versus 4hr Hibernate™ storage cultures (**A, right**). The average percentage of astrocytes is shown (**B**) (n=4, mean ± SEM).*

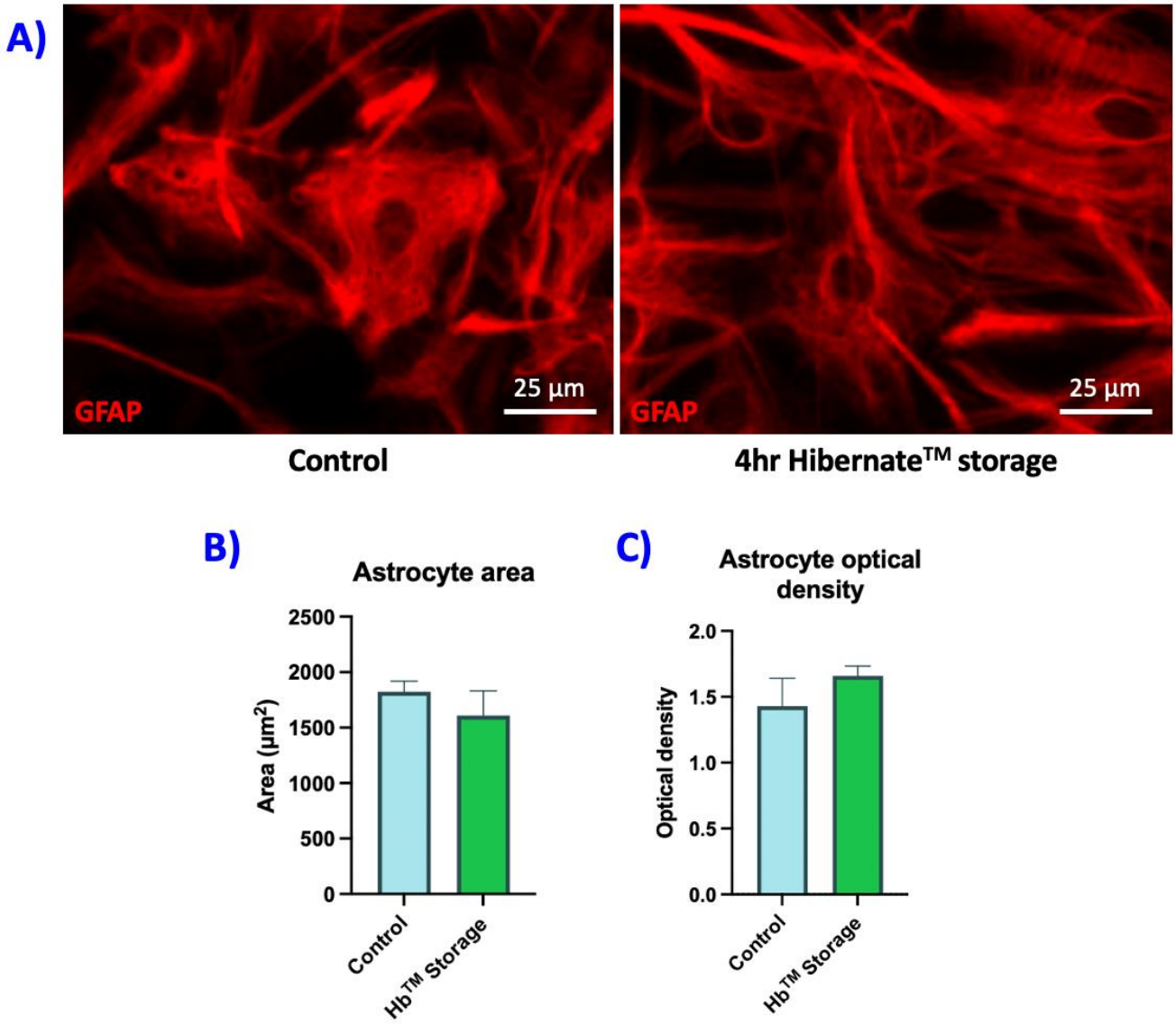

Figure 3.8 High magnification fluorescence images of GFAP staining showing astrocyte morphologies. *There was no immediately visible difference in astrocyte morphology, in their area or in 'brightness' of GFAP stain uptake, in control (**A, left**) versus 4hr Hibernate™ storage cultures (**A, right**). The average percentage of astrocyte area (**B**) and astrocyte optical density (**C**) are both shown (n=4, mean ± SEM respectively).*

3.3A.7 Hibernate™ storage of established primary mixed cortical glial cultures does not adversely alter oligodendrocyte cell proportion or maturation

Oligodendrocytes were not evenly distributed in culture, and some areas showed many oligodendrocytes in close proximity with other areas showing few individual cells in low density patches. This pattern was present in control and Hibernate™ storage cultures indicating this was not an effect of storage but likely the natural growth pattern of oligodendrocytes in the glial cultures. When cell proportions were analysed (total number of MBP positively stained cells as a percentage of total DAPI stained nuclei), images of clear and even MBP staining of both low density and high-density areas were taken, (method of imaging discussed previously in chapter 2). There was a non-significant increase in oligodendrocyte cell proportion in 4hr Hibernate™ storage cultures (**figure 3.9 (B)**, n=4: control: 1.23 ± 0.56% vs storage: 1.60 ± 1.14%, Welch's t-test **P=0.7702**), indicating storage does not cause oligodendrocyte detachment or death relative to other cell types. When assessing morphology, oligodendrocytes of varying morphologies were identified with some highly mature cells exhibiting large, complex 'spider-web' or 'fried-egg' morphologies (**figure 3.10 (A)**). This did not differ across control and storage conditions. Oligodendrocyte area, a marker for oligodendrocyte maturation was not significantly different between control and storage conditions. There was a marginal increase in cell area (**figure 3.10 (B)**, n=4: control: 4586 ± 649 μm^2 vs storage: 5655 ± 1677 μm^2, Welch's t-test **P=0.5633**). Classifying cells into their 'Stages of Maturation' (criteria for which are outlined previously in chapter 2: methods) did not show any significant changes in cell development, with a majority of oligodendrocytes being mature (**figure 3.11**). Non-significant increases and decreases within each stage across control and 4hr Hibernate™ storage cultures were statistically analysed as follows (**figure 3.11**; n=4, Welch's t-test for all: Immature: control 11.1 ± 8.1% vs storage 13.0 ± 9.4%, P**=0.9155**; Intermediate-1: control 13.1 ± 7.5% vs storage 12.4 ± 5.5%, **P=0.9608**; Intermediate-2: control 23.7 ± 11.3% vs storage 15.7 ± 6.5%, **P=0.2310**; Mature: 52.2 ± 9.2% vs storage 58.9 ± 20.7%, **P=0.8410**). In summary, this shows there is no clear evidence of 4hr Hibernate™ storage being a detriment to oligodendrocyte differentiation or maturation.

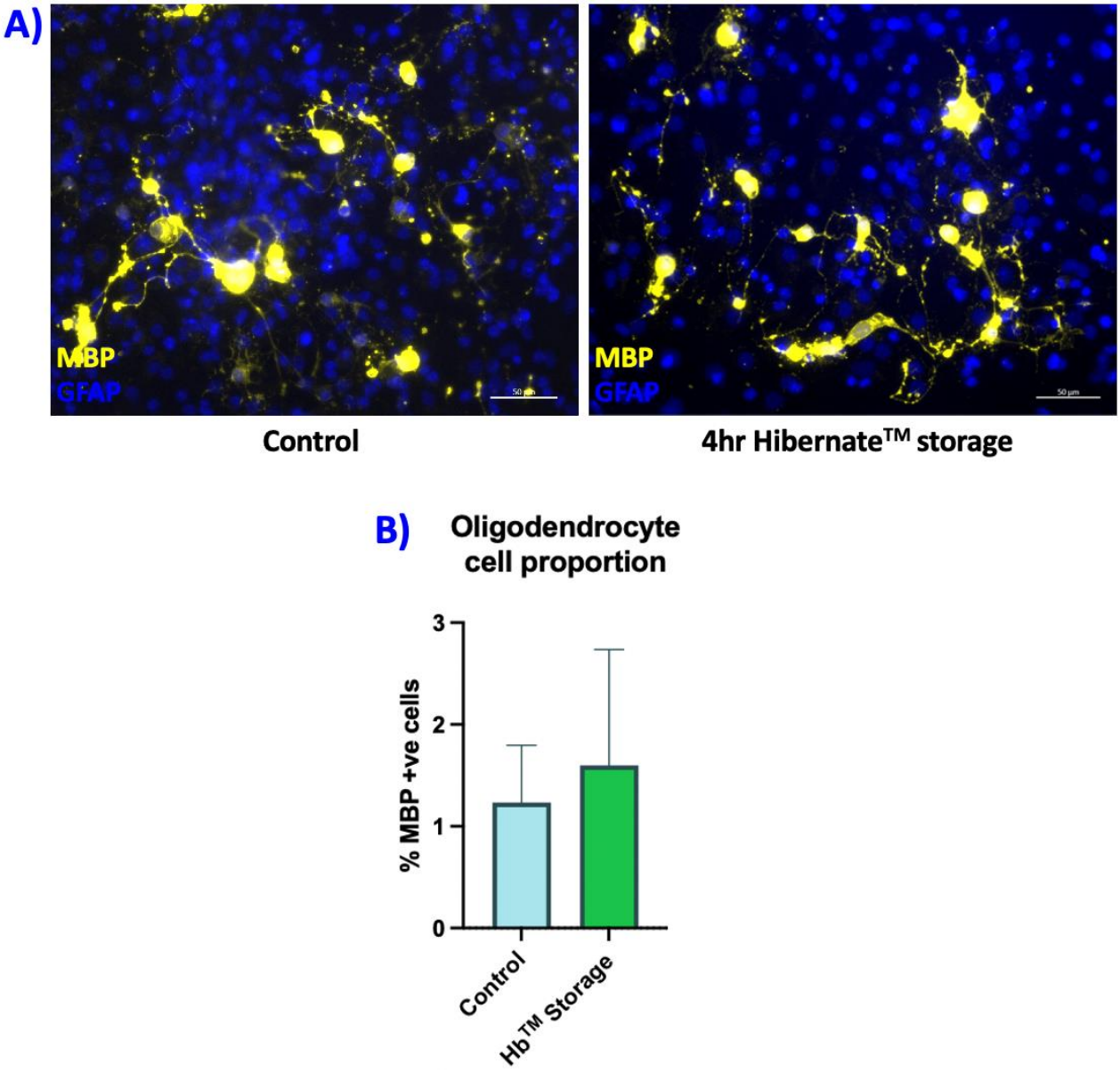

Figure 3.9 Low magnification microscopy images of MBP and DAPI staining showing oligodendrocyte cell proportion. *There are patches of high-density oligodendrocytes clearly and evenly stained with various morphologies and no obvious differences visible in control (**A, left**) versus 4hr Hibernate™ storage cultures (**A, right**). The average percentage of oligodendrocytes is shown (**B**) (n=4, mean ± SEM).*

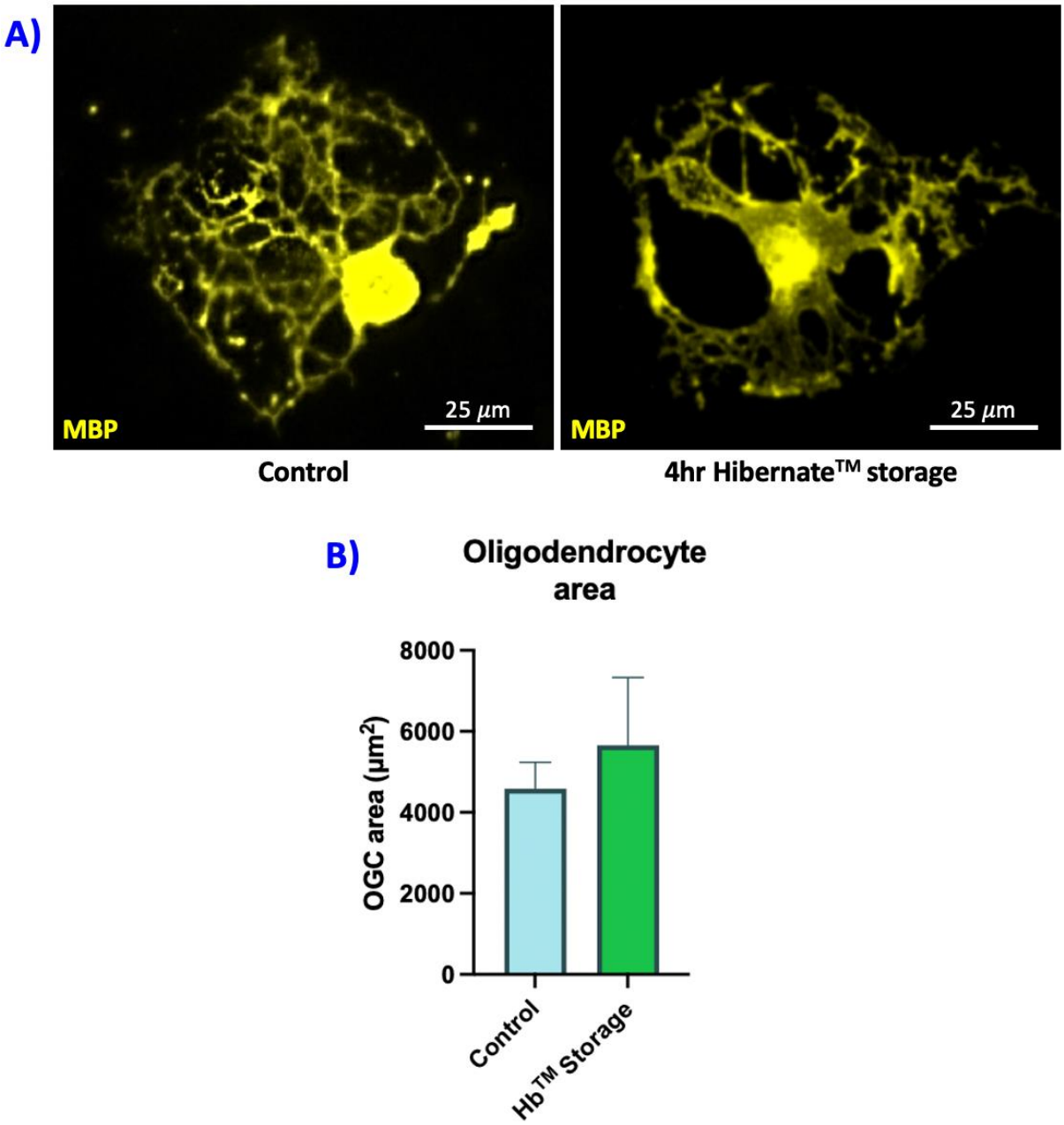

Figure 3.10 High magnification fluorescence images of MBP showing oligodendrocyte morphology. *Individually visible, clearly stained oligodendrocytes showed complex, multipolar 'spider-web' or 'fried-egg' morphologies with no obvious differences visible in control (**A, left**) versus 4hr Hibernate™ storage cultures (**A, right**). The average area of analysed oligodendrocytes is shown (**B**) (n=4, mean ± SEM).*

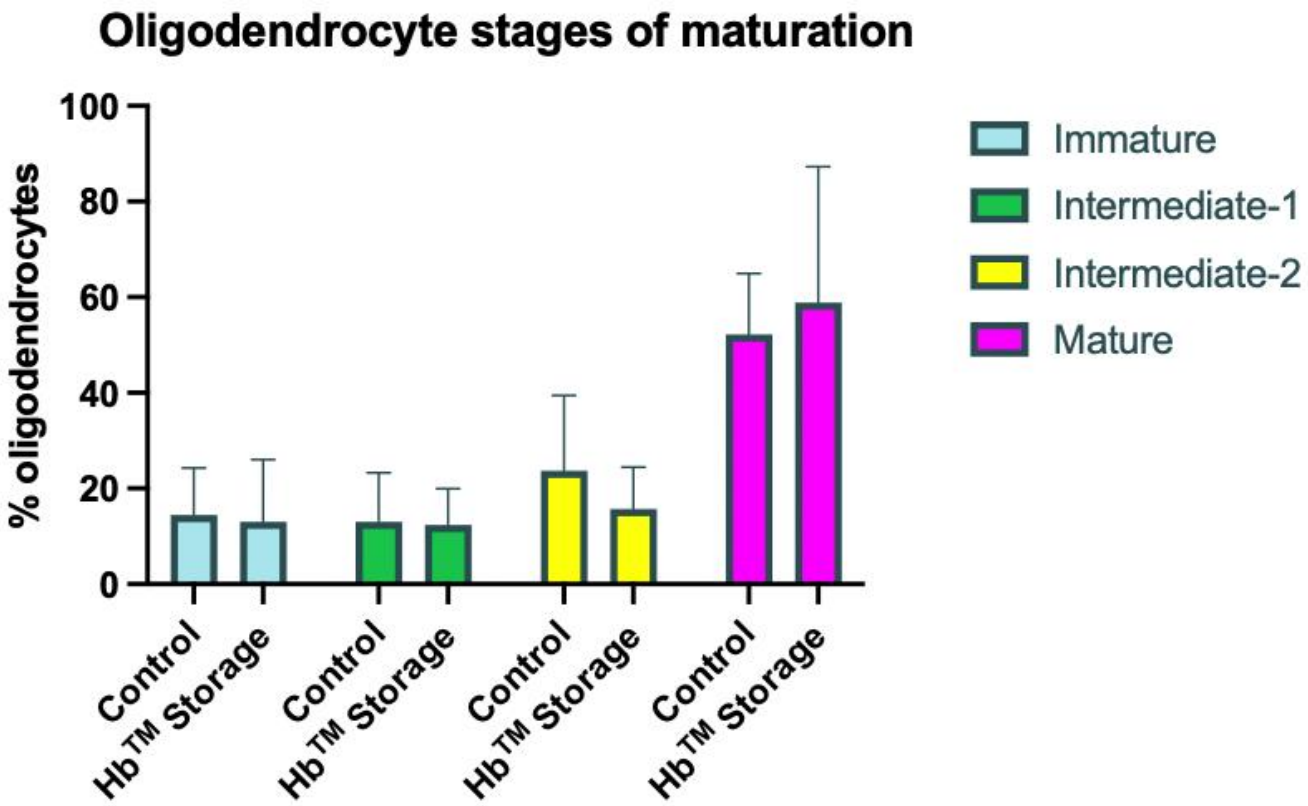

Figure 3.11 Oligodendrocyte morphology: Stages of Maturation *showing distribution of immature to mature oligodendrocytes in control and 24 hrs post 4 hr Hibernate™ storage (n=4, mean ± SEM).*

3.3A.8 Hibernate™ storage of established primary mixed cortical glial cultures does not adversely alter microglial cell proportion or reactivity

A substantial proportion of the cells in the glial cultures were microglia, with similar proportions identified in 4hr Hibernate™ storage cultures compared to controls (**figure 3.12**, n=2: control 28.2 ± 10.8 % vs storage 24.1 ± 8.1%, Welch's t-test **P=0.8491**). When assessing cell reactivity, several morphological parameters were used (**figure 3.13**) that were found to be overall similar in both control and 4hr Hibernate™ storage conditions: circle value (**figure 3.13 (E)**; n=2: control 0.185 ± 0.062 vs storage 0.171 ± 0.063, Welch's t-test **P=0.8853**); microglial roundedness index (**figure 3.13 (F)**; n=2: control 0.505 ± 0.043 vs storage 0.576 ± 0.037, Welch's t-test **P=0.3359**); microglial area (**figure 3.13 (G)**, n=2: control 1097 ± 62 μm^2 vs storage 1313 ± 94 μm^2, Welch's t-test **P=0.1939**) and percentage ramified microglia (**figure 3.13 (H)**, n=2: control 93.7 ± 0.6% vs storage 97.2 ± 1.4%, Welch's t-test **P=0.1462**). These small differences in morphological parameters, with some indicating small increases in reactivity and others indicating decreases in reactivity show an overall trend that storage has no effect on the overall reactivity of microglia, however more experimental repeats are required to conclude for certain.

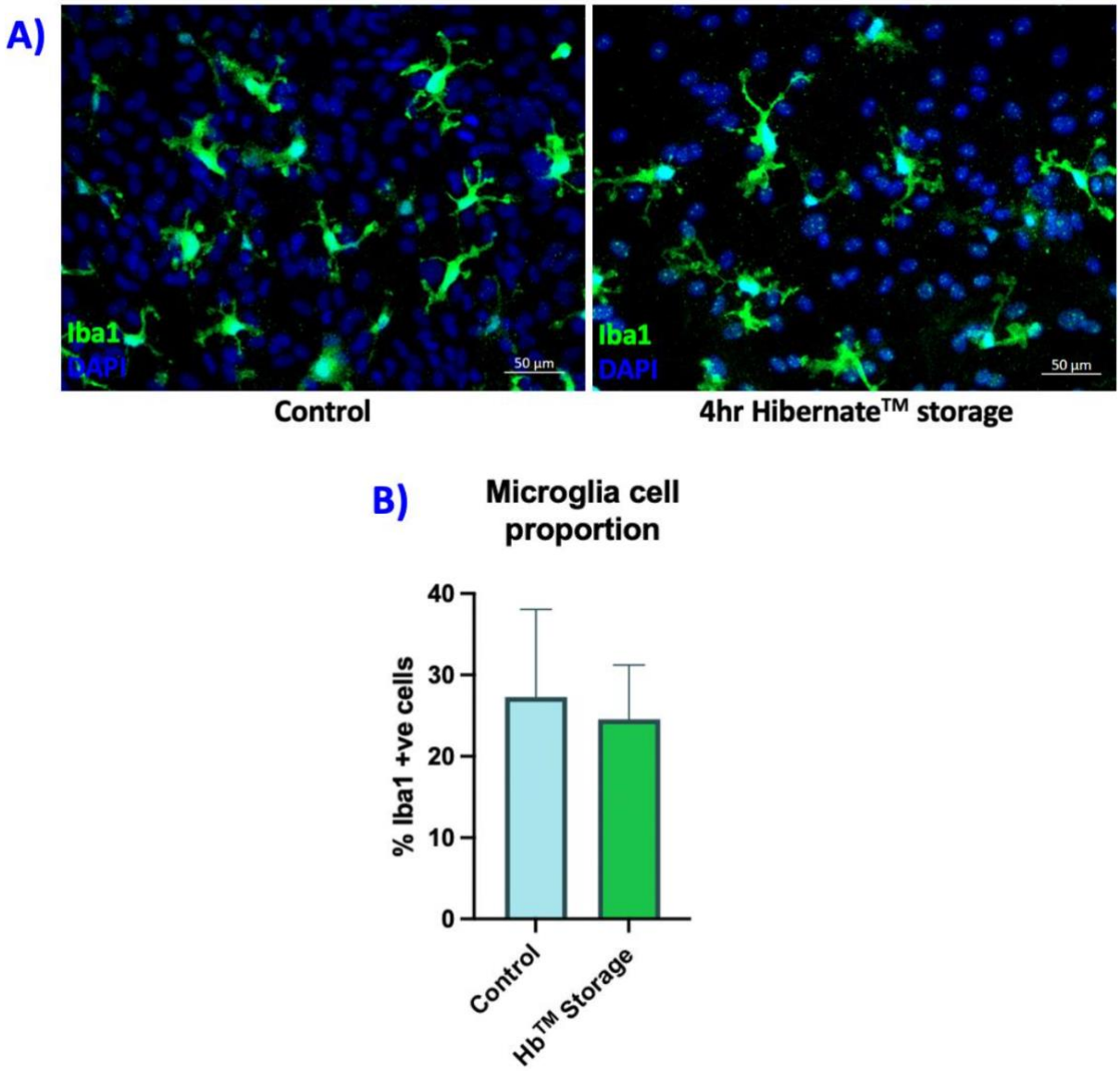

Figure 3.12 Low magnification fluorescence images of Iba1 and DAPI staining showing microglia cell proportion. *There were several clearly and evenly stained, mostly ramified microglia visible in control (**A, left**) and 4hr Hibernate™ storage (**A, right**) where no obvious differences were obviously identifiable. Average microglia cell proportion is also shown (**B**) (n=3, mean ± SEM).*

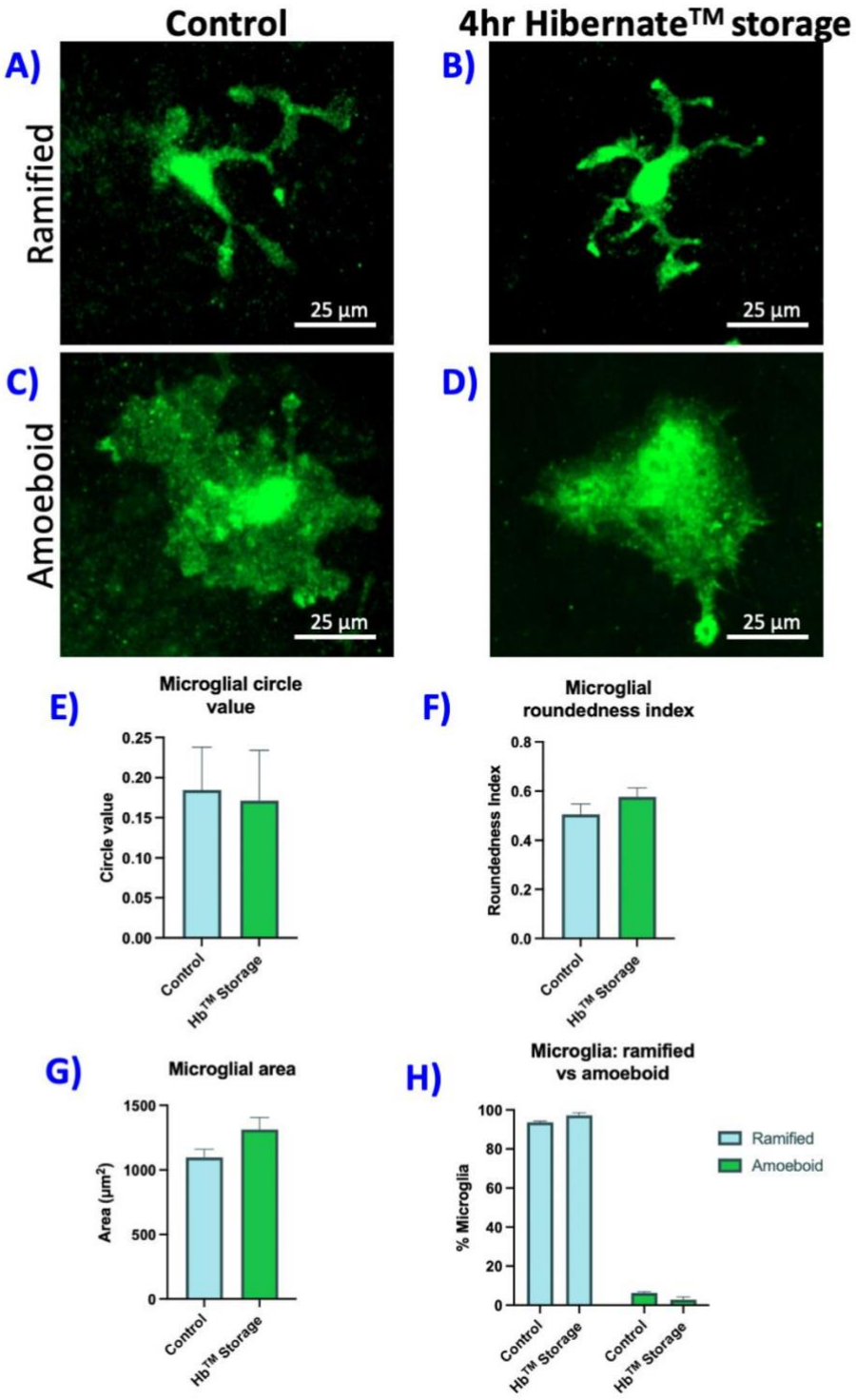

Figure 3.13 High magnification fluorescence images of Iba1 staining showing microglia morphologies. *Of the clearly and individually identifiable microglia, various cellular morphologies were identified in control (**(A)**: ramified, **(C)**: amoeboid) versus 4hr Hibernate™ storage cultures (**(B)**: ramified, **(D)**: amoeboid). Different parameters of microglial morphology are shown including **(E)**:*

*circle value, **(F)**: roundedness index, **(G)**: area, and **(H)**: ramified vs amoeboid proportions, (n=3, mean ± SEM for all).*

3.3B Evaluating the feasibility of storing primary mixed neuronal cultures in Hibernate™

3.3B.1 Normal establishment of primary mixed neuronal cultures

Primary mixed neuronal cultures showed defined changes in their maturation status and progressive appearance and development of individual glial and neuronal cell types which is shown in **figure 3.14**.

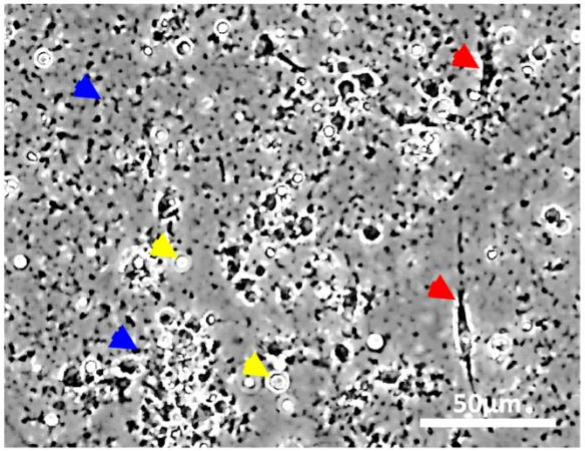

Day 1

Significant debris (blue arrows) and small, bright round dots, likely dead cells (yellow arrows), of which significant numbers are present

Dark bipolar cells (red arrows) with short processes, likely immature neurons which were cells attached to the glass coverslip

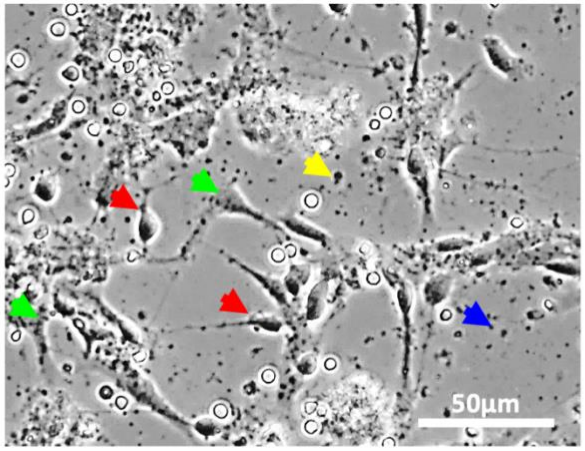

Day 3

Debris (blue arrows) and small, bright round dots, likely dead cells (yellow arrows), still present

Small, dark round bodies (red arrows) with thin processes establishing into a network

Larger, 'flatter' gray cells (green arrows), with thick 'muscular' processes which are likely attached astrocytes

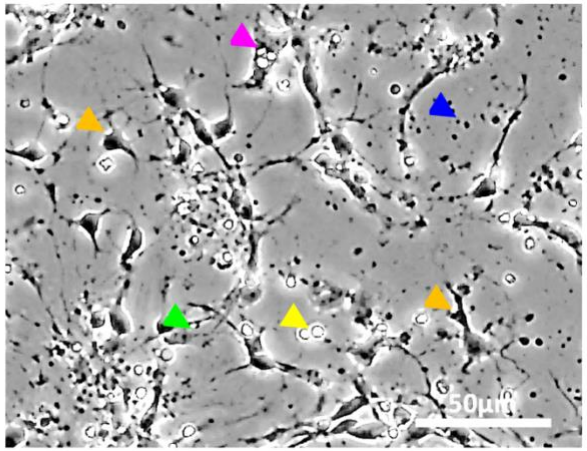

Day 6

Debris (blue arrows) and dead cells (yellow arrows) still present although less prominent

small dark bodies with multiple, thin processes, likely multipolar OPC/oligodendrocyte morphologies (orange arrows)

Larger, 'flat' gray cells, likely astrocytes, with thick 'muscular', 'astrocytic pavement' forming (green arrows)

Small, dark cells with short, thick processes (purple arrows) with small bright circles within cells (vesicles): likely microglia

Figure 3.14 Features of normal establishment of a primary mixed cortical neuronal culture

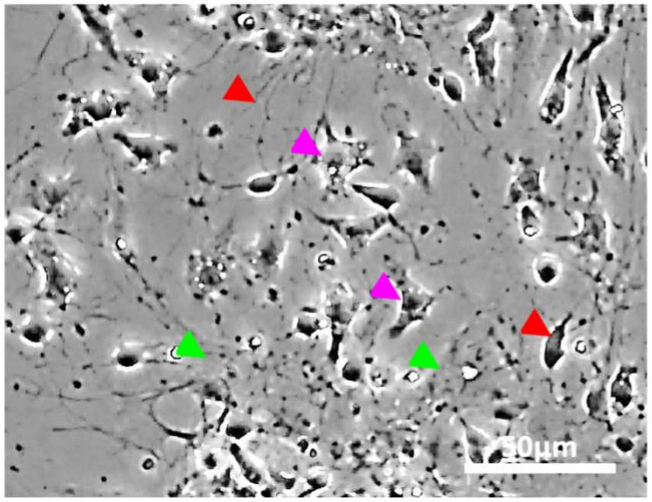

Day 8

Formation of a 'network' of thin processes (red arrows) as neuronal outgrowths become longer, denser, more connections forming becoming

'Astrocyte pavement' (green arrows) forming in patches

Increased, dark microglia with short, thick processing (purple arrows)

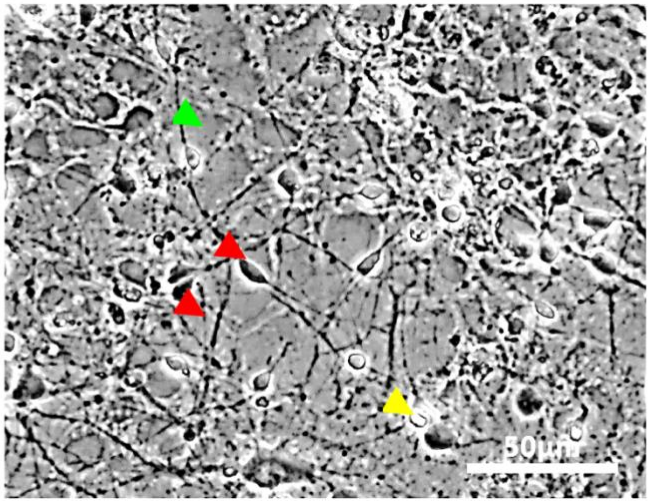

Day 10

Small, round dark neurons and longer neuronal processes (red arrows) forming dense network

Large, 'flat' gray astrocytes forming 'astrocytic pavement' (green arrows) more established and confluent

Few small bright round cells, dead cells, still present (yellow arrows)

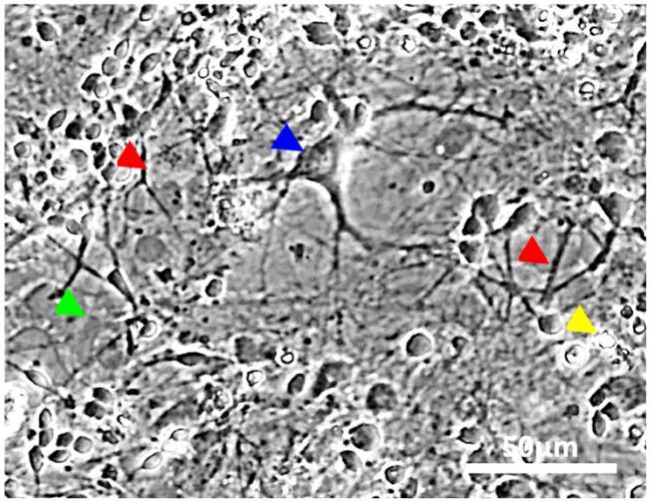

Day 13

Multiple small, round dark neurons and longer, thicker neuronal processes (red arrows) forming dense network

'Astrocyte pavement' (green arrows) mostly confluent

Large, round neuronal somas with thicker, longer processes now present, (blue arrow) likely mature neurons establishing

Round, bright dots, dead cells still present (yellow arrows)

Figure 3.14 Features of normal establishment of a primary mixed cortical neuronal culture cont.

3.3B.2 Confluency and adherence of established primary mixed cortical neuronal cultures were similar between control and 4hr storage in Hibernate™ at RT conditions

After 24hr recovery post 4hr Hibernate™ storage, there is no evidence of increased numbers of small bright bodies (dead cells). In both conditions, there were patches of multiple dense small round cell bodies, likely neurons, with thin, long processes that form a neuronal network (**figure 3.15**). There is also a confluent layer of larger, flat, gray cells, astrocytes, forming a 'pavement' underneath the network (**figure 3.15**). After storage, there is no evidence of detachment of cells, of disruption of the confluent astrocyte pavement or of the network of dense neuronal processes. No immediate signs of cell detachment were identified from phase images or prior to fixation and ICC staining.

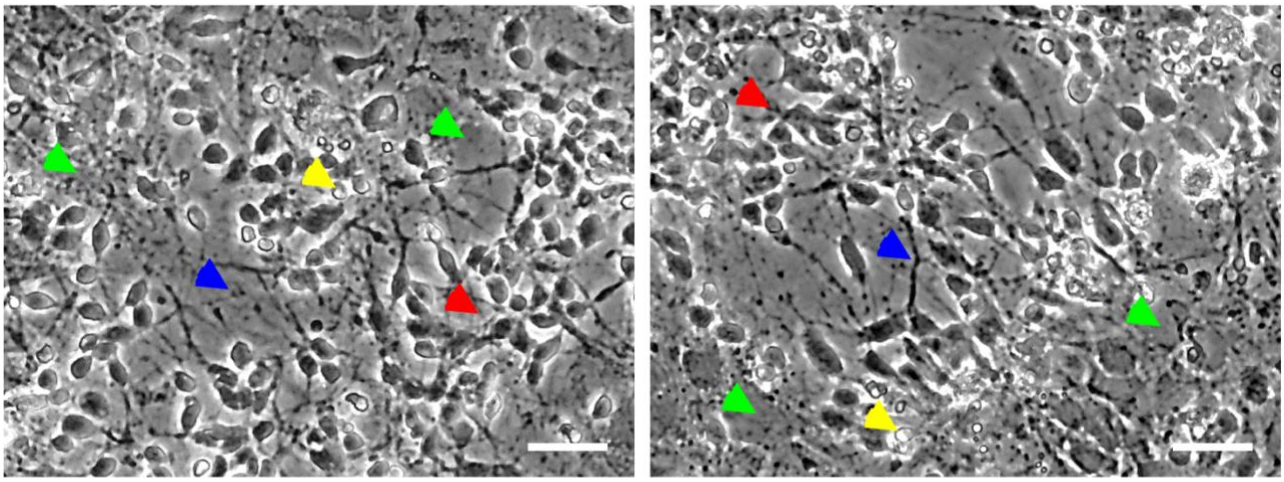

Figure 3.15 High magnification phase images showing a range of morphologies of different cell types in control and 4hr Hibernate™ storage conditions. *Red arrows indicate multiple, dense small dark bodies with thin processes (immature neurons). Blue arrows indicate areas of dense process networks. Yellow arrows indicate small, bright white dots (dead cells).*

3.3B.3 Primary mixed cortical neuronal cultures do not show changes in cell viability after storage in Hibernate^{TM} medium for 4 hours at RT

After calcein-AM and ethidium homodimer-1 staining, the majority of cells were stained green, with small nuclear fragments stained red (**figure 3.16**). A background confluent layer of astrocytes was stained green, the borders between cells can be seen in high magnification microscopy images (**figure 3.17 (A)**) with patches of overlying smaller, brighter cells, usually with long, fine processes also visible (**figure 3.17 (A)**, **black arrows**). This expected range of morphologies displayed amongst different cell types is evident in storage condition cultures. There are also speckles of red dots where dead nuclear fragments take up the ethidium stain that have not increased post storage (**figure 3.16**, **white arrows**). Cell viability was not significantly different between control and storage conditions (**figure 3.17 (B)**, n=5: control 83.2 ± 4.4% vs storage 81.6 ± 3.0%, Welch's t-test **P=0.8018**).

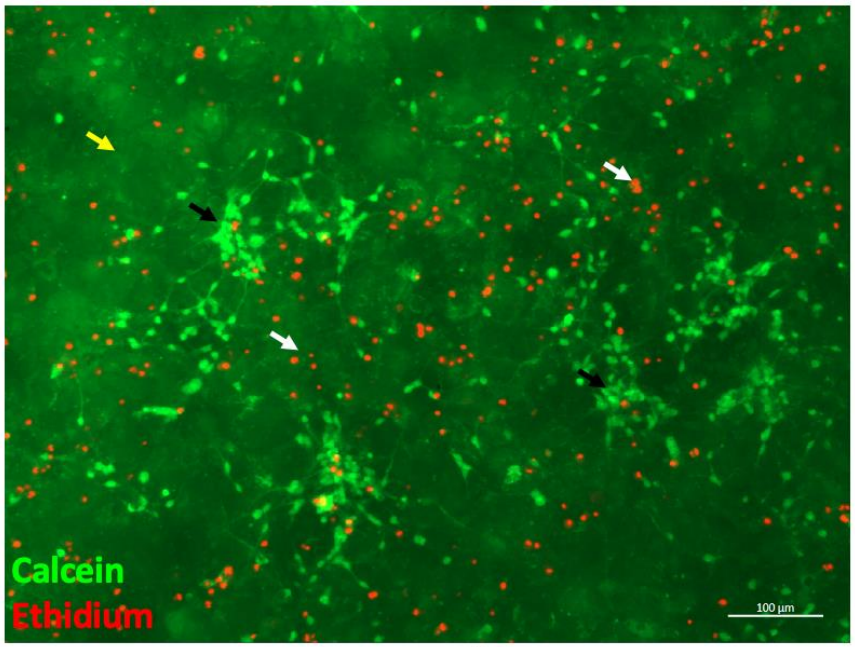

Control

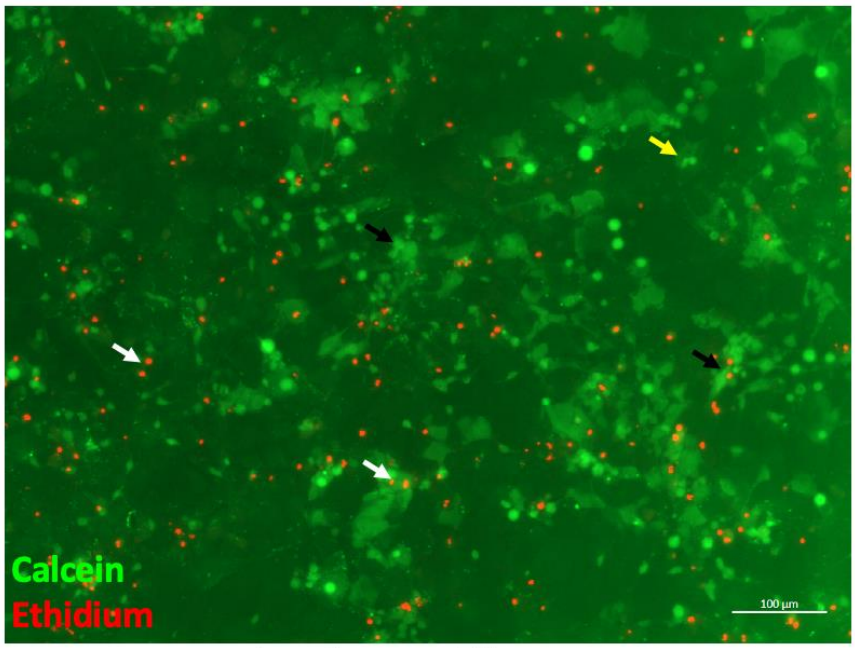

4hr Hibernate™ storage

Figure 3.16 Low magnification fluorescence images of calcein-AM and ethidium homodimer-1 staining showing high proportion of live cells*. In both control (**top**) and 4hr Hibernate™ storage cultures (**bottom**) multiple small red dots (dead nuclear fragments) are shown by white arrows and are not noticeably increased on microscopic observation. There is clear and even green staining across the image, showing the confluency of all live cells, shown by yellow arrows, with brighter green patches of small cell bodies with long thin processes forming into networks (neurons) shown by black arrows.*

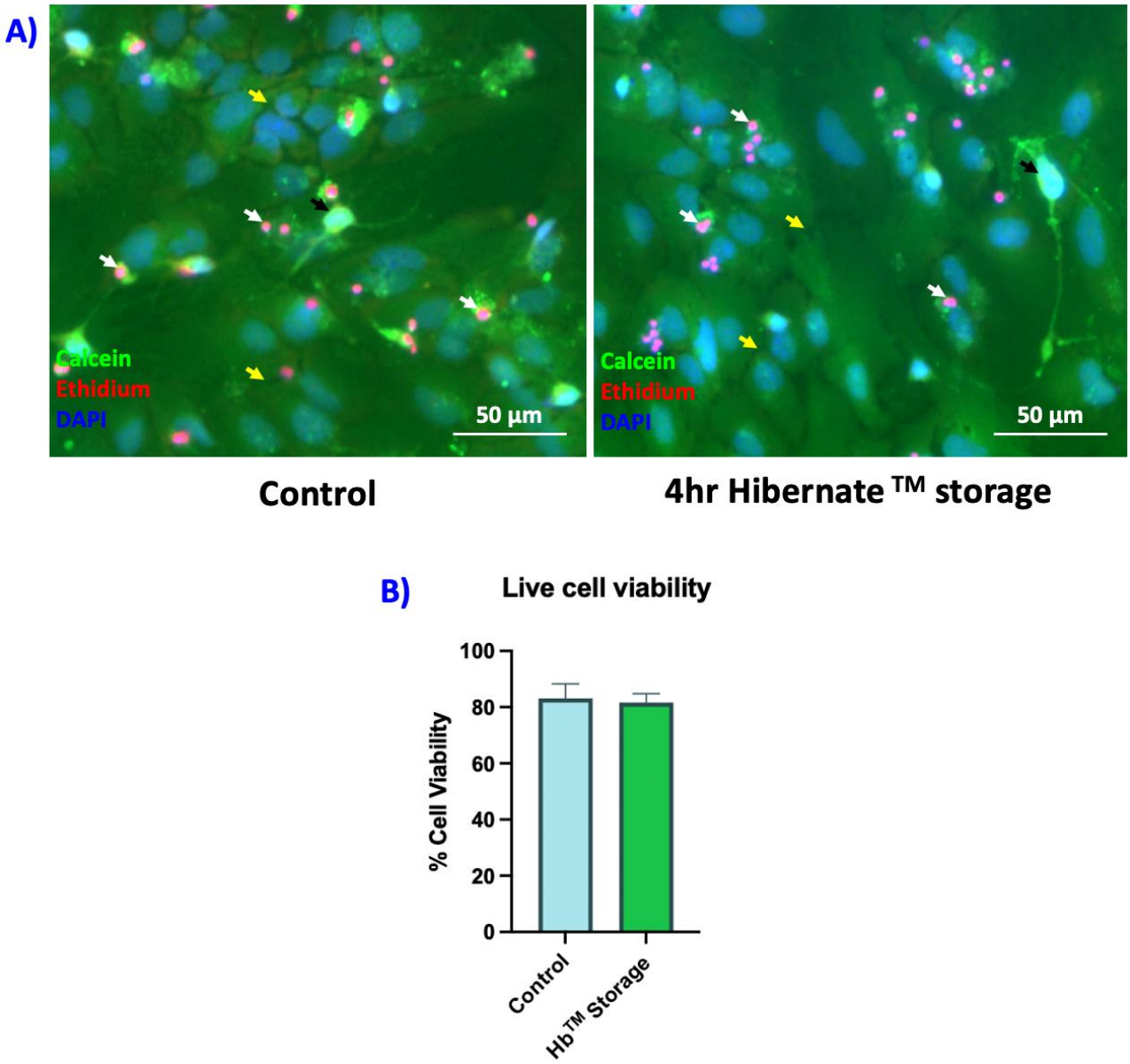

Figure 3.17 High magnification fluorescence images of calcein-AM and ethidium homodimer-1 staining showing high proportion of live cells*. In both control (**A, left**) and 4hr Hibernate™ storage cultures (**A, right**) there is clear and even green staining across the image with morphologies of individual cell morphologies now visible. Astrocytes in a confluent layer are visible, with the edges of cells clearly shown by the **yellow arrows**. There are multiple small red dots of nuclear fragments visible, shown by **white arrows**. Small, bright green bodies with thin processes, showing a bipolar morphology are shown overlying the astrocyte pavement, shown by **black arrows**. These are likely either neurons or OPCs. Percentage live cells in each condition are shown **(B)** (n=5, mean ± SEM).*

3.3B.4 All major neural types were identified in primary cortical neuronal cultures in control and 4hr Hibernate^{TM} storage conditions

Neurons with a range of morphologies and cell process lengths can be seen in a dense network of processes (as shown in **figure 3.18** and **figure 3.19**). A confluent layer of astrocytes can be seen with areas of brighter and dimmer staining reflecting differences in GFAP regulation across different cells. Oligodendrocytes can be in a range of maturation stages from small, unipolar cells, to bipolar and multipolar morphologies with longer processes (shown in **figure 3.18** and **figure 3.19**). Specific analyses of each cell type are identified below.

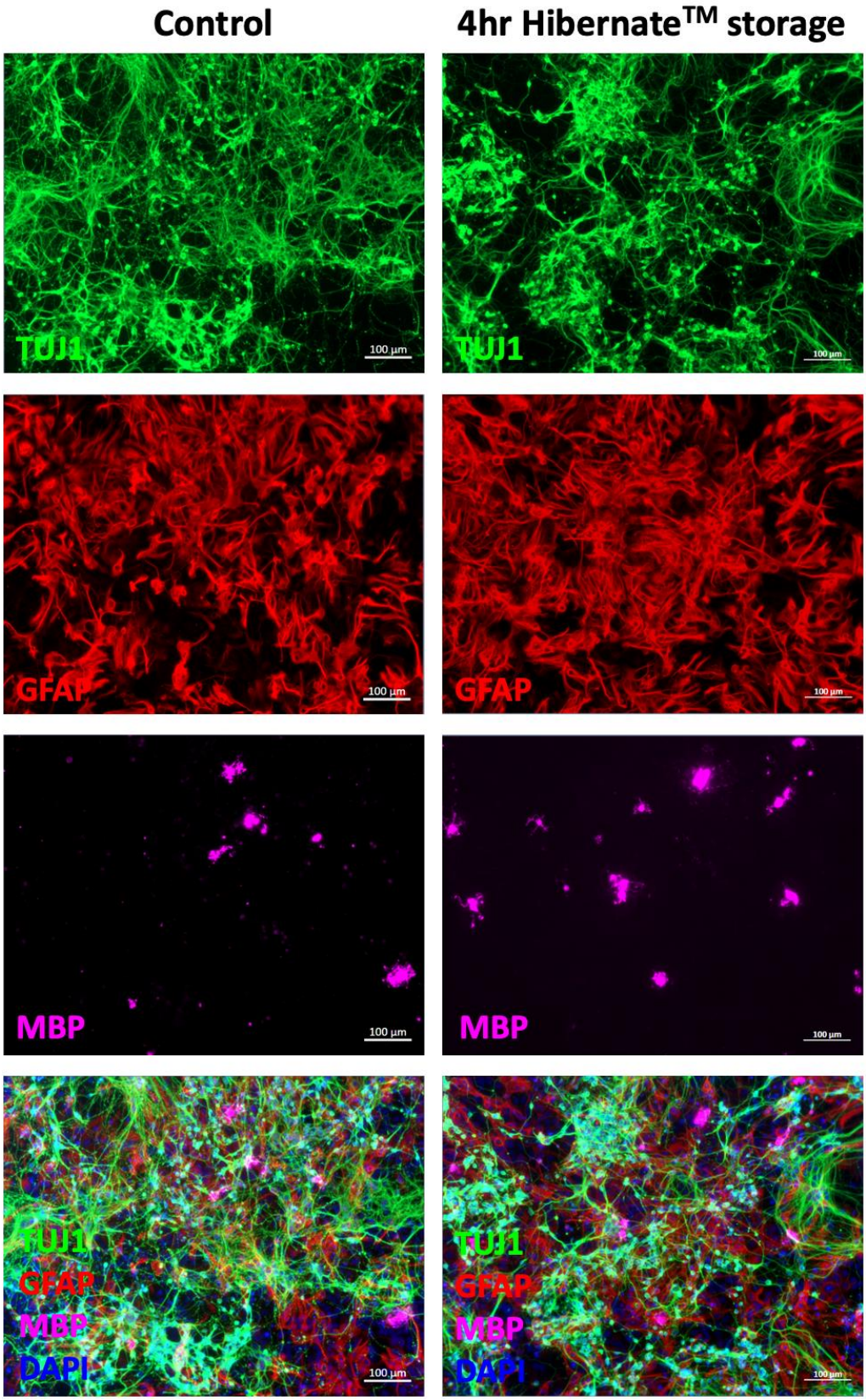

Figure 3.18 Low magnification fluorescence images of TUJ1, GFAP, MBP and DAPI staining to show all major neural cell types. *Tuj1 (neurons), GFAP (astrocytes) and MBP (oligodendrocytes) were all identified in control (**left panel**) and 4hr Hibernate™ storage conditions (**right panel**) showing various cell proportions. (Microglia are imaged below).*

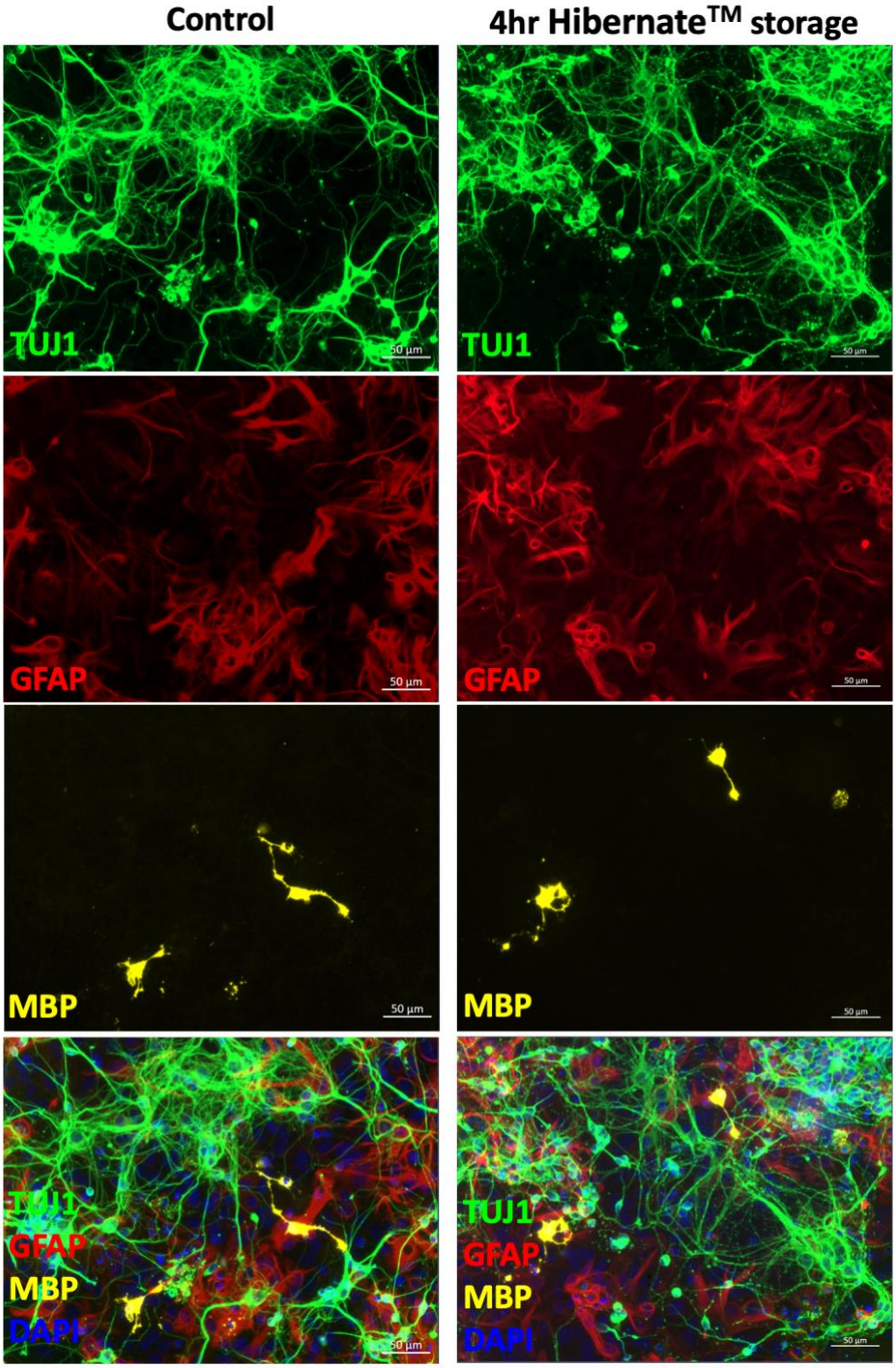

Figure 3.19: High magnification fluorescence images of neurons, astrocytes and oligodendrocytes with nuclear (DAPI) stain. *Tuj1 (neurons), GFAP (astrocytes) and MBP (oligodendrocytes) were all identified and show various morphologies in control (**left panel**) and 4 hr Hibernate™ storage conditions (**right panel**). (Microglia are imaged below).*

3.3B.5 Hibernate^{TM} storage of established primary mixed cortical neuronal cultures does not adversely alter neuronal cell proportion or maturation

In a mature culture, there are a high density of neurons forming a dense network of processes. This is present in control cultures and is not disrupted by storage, as seen in **figure 3.19** and **figure 20 (A)**. When quantified, there is no significant difference in the relative proportions of neuronal cells (**figure 3.20 (B)**, n=5: control 23.7 ± 7.3% vs storage 25.2 ± 5.8%, Welch's t-test **P=0.9377**). When assessing neurite process length, **figure 3.21** show high magnification images of Tuj1 staining in low density areas such that individual somas and their associated processes can be identified. There is also no significant difference in neurite length after storage (**figure 3.21 (B)**, n=5: control 98.6 ± 5.5 µm vs storage 88.9 ± 10.5 µm, Welch's t-test **P=0.4399**). Thus, there was no evidence of neuronal detachment or morphological changes signifying altered neuronal development as a result of storage.

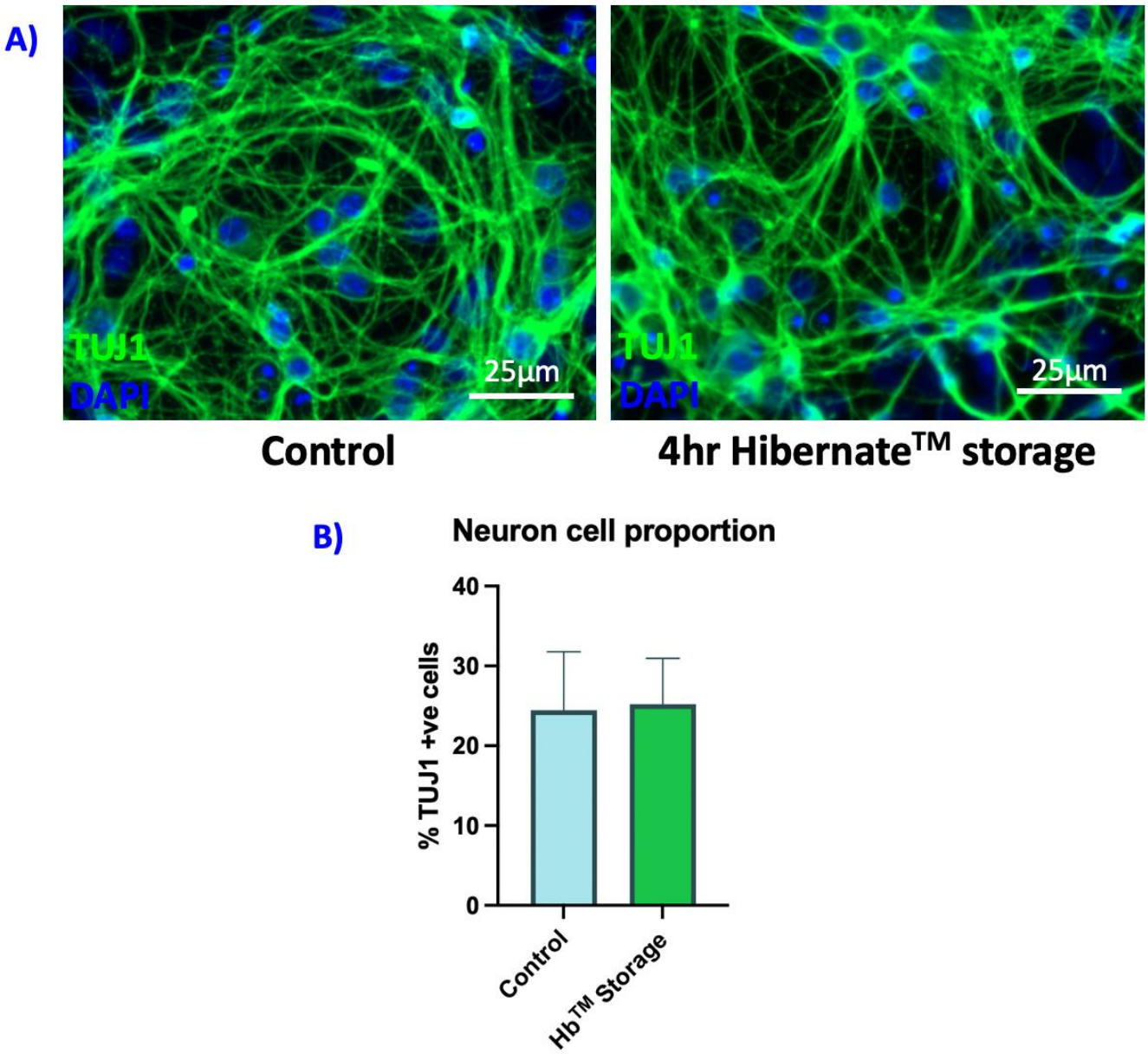

Figure 3.20 High magnification fluorescence images of Tuj1 and DAPI staining showing a high neuronal cell proportion. *Patches of high-density neuronal cell bodies with long, fine processes forming a dense network were identified in control (**A, left**) and 4hr Hibernate™ storage conditions (**A, right**). The percentage of Tuj1 positive cell nuclei, neuronal cell proportion, is shown in **(B)** (n=5, mean ± SEM).*

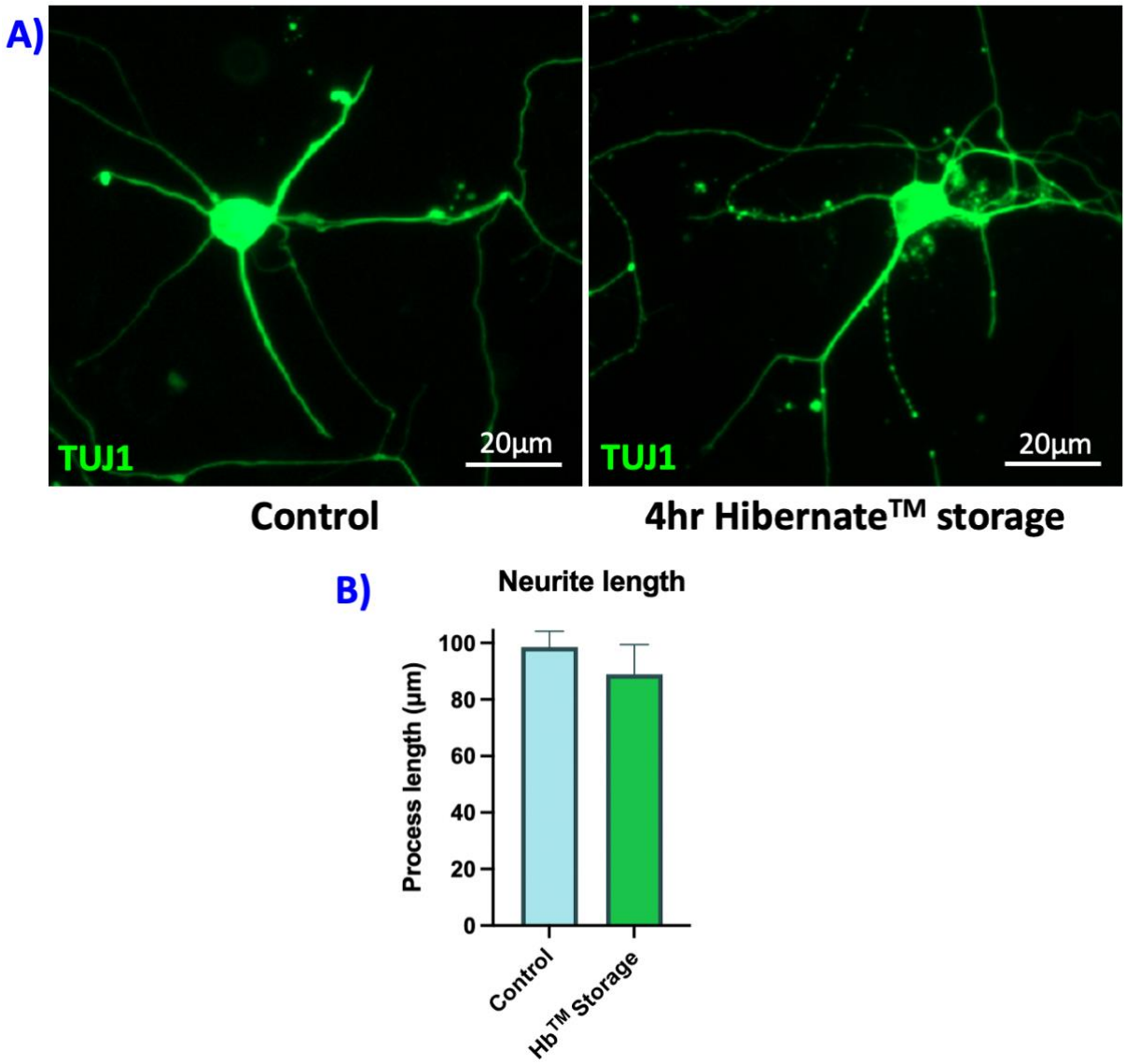

Figure 3.21 High magnification fluorescence images of Tuj1 staining showing neurite process length*. Within patches of low-density neurons, individual neurons clearly stained were visible. Neuronal cell bodies exhibited a range of morphologies, from small cell bodies with short processes in a bipolar morphology to multipolar cells with long thin processes from 50 to up to 100 µm shown here. These were identified in control* ***(A, left)*** *and 4 hr Hibernate™ storage cultures* ***(A, right)****. Average neurite process length is also shown* ***(B)*** *(n=5, mean + SEM).*

3.3B.6 Hibernate™ storage of established primary mixed cortical neuronal cultures does not adversely alter astrocyte cell proportion or reactivity

As evidenced in **figure 3.22 (A)** and **figure 3.23 (A)**, there was no sign of cell detachment, cell death or markers of cell reactivity in the astrocyte population. There was a non-significant difference in astrocyte cell proportion (**figure 3.22 (B)**, n=5: control 67.4 ± 6.9% vs storage 67.8 ± 4.2%, Welch's t-test **P=0.9563**) evidencing normal specific cell marker expression and normal cell attachment, and no evidence of increased cell death comparable to other cell types. Astrocyte reactivity was not significantly altered as a result of storage as there was a slight increase in astrocyte area (**figure 3.23 (C)**, n=5: control 1640 ± 177 μm^2 vs storage 1677 ± 190 μm^2 Welch's t-test **P=0.8907)** and astrocyte optical densities in both conditions were similar (**figure 3.23 (D)**, n=5: control 1.864 ± 0.289 vs storage 1.833 ± 0.162, Welch's t-test **P=0.9378**) signifying no signs of astrocyte hypertrophy or GFAP antigen upregulation as a result of cell stress.

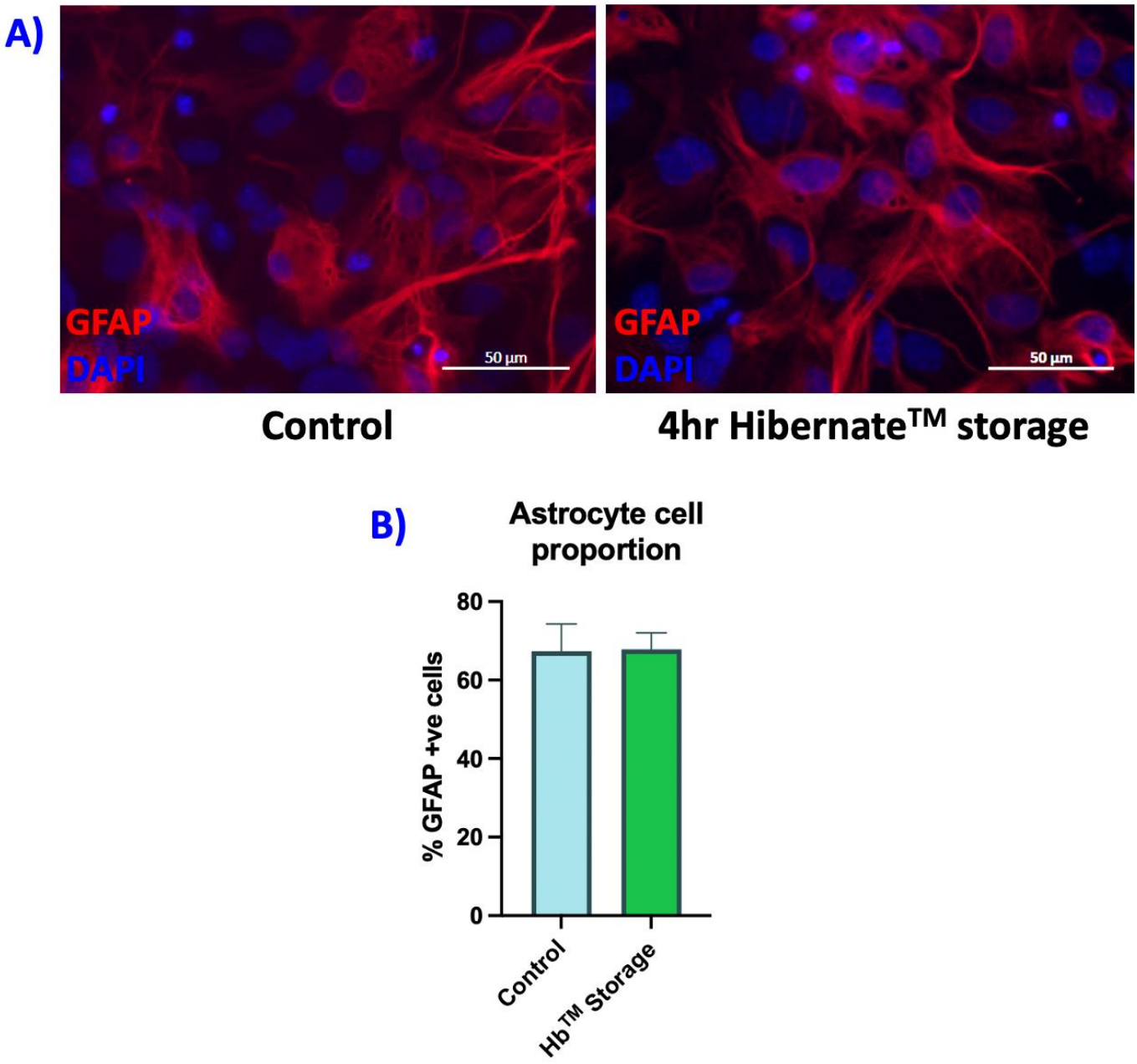

Figure 3.22 Low magnification fluorescence images of GFAP and DAPI staining showing a high astrocyte cell proportion. *A high density of astrocytes was clearly and evenly stained showing their growth into a confluent layer, similar to astrocytes identified in phase images, in control* ***(A, left)*** *versus 4 hr Hibernate™ storage conditions* ***(A, right)****. Astrocyte percentage cell proportion is also depicted* ***(B)*** *(n=5, mean ± SEM).*

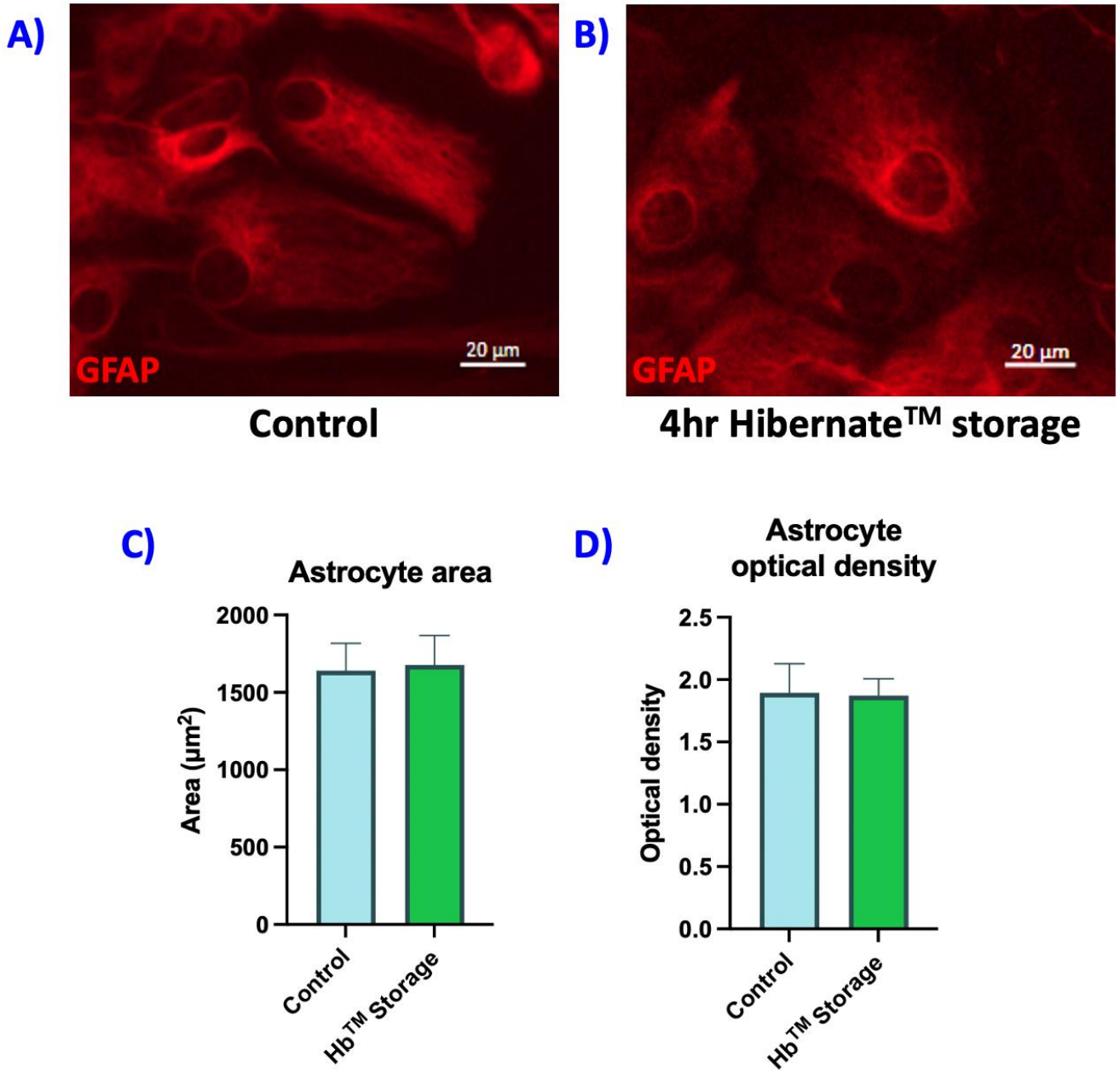

Figure 3.23 High magnification fluorescence images of GFAP staining showing astrocyte morphology. *Astrocytes of varying morphologies in low density patches in both control* ***(A)*** *and 4 hr Hibernate™ storage conditions* ***(B)*** *showed no immediately visible difference astrocyte area or 'brightness' of staining. Average astrocyte area is depicted in* ***(C)*** *and average optical density of GFAP staining is shown in* ***(D)****, (n=5, mean ± SEM for both).*

3.3B.7 Hibernate™ storage of established primary mixed cortical neuronal cultures does not adversely alter oligodendrocyte cell proportion or maturation

Oligodendrocytes identified in control and in 24 hrs post 4hr Hibernate™ storage cultures exhibited a range of morphologies, showing varied levels of development. Cells exhibited expected patterns of MBP expression shown in (**figure 3.24 (A)**) where cells portrayed similar numbers, similar morphologies with clear and even staining. When the cell proportions were quantified, similar numbers were identified in both control and 4hr Hibernate™ storage cultures (**figure 3.24 (B)**, n=4: control 0.96 ± 0.24% vs. storage 1.06 ± 0.38%, Welch's t-test **P=0.8623**). Large, mature oligodendrocytes were also identified in both conditions (**figure 3.25 (A)**), cells with multiple processes, 'fried-egg' morphologies with lots of fine processes forming 'netting' were identified. When quantifying the oligodendrocyte area, there was a non-significant increase (**Figure 3.25 (B)**, n=4: control 6166 ± 1712 μm^2 vs storage 7145 ± 2054 μm^2 Welch's t-test **P=0.7216**). Classifying oligodendrocytes into 'stages of maturation' and comparing these found there was non-significant differences between control and storage conditions within each stage as evidenced above (**Figure 3.26,** n=4, Welch's t-test for all: immature, control 32.3 ± 13.6% vs storage 19.3 ±13.5%, **P=0.5225**; intermediate-1, control 25.5 ± 10.5% vs storage 32.0 ± 14.1%, **P=0.7218**; intermediate-2, control 7.3 ± 4.8% vs storage 23.7 ± 8.8%, **P=0.1515**; mature, control 35.0 ± 23.6% vs storage 25.0 ± 25.0%, **P=0.7811**).

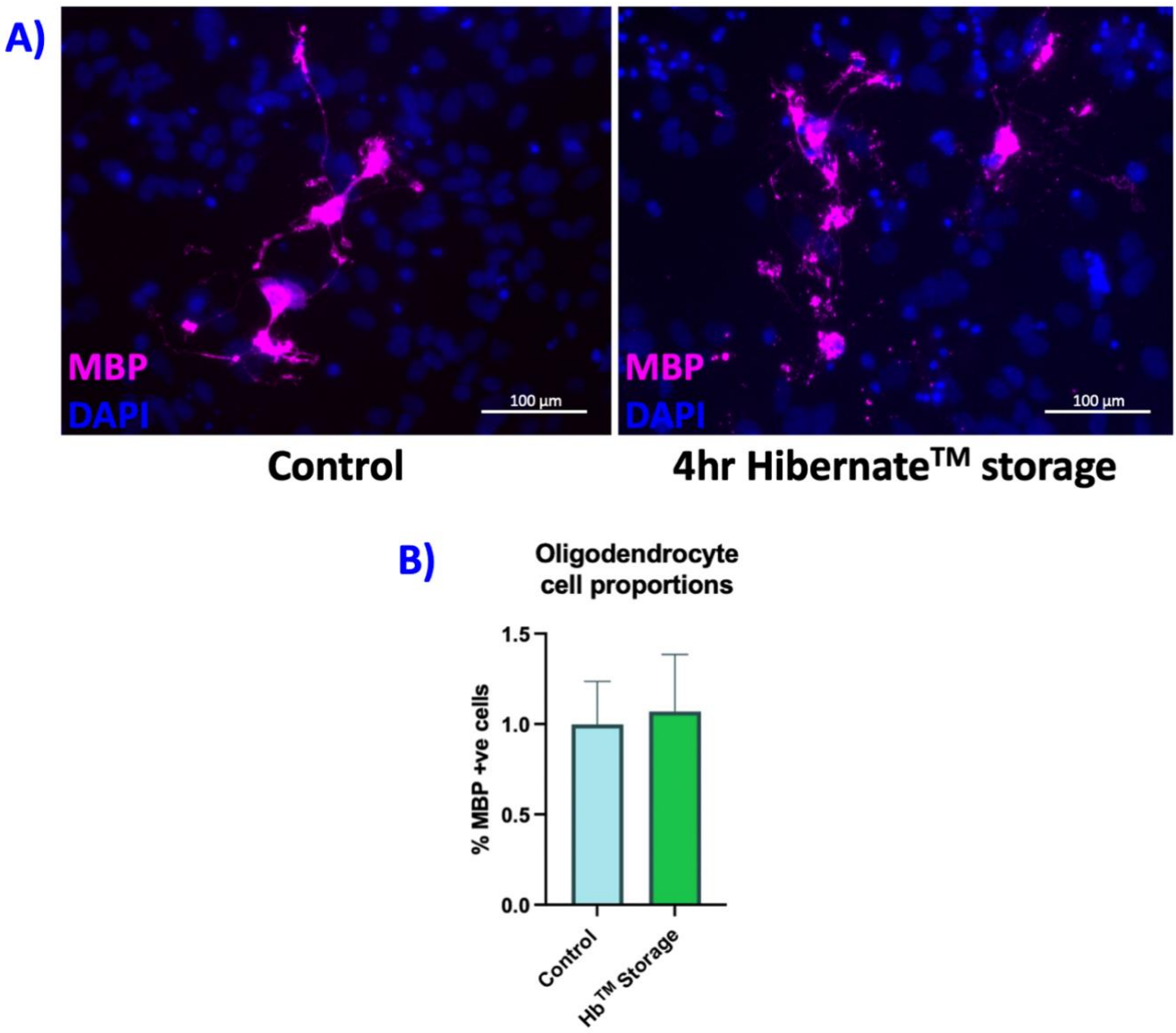

Figure 3.24 Low magnification fluorescence images of MBP and DAPI staining showing oligodendrocytes proportions. *There were several oligodendrocytes with various morphologies identified in areas of clear in even staining in control* ***(A, left)*** *and in 4 hr Hibernate™ storage* ***(A, right)*** *cultures. Average oligodendrocyte cell proportions are also depicted* ***(B)*** *(n=4, mean + SEM).*

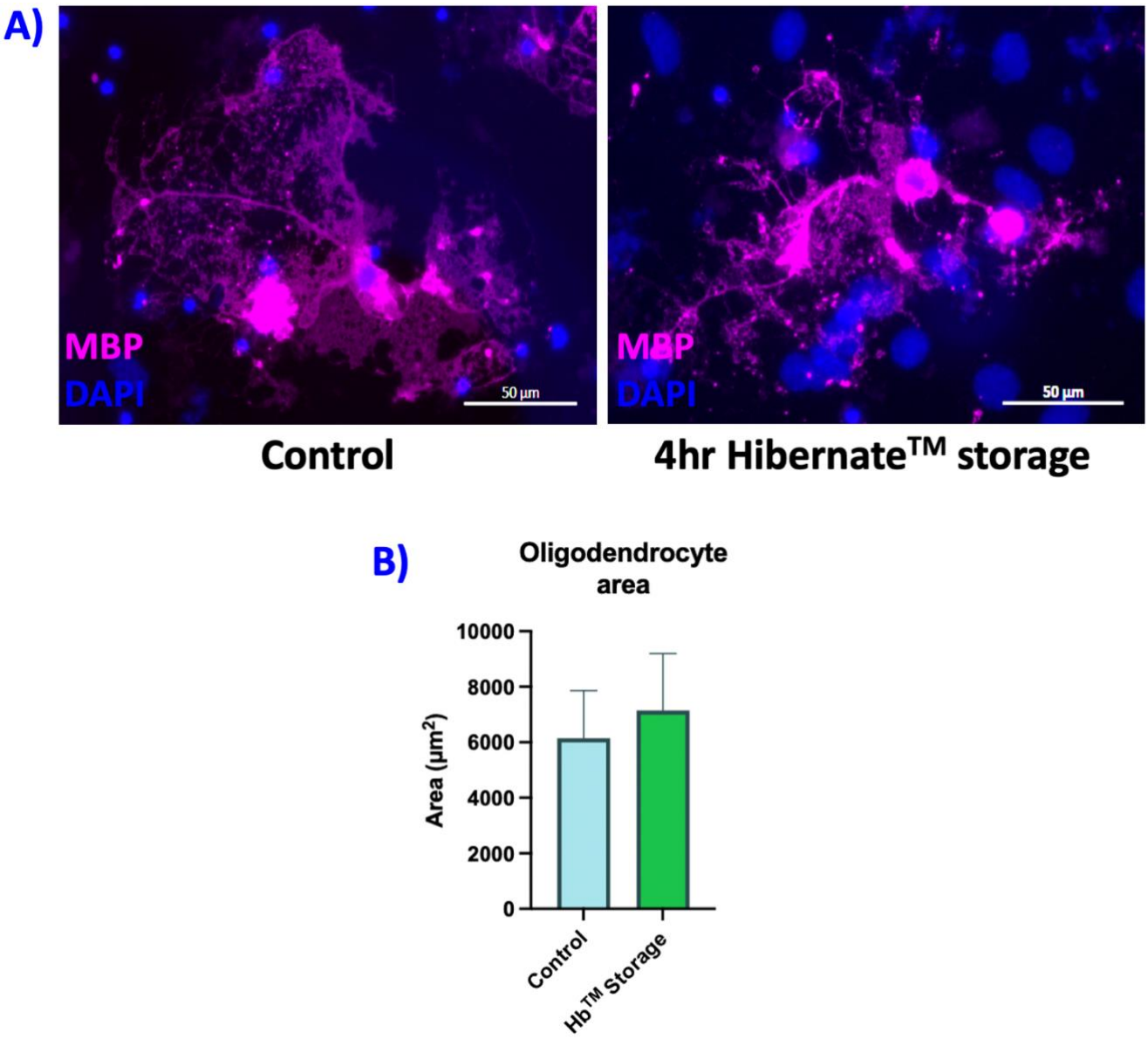

Figure 3.25 High magnification fluorescence images of MBP and DAPI staining showing oligodendrocyte cell morphology. *Large, highly mature oligodendrocytes were identified in control* ***(A, left)*** *and in 24 hr post 4 hr Hibernate™ storage cultures* ***(A, right)****. Mature cells had multiple thicker and fine processes, exhibiting 'fried-egg' or 'spider-web' morphologies in storage cultures comparable to those identified in control cultures. Average oligodendrocyte cell proportions are also shown* ***(B)*** *(n=4, mean ± SEM).*

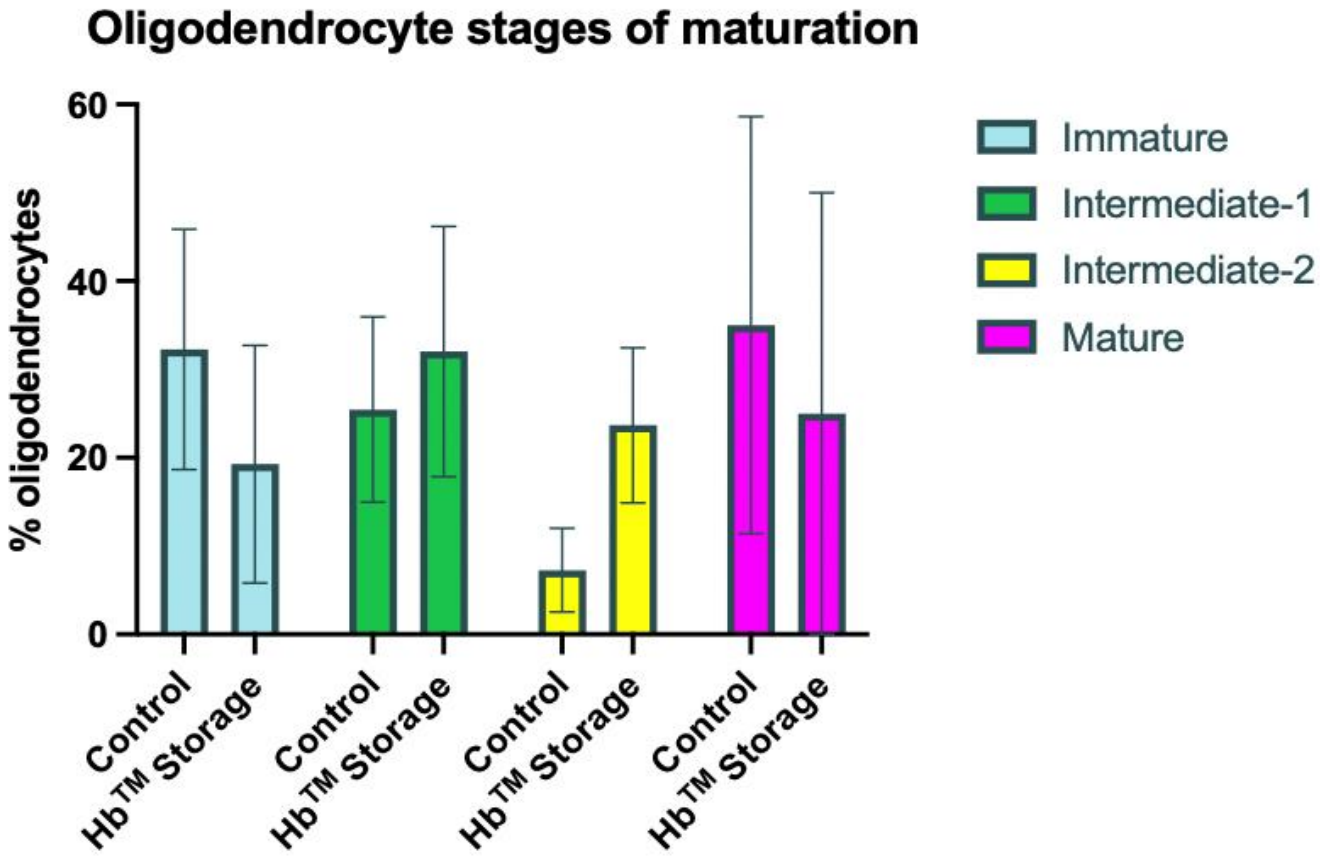

Figure 3.26 Oligodendrocyte morphology: Stages of Maturation *showing distribution of immature to mature oligodendrocytes in control and 24 hrs post 4 hr Hibernate™ storage (n=4, mean ± SEM).*

3.3B.8 Hibernate™ storage of established primary mixed cortical neuronal cultures does not alter microglial cell proportion or reactivity

Iba1 staining showed many clearly and evenly stained microglia that were identifiable with varying densities across cultures (**figure 3.27 (A)**). When counted, a relatively small proportion of the cells in the neuronal cultures were microglia, showing similar proportions across control and storage conditions (**figure 3.27 (B)**, n=3: control 2.9 ± 1.3% vs storage 2.8 ± 0.6%, Welch's t-test **P=0.9567**). This means there is likely no cell detachment or increase in microglial death compared to other cell types as a result of storage. Microglia displayed various morphologies across cultures indicating many cells with different reactivities (**figure 3.28 (A-D)**). Several morphological parameters were assessed (**figure 3.28 (E-H**). Morphologies were identified to be mostly similar in circle value (**figure 4.17 (E)**; n=3: control 0.272 ± 0.112 vs storage 0.242 ± 0.045, Welch's t-test **P=0.7084**), in microglial roundedness (**figure 4.17 (F)**; n=3: control 0.608 ± 0.031 vs storage 0.568 ± 0.084, Welch's t-test **P=0.5546**), in microglial area (**figure 4.17 (G)**; n=3: 2020 ± 589 μm^2 vs storage 2437 ± 416 μm^2 Welch's t-test **P=0.8707**) and in percentage ramified microglia (**figure 4.17 (H)**; n=3: 71.7 ± 12.6% vs storage 90.4 ± 5.3%, Welch's t-test **P=0.3662**) (with a converse decrease in percentage amoeboid microglia). The lack of statistical significance in any parameters means there is not sufficient evidence to conclude storage in Hibernate™ does increase microglial reactivity, with the current trend of the evidence suggesting it does not.

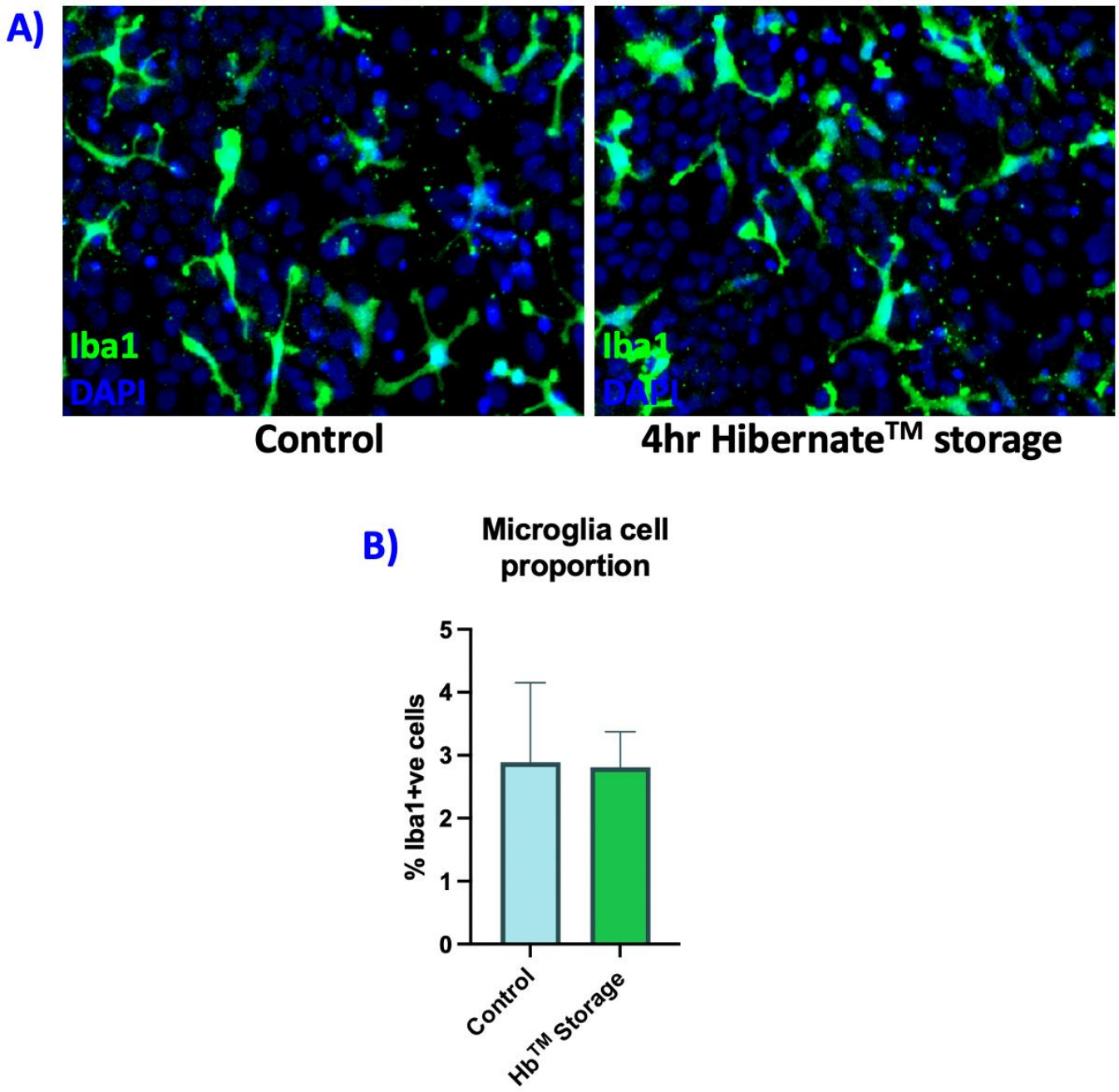

Figure 3.27 Low magnification fluorescence images of Iba1 and DAPI staining showing microglial proportions. *Clear and evenly stained high-density patches of microglia showing various morphologies were identified in control* ***(A, left)*** *and 24 hrs post 4 hr Hibernate™ storage cultures* ***(A, right)****. Average microglial cell proportions are also depicted* ***(B)*** *(n=3, mean ± SEM).*

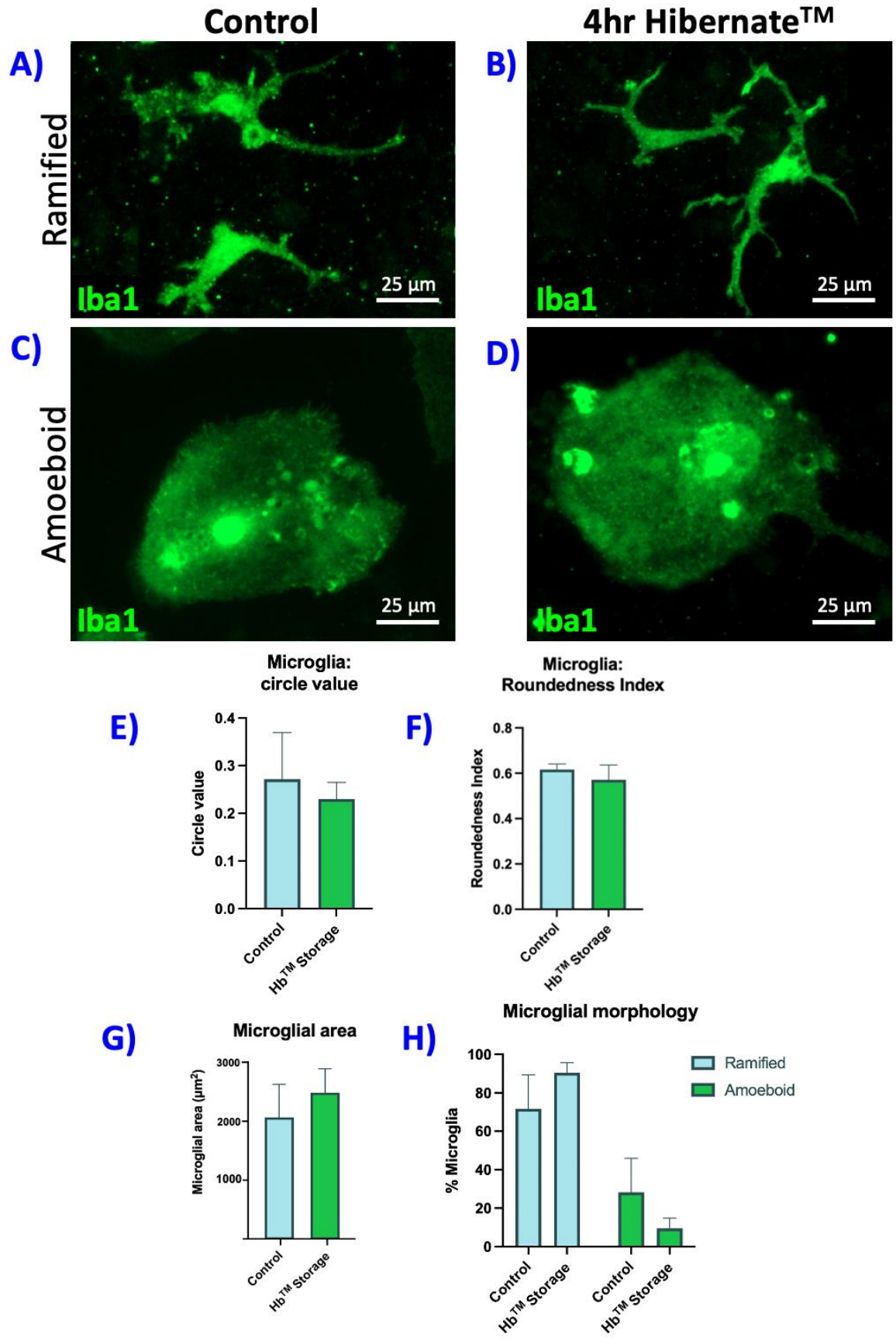

Figure 3.28 High magnification fluorescence images of Iba1 staining showing various microglial morphologies. *Of the clearly and individually identifiable microglia, various cell morphologies were*

*identified in control (**(A)**: ramified, **(C)**: amoeboid) and 4 hr Hibernate™ storage conditions (**(B)**: ramified, **(D)**: amoeboid). Different parameters of morphologies are depicted as following: average microglial circle value **(E);** average microglial roundedness **(F)**; average microglial area **(G)**; average microglial ramified vs amoeboid proportions **(H)**, (n=3, mean ± SEM for all).*

Discussion

This study has demonstrated for the first time that it is feasible to store cultured and established multicellular neural tissue models at room temperature without any detriment to cell viability, maturation or reactivity confirmed by phase microscopy, ICC staining and morphological analysis. Our laboratory has previously shown the ability to store oligodendroglial cells (mature cells and OPCs) at RT [54]. However, so far, storage of other glial cell types on their own or the storage of cells as an established complex monolayer model has not been attempted.

Additionally, for the first time, our laboratory's mixed neuronal model of pTBI has been shown to be able to be kept in storage at RT. A single study has been shown previously to store cultured primary neurons with a view of transportation [63], and limitations to the study involved only the use of hippocampal neurons, instead of a multicellular culture, which has disadvantages as a neural tissue model, and the use of cold chain transport where Hibernate™ was cooled to 4 °C. The model itself showed significant loss of viability when cultures older than 2 days *in vitro* where shipped. The reason for this is not discussed, however this study has shown the ability to maintain viability of cultures that were up to two weeks old in storage at RT. As a purely neuronal model, it ultimately lacks the completeness of a multicellular model, particularly for this study's purpose and context, which is for pTBI.

While it is outside of the scope of this study to directly compare and analyse the glial and neuronal cell models, the same assays were used for both experiments and thus some interesting comparisons can be made. The microglial profile showed differences between models, with microglia making up a larger proportion of all cells in the glial model. This could just be due to the additional neuronal component increasing the total number of cells; however the microglia also seem overall more reactive. Several morphological parameters indicate this, average microglial area in the glial and neuronal cultures being 1097 μm^2 and 2020 μm^2 respectively (**figure 3.13** (G) and **figure 3.29 (G)** respectively). There were also increases in microglial circle value, roundedness index and percentage amoeboid microglia in neuronal versus glial cultures. While no specific studies have looked into why this could be, the culture medium for the glial cultures, D10, is made up of 10% FBS, which may include a host of growth factors that influence or increase microglial proliferation [68]. The absence of any factors in the serum-free culture in the neuronal cultures could be contributing to a lower proliferative capacity of the microglia, resulting in fewer numbers which become reactive to any cellular cultural debris. Evidence of this can also be seen in the normal establishment of glial and neuronal cultures (**figure 3.2** and **figure 3.14**) where both cultures initially have significant debris present, however glial cultures are very clean with minimal debris by 13 days *in vitro* in comparison to neuronal cultures which still have bright bodies of dead cells still present, which may drive an increased reactivity in the fewer microglia that are present.

However, more specific analyses would need to be completed to understand how the different culturing media impact the cellular profile and establishment of each type during establishment. This can be useful in understanding which model can be ideal for different studies. For example, studies looking at specific microglial behaviours may benefit from using the glial model, which have more cells, more of which are in their 'normal' resting state. Alternatively,, a study looking at microglial uptake of anti-inflammatory pharmaceutical agents in response to injury may benefit from using the neuronal model, where more reactive microglia are more likely to take up a drug. This is only an example of how small differences between both mini-cultures may make one more suitable than the

other depending on the context and aims of the study, and both have their place as viable cultures that can be selected for transport and collaboration.

The applicability of a facile method of storage and transportation of complex neural tissue is widespread in any field involving working with neural tissue. This study proves the ability to store several neural cell types at room temperature, which would normally cause loss of viability to the cells. The ability to keep cultured, established neural models alive and viable at room temperature for even four hours can allow for a big improvement in how neuroscience research, specifically pTBI research, is currently carried out. If travelling by car, from Keele University, neural tissue can be transported as far down south as Southampton or north up to Newcastle upon Tyne (**figure 3.29**), within which are easily over a hundred universities that now have the access to complex, multicellular pTBI models for testing and collaboration. This is also without the use of cold chain transport which is the usual relied upon method for tissue transport and which adds further costs and logistical challenges while transporting. As outlined, the resources for transportation is just a single medium within which the culture can be suspended. A distal, collaborative site would only need to remove the transport/storage medium and add the growth medium once obtaining the established culture for experimentation, which is a drastic improvement than having to establish primary cultures from scratch. This can improve the efficiency of neuroscientific research, and primarily increases the ease with which interdisciplinary collaboration can occur, which is a key limiting factor in not only pTBI research, but across all of regenerative neuroscience research.

Figure 3.29. Map of the United Kingdom showing an estimated distance that can be travelled by car within four hours

Chapter 4: Conclusions and Future Directions

Conclusions

Here, Hibernate™ medium has been proved as a viable storage medium to store two complex, mixed neural cell culture models without any effects on:

- Culture confluency and adherence
- Cell viability
- Astrocyte viability and reactivity in glial and neuronal monolayer cultures
- Oligodendrocyte viability and maturation in glial and neuronal monolayer cultures
- Microglial viability and reactivity in glial and neuronal monolayer cultures
- Neuronal cell viability and maturation in neuronal monolayer cultures

This information can hopefully be applied directly and quickly to increase the ease with which these models and resources are available and enhance accessibility and collaboration within pTBI regenerative research. Ultimately however, this information can be useful to any neuroscientists working on a regenerative neurotherapy.

Future directions

As elaborated, four hours can be significant time to travel to many distal sites within the UK. Particularly from a centralised location, collaboration with many universities undertaking pTBI research is now possible. However, from previous studies from our laboratory looking at the use of Hibernate™ as a RT neural cell storage medium [54], there is evidence that increasing the radius of transport is possible, storage for up to 24 hours or more at RT can be a valuable additional timepoint. If including public/air travel, 24 hours can make transport to most neighbouring countries

possible, introducing the potential for international collaborative studies. The effect of storage for increasing timepoints on neural tissue would be valuable information to enable this option.

The success of this study is based on the formulation of Hibernate™ medium. As mentioned previously, Hibernate™ is a derivative of Neurobasal-A medium, the growth medium that the primary neuronal cultures are grown in. The only changes are in the pH buffering capacity, with a much lower bicarbonate ion concentration and alternative use of MOPS instead of HEPES, adapting the medium for much lower ambient carbon dioxide concentrations than Neurobasal-A, which is suited for the 5% carbon dioxide of standard culturing conditions. This may be the likely reason why the neuronal model is able to fare well in RT storage in Hibernate™. A direct comparison between Neurobasal-A medium used as a RT storage medium and Hibernate™ may be useful to identify if cells would actually deteriorate if just kept in their original growth medium outside of its usual culturing conditions, and if so to map this deterioration over longer timepoints in comparison to any declines in viability seen in longer-term Hibernate™ storage. Additionally, it may also be useful to know if there is any effect of Hibernate™ medium further to just balancing the pH of cultures for a lower ambient carbon dioxide concentration. The only difference in storage conditions to culturing conditions that are not accounted for is the lower temperature, from 37 °C to RT, which is there is no indication in the formulation that Hibernate™ modifies the cellular environment to account for. This is likely as its original formulation as the use of a hypothermic storage medium, which would cool cells right down, and not for use as a RT storage medium. It could be useful keeping cultures in Hibernate™ in ambient carbon dioxide but various temperatures for longer time points in storage, to identify if there is any difference in keeping cells in Hibernate™ at ambient carbon dioxide and keeping cells in Neurobasal at 5%, with temperature controlled for (which would identify if there is any additional element to the effect of Hibernate™ on cultures aside from pH control), or to see the effect of different temperatures of Hibernate™ storage on cell viability, and to map this across longer timepoints.

The growth medium of the glial culture, however, is a completely different formulation than Hibernate™. D10 is based on DMEM with added FBS and sodium pyruvate with few other additives (as outlined above). The complete switch in chemical medium from a serum based medium to something with a completely different formulation, serum free, may have unknown longer-term stressful effects on the viability, maturation or cell type ratios if kept in Hibernate™ for a much longer period of time. Considering Hibernate™'s formulation being very similar to Neurobasal-A's formulation, there is no indication of what would occur if cells developed in a glial culturing medium are suddenly kept in a neuronal culturing medium, what effect this would have. As mentioned already there are a host of serum associated proteins and factors that can influence the proliferation of glial cells [91] [92], which would not be present in the neuronal culturing medium. While there was no directly observable change to identify in the glial cultures after 4 hours in storage, as already mentioned, repeating these experiments with storage times up to 24 hours, 48 or 72 hours can be useful to identify any subtle changes that progress. After longer times in storage, it may also be useful to keep cultures in standard conditions for longer than 24 hours post storage, as was done for this study, to observe any longer time changes in culture or cell viability.

Additionally, this study has focussed on the storage of tissue, keeping cells alive at room temperature. Obviously, storage and transport are not the same, meaning it would be valuable to attempt to actually transport cells, keep them at room temperature and travel to a nearby city a few hours away. During storage, cultures are kept stationary in the dark, they are not exposed to the mechanical forces, turbulence and potential damage that can occur during transportation. Cultures are 2D established on glass coverslips, where if cells, particularly neurons, are jolted or moved too much, cells can detach. It would be important to establish the effects of actual transport or develop a method of preventing the mechanical disruption of the culture.

A potential solution for this is in the use of 3D hydrogels or polymers for the use of keeping cells in storage. Atelerix Ltd, Newcastle upon Tyne, is a company that have already formulated the use of

alginate polymers that form into gels for the specific encapsulation and storage for transport of cell tissues at hypothermic temperatures. Once it reaches its destination, a solution for the gel's dissolution can be added, and the solution replaced with its regular growth medium. The technology has been formulated for cells in suspension, for tissues in suspension, and, critical to this study, for already established and adherent cultures, called WellReady™. While this has been trialled on a variety of tissues, they only cite a poster on the encapsulation of microglia in suspension [69], no other neural tissue has been trialled with this technology, however there is previous data to suggest the use of alginate as a hydrogel biomaterial in nerve repair, such as in spinal cord injury [70] and peripheral nerve disease [71]. It would be interesting to identify if alginate could be used to store cells combined with Hibernate™ solution to keep cultures in transit over a longer period of time, and without the use of cold chain transport. This could combine the ability of Hibernate™ to keep cells at RT and ambient CO_2 conditions with the mechanical protection of the alginate hydrogel during transit.

Furthermore, assays used to establish if there was any sign of disrupted maturation or increased reactivity depending on morphological analysis using ICC staining only. While this is useful for microglial and astrocyte analysis, where morphology is significant influenced by the reactive state the cell is in, would be beneficial to investigate if there were any physiological parameters that were altered as a result of storage that may not influence morphology. Other assays to investigate changes in cell behaviour or physiology could be useful. For example, electroconductive studies [72] looking at neuronal or glial behaviour would can establish a baseline physiology of a culture and see if this is influenced in any way by storage. Any alterations to electroconductivity may not be immediately obvious through cell morphology, making electroconductive studies useful. Proteomic or genomic studies could also be useful to investigate if there are changes in protein or gene expression linked to damage, stress or inflammation. These may identify early signs of cell stress that are not enough to influence cell morphology and may predict altered cell behaviour for longer time periods after storage.

References

[1] T. Lawrence, A. Helmy, O. Bouamra, M. Woodford, F. Lecky and P. J. Hutchinson, "Traumtic brain injury in England and Wales: prospective audit of epidemiology, complications and standardised mortality," *BMJ Open,* vol. 6, no. 11, pp. 1-8, November 2016.

[2] C. E. Takahashi, D. Virmani, D. Y. Chung, C. Ong and A. M. Cervantes-Arslanian, "Blunt and Penetrating Severe Traumatic Brain Injury," *Neurologic Clinics,* vol. 39, pp. 443-69, 2021.

[3] B. Joseph, H. Aziz, V. Pandit, N. Kulvatunyou, T. O'Keeffe, J. Wynne, A. Tang , R. S. Friese and P. Rhee, "Improving survival rates after civilian gunshot wounds to the brain," *Journal of the American College of Surgeons,* vol. 218, no. 1, pp. 58-65, 2014.

[4] G. W. J. Hawryluk and G. T. Manley, "Classification of traumtic brain injury: past, present, and future," *Handbook of Clinical Neurology,* vol. 127, no. 3, pp. 15-21, 2015.

[5] T. Alao and M. Waseem, "Penetrating Head Trauamtia," in *StatPearls [Internet]*, Florida, StatPearls Publishing, 2021.

[6] A. Capizzi, J. Woo and M. Verduzco-Gutierrez, "Traumatic Brain Injury An Overview of Epidemiology, Pathophysiology, and Medical Management," *Medical Clinics of North America,* vol. 104, no. 2, pp. 213-38, March 2020.

[7] W. Ruland-Brown, J. A. Langlois, K. E. Thomas and Y. L. Xi, "Incidence of traumatic brain injury in the United States, 2003," *Journal of Head Trauma Rehabilitation,* vol. 21, no. 6, pp. 544-8, November-December 2006.

[8] K. J. Dixon, “Pathophysiology of Traumatic Brain Injury,” *Physical Medicine and Rehabilitation Clinics of North America,* vol. 28, no. 2, pp. 215-25, March 2017.

[9] S. Solumsmoen, A. Lilija-Cyron, K. F. Buch and J. Kelsen, “[Penetrating traumatic head injury],” *Ugeskr Laeger,* vol. 180, no. 51, pp. 2-6, 2018.

[10] M. T. Vakil and A. K. Singh, “A review of penetrating brain trauma: epidemiology, pathophysiology, imaging assessment, complications, and treatment,” *Emergency Radiology,* vol. 24, no. 3, pp. 301-9, 2017.

[11] J. E. Burda and M. V. Sofroniew, “Reactive gliosis and the multicellular response to CNS damage and disease,” *Neuron,* vol. 81, no. 2, pp. 229-48, 2014.

[12] M. Krings, A. Höllig, J. Liu, L. Grüsser, R. Rossaint and M. Coburn, “Desflurane impairs outcome of organotypic hippocampal slices in an in vitro model of traumatic brain injury,” *Medical Gas Research,* vol. 6, no. 1, pp. 3-9, 2016.

[13] K. G. Swan and R. C. Swan, “Man's best friend or man?,” *Physiologist,* vol. 27, no. 5, pp. 347-50, 1984.

[14] A. Quiñones-Hinojosa, Schmidek and Sweet Operative Neurosurgical Techniques, USA: Saunders, 2012.

[15] J. Ghajar, “Traumatic brain injury,” *The Lancet,* vol. 356, no. 9233, pp. 923-9, September 2000.

[16] T. Pakkanen, I. Virkkunen, A. Kamarainen, H. Huhtala, T. Silfvast, J. Virta, T. Randell and A. Yli-Hankala, “Pre-hospital severe traumatic brain injury – comparison of outcome in paramedic versus physician staffed emergency medical services,” *Scandinavian Journal of Trauma, Resuscitation and Emergency Medicine,* vol. 24, no. 62, 2016.

[17] L. S. Murray, G. M. Teasdale, G. D. Murray, D. J. Miller, J. D. Pickard and M. D. Shaw, “Head injuries in four British neurosurgical centres,” *British Journal of Neurosurgery,* vol. 13, no. 6, pp. 564-9, 1999.

[18] D. P. Esposito and J. B. Walker, “Contemporary Management of Penetrating Brain Injury,” *Neurosurgery Quarterly,* vol. 19, no. 4, pp. 249-54, 2009.

[19] National Institute of Heatlh and Care Excellence, “Head injury: assessment and early management,” 2014.

[20] R. S. Bell, C. M. Mossop, M. S. Dirks, F. L. Stephens, L. Mulligan, R. Ecker, C. J. Neal, A. Kumar, T. Tigno and R. A. Armonda, “Early decompressive craniectomy for severe penetrating and closed head injury during wartime,” *Neurosurgery Focus,* vol. 28, no. 5, 2010.

[21] J. Gu, H. Huang, Y. Huang, H. Sun and H. Xu, “Hypertonic saline or mannitol for treating elevated intracranial pressure in traumatic brain injury: a meta-analysis of randomized controlled trials,” *Neurosurgical Review,* vol. 42, no. 2, pp. 499-509, 2019.

[22] E. Dereeper, J. Berré, A. Vandesteene, F. Lefranc and J.-L. Vincent, “Barbiturate coma for intracranial hypertension: clinical observations,” *Journal of Critical Care,* vol. 17, no. 1, pp. 58-62, 2002.

[23] E. Maloney-Wilensky, V. Gracias, A. Itkin, K. Hoffman, S. Bloom, W. Yang, S. Christian and P. LeRoux, “Brain tissue oxygen and outcome after severe traumatic brain injury: A systematic review,” *Critical Care Medicine,* vol. 37, no. 6, pp. 2057-63, 2009.

[24] P. J. D. Andrews, H. L. Sinclair, A. Rodriguez, B. A. Harris, C. G. Battison, J. K. Rhodes and G. D. Murray, “Hypothermia for Intracranial Hypertension after

Traumatic Brain Injury," *The New England Journal of Medicine,* vol. 374, no. 14, p. 1385, 2015.

[25] E. Sydenham, I. Roberts and P. Alderson, "Hypothermia for traumatic head injury," *Cochrane Database Systematic Reviews,* vol. 2, 2009.

[26] E. J. Chung, L. Leon and C. Rinaldi, Nanoparticles for Biomedical Applications, vol. 1, Elsevier, 2019, pp. 89-107.

[27] S.-D. Li and L. Huang, "Nanoparticles evading the reticuloendothelial system: role of the supported bilayer," *Biochimica et Biophysica Acta,* vol. 1788, no. 10, pp. 2259-66, 2009.

[28] R. Liao, T. R. Wood and E. Nance, "Nanotherapeutic modulation of excitotoxicity and oxidative stress in acute brain injury," *Nanobiomedicine,* vol. 7, 2020.

[29] E. Blanco, H. Shen and M. Ferrari, "Principles of nanoparticle design for overcoming biological barriers to drug delivery," *Nature Biotechnology,* vol. 33, no. 9, pp. 941-51, 2015.

[30] A. B. Chinen, C. M. Guan, J. R. Ferrer, S. N. Barnaby, T. J. Merkel and C. A. Mirkin, "Nanoparticle Probes for the Detection of Cancer Biomarkers, Cells, and Tissues by Fluorescence," *Chemical Reviews,* vol. 115, no. 19, pp. 10530-74, 2015.

[31] P. J. Horner and F. H. Gage, "Regenerating the damaged central nervous system," *Nature,* vol. 407, pp. 963-70, 2000.

[32] M. R. Chrostek, E. G. Fellows, A. T. Crane, A. W. Grande and W. C. Low, "Efficacy of stem cell-based therapies for stroke," *Brain Research,* vol. 1722, 2019.

[33] R. A. Barker, J. Barrett, S. L. Mason and A. Björklund, "Fetal dopaminergic transplantation trials and the future of neural grafting in Parkinson's disease," *Lancet Neurology,* vol. 12, no. 1, pp. 84-91, 2013.

[34] G. Schepici, S. Silvestro, P. Bramanti and E. Mazzon, “Traumatic Brain Injury and Stem Cells: An Overview of Clinical Trials, the Current Treatments and Future Therapeutic Approaches,” *Medicina,* vol. 56, no. 3, p. 137, 2020.

[35] D. Ferrari, M. Gelati, D. C. Profico and A. L. Vescovi, “Human Fetal Neural Stem Cells for Neurodegenerative Disease Treatment,” in *Results and Problems in Cell Differentiation,* Springer, 2018, pp. 307-29.

[36] J. Sanchez-Ramos, S. Song, F. Cardozo-Pelaez, C. Hazzi, T. Stedeford, A. Willing, T. B. Freeman, S. Saporta, W. Janssen, N. Patel, D. R. Cooper and P. R. Sanberg, “Adult Bone Marrow Stromal Cells Differentiate into Neural Cells in Vitro,” *Experimental Neurology,* vol. 164, no. 2, pp. 247-56, 2000.

[37] R. Zhang, Y. Liu, K. Yan, L. Chen, X.-R. Chen, P. Li, F.-F. Chen and X.-D. Jiang, “Anti-inflammatory and immunomodulatory mechanisms of mesenchymal stem cell transplantation in experimental traumatic brain injury,” *Journal of Neuroinflammation,* vol. 10, no. 106, 2013.

[38] Z. Yunxiang, A. Shao, W. Xu, H. Wu and Y. Deng, “Advance of Stem Cell Treatment for Traumatic Brain Injury,” *Frontiers in Cellular Neuroscience,* vol. 13, p. 301, 2019.

[39] P. Ludwig, F. G. Thankam, A. A. Patil, A. J. Chamczuk and D. K. Agrawal, “Brain injury and neural stem cells,” *NEural Regeneration Research,* vol. 13, no. 1, pp. 7-18, 2018.

[40] D. L. Haus, L. López-Velàzquez, E. M. Gold, K. M. Cunningham, H. Perez, A. J. Anderson and B. J. Cummings, “Transplantation of human neural stem cells restores cognition in an immunodeficient rodent model of traumatic brain injury,” *Experimental Neurology,* vol. 281, pp. 1-16, 2016.

[41] C. Jiang, B.-R. Hou, Z.-N. Wang, Y. Chen, D. Wang and H.-J. Ren, “How neural stem cells promote the repair of brain injury through immunoregulation,” *Chinese Medical Journal,* vol. 133, no. 19, pp. 2365-7, 2020.

[42] S. S. Shin, E. Dixon, D. O. Okonkwo and M. R. Richardson, “Neurostimulation for traumatic brain injury,” *Journal of Neurosurgery,* vol. 121, pp. 1219-31, 2014.

[43] A. P. Diaz, M. L. Schwarzbold, R. Guarnieri, M. E. Rodrigues de Oliveira Thais, F. C. Freitas, F. Zanela da Silva Areas, N. M. Linhares, R. Walz, S. S. Shin, C. E. Dixon and D. Okonwko, “Early non-invasive brain stimulation after severe TBI,” *Journal of Neurosurgery,* vol. 123, p. 476, 2015.

[44] Y. Li, B. E. Hawkins, D. S. DeWitt, D. S. Prough and W. Maret, “The relationship between transient zinc ion fluctuations and redox signaling in the pathways of secondary cellular injury: Relevance to traumatic brain injury,” *Brain Research,* vol. 1330, pp. 131-41, 2010.

[45] M. J. Kane, H. Hatic, V. Delic, J. S. Dennis, C. L. Butler, J. N. Saykally and B. A. Citron, “Modeling the pathobiology of repetitive traumatic brain injury in immortalized neuronal cell lines,” *Brain Research,* vol. 1425, pp. 123-31, 2011.

[46] G. C. Buehring, E. A. Eby and M. J. Eby, “Cell line cross-contamination: how aware are Mammalian cell culturists of the problem and how to monitor it?,” *In Vitro Cellular & Developmental Biology - Animal,* vol. 40, no. 7, pp. 511-5, 2004.

[47] R. Campos-Pires, A. Yonis, W. Macdonald, K. Harris, C. J. Edge, P. F. Mahoney and R. Dickinson, “A Novel In Vitro Model of Blast Traumatic Brain Injury,” *Journal of Visual Experiments,* no. 142, 2018.

[48] E. Bar-Kochba, M. T. Scimone, J. B. Estrada and C. Franck, “Strain and rate-dependent neuronal injury in a 3D in vitro compression model of traumatic brain injury,” *Scientific Reports,* vol. 6, p. 30550, 2016.

[49] A. P. Weightman, M. R. Pickard, Y. Yang and D. M. Chari, “An in vitro spinal cord injury model to screen neuroregenerative materials,” *Biomaterials,* vol. 35, no. 12, pp. 3756-65, 2014.

[50] G. Rossi, A. Manfrin and M. P. Lutolf, “Progress and potential in organoid research,” *Nature Reviews Genetics,* vol. 19, no. 11, pp. 671-87, 2018.

[51] Y. Sasai, “Cytosystems dynamics in self-organization of tissue architecture,” *Nature,* vol. 493, no. 7432, pp. 318-26, 2013.

[52] A. M. Turing, “The Chemical Basis of Morphogenesis,” *Philosophical Transactions of the Royal Society of London,* vol. 237, no. 641, pp. 37-72, 1962.

[53] T. Sato, R. G. Vries, H. J. Snippert, M. vn de Wetering, N. Barker, D. E. Stange, J. H. van Es, A. Abo, P. Kujala, P. J. Peters and H. Clevers, “Single Lgr5 stem cells build crypt-villus structures in vitro without a mesenchymal niche,” *Nature,* vol. 459, pp. 262-265, 2009.

[54] J. R. Spence, C. N. Mayhew, S. A. Rankin, M. F. Kuhar, J. E. Vallance, K. Tolle, E. E. Hoskins, V. V. Kalinichenko, S. I. Wells, A. M. Zorn, N. F. Shroyer and J. M. Wells, “Directed differentiation of human pluripotent stem cells into intestinal tissue in vitro,” *Nature,* vol. 470, no. 7332, pp. 105-9, 2011.

[55] S. Boj, C.-I. Hwang, L. Baker, I. I. Chio, D. D. Engle, V. Corbo, M. Jager, M. Ponz-Sarvise, H. Tiriac, M. S. Spector, A. Gracanin, T. Oni, K. Yu, R. van Boxtel, M. Huch and K. Rivera, “Organoid models of human and mouse ductal pancreatic cancer,” *Cell,* vol. 160, no. 1-2, pp. 324-38, 2015.

[56] T. Takebe, K. Sekine, M. Enomura, H. Koike, M. Kimura, T. Ogaeri, R.-r. Zhang, Y. Ueno, Y.-W. Zheng, N. Koike, S. Aoyama, Y. Adachi and H. Tanijuchi, "Vascularized and functional human liver from an iPSC-derived organ bud transplant," *Nature,* vol. 499, pp. 481-4, 2013.

[57] A. P. Wong, C. E. Bear, S. Chin, P. Pasceri, T. O. Thompson, L.-J. Huan, F. Ratjen, J. Ellis and J. Rossant, "Directed differentiation of human pluripotent stem cells into mature airway epithelia expressing functional CFTR protein," *Nature Biotechnology,* vol. 30, no. 9, pp. 876-82, 2012.

[58] A. A. Kurmann, M. Serra, F. Hawkins, S. A. Rankin, M. Mori, I. Astapova, S. Ullas, S. Lin, M. Bilodeau, J. Rossant, J. C. Jean, L. Ikonomou, R. R. Deterding, J. M. Shannon, A. M. Zorn and A. Hollenberg, "Regeneration of Thyroid Function by Transplantation of Differentiated Pluripotent Stem Cells," *Cell Stem Cell,* vol. 17, no. 5, pp. 527-42, 2015.

[59] B. S. Freedman, C. R. Brooks, A. Q. Lam, H. Fu, R. Morizane, V. Agrawal, A. F. Saad, M. K. Li, M. R. Hughes, R. V. Werff, D. T. Peters, J. Lu, A. Baccei, A. M. Siedlecki, T. M. Valerius and Mu, "Modelling kidney disease with CRISPR-mutant kidney organoids derived from human pluripotent epiblast spheroids," *Nature Communications,* vol. 6, no. 8715, 2015.

[60] M. A. Lancaster, M. Renner, C.-A. Martin, D. Wenzel, L. S. Bicknell, M. E. Hurles, T. Homfray, J. M. Penninger, A. P. Jackson and J. A. Knoblich, "Cerebral organoids model human brain development and microcephaly," *Nature,* vol. 501, no. 7467, pp. 373-9, 2013.

[61] M. Eiraku, K. Watanabe, M. Matsuo-Takasaki, M. Kawada, S. Yonemura, M. Matsumura, T. Watay, A. Nishiyama, K. Muguruma and Y. Sasai, "Self-organized

formation of polarized cortical tissues from ESCs and its active manipulation by extrinsic signals," *Cell Stem Cell,* vol. 3, no. 5, pp. 519-32, 2008.

[62] H. Sakaguchi, T. Kadoshima, M. Soen, N. Narii, Y. Ishida, M. Ohgushi, J. Takahashi, M. Eiraku and Y. Sasai, "Generation of functional hippocampal neurons from self-organizing human embryonic stem cell-derived dorsomedial telencephalic tissue," *Nature Communications,* vol. 8, no. 8896, 2015.

[63] S. Ramirez, A. Mukherjee, S. Sepulveda, A. Becerra-Calixto, N. Bravo-Vasquez, C. Gherardelli, M. Chavez and C. Soto, "Modeling Traumatic Brain Injury in Human Cerebral Organoids," *Cells,* vol. 10, no. 10, p. 2683, 2021.

[64] D. Qin, Y. Xia and G. M. Whitesides, "Soft lithography for micro- and nanoscale patterning," *Nature protocols,* vol. 3, no. 5, pp. 491-502, 2010.

[65] A. B. Shrirao, F. H. Kung, A. Omelchenko, R. S. Schloss, N. N. Boustany, J. D. Zahn, M. L. Yarmush and B. L. Firestein, "Microfluidic platforms for the study of neuronal injury in vitro," *Biotechnology and Bioengineering,* vol. 115, no. 4, pp. 815-30, 2018.

[66] S. Currle, J. S. Hu, A. Kolski-Andreaco and E. S. Monuki, "Culture of Mouse Neural Stem Cell Precursors," *Journal of Visualized Experiments,* vol. 2, p. 1, 2007.

[67] B. Vagaska, O. Gillham and P. Ferretti, "Modelling human CNS injury with human neural stem cells in 2- and 3-Dimensional cultures," *Scientific Reports,* vol. 10, p. 6785, 2020.

[68] R. H. Basit, N. Tzerakis, S. I. Jenkins and D. M. Chari, "In vitro model of traumatic brain injury to screen neuro-regenerative biomaterials," *Materials Science and Engineering: C,* vol. 128, no. 112253, 2021.

[69] M. García-Roa, M. d. C. Vicente-Ayuso, A. M. Bobes, A. C. Pedraza, A. González-Fernández, M. Paz Martín, I. Sáez, J. Seghatchian and L. Gutiérrez, "Red blood cell

stroage time and transfusion: current practice, concerns and future perspectives," *Blood Transfusion,* vol. 15, pp. 222-31, 2017.

[70] J. R. Hess, N. Rugg, A. D. Knapp, J. F. Gormas, E. B. Silberstein and T. J. Greenwalt, "Successful storage of RBCs for 9 weeks in a new additive solution," *Transfusion,* vol. 40, pp. 1007-11, 2000.

[71] National Health Service, Blood and Transplant, "NHS Tissue and Eye Services, Storing tissue safely," National Health Service, [Online]. Available: https://www.nhsbt.nhs.uk/tissue-and-eye-services/support/storing-tissue-safely/. [Accessed 27 06 2022].

[72] Y. Yoshimoto, I. Date and T. Ohmoto, "Improved cryopreservative medium suitable for the freeze-storage and transplantation of fetal neural tissues," *Restorative Neurology and Neuroscience,* vol. 6, pp. 73-81, 1993.

[73] A. G. E. Day, K. S. Bhangra, C. Murray-Dunning, L. Stevanato and J. B. Phillips, "The Effect of Hypothermic and Cryogenic Preservation on Engineered Neural Tissue," *Tissue engineering & regenerative medicine international society,* vol. 23, no. 10, pp. 575-82, 2017.

[74] J. C. Kawamoto and J. N. Barrett, "Cryopreservation of Primary Neurons for Tissue Culture," *Brain Research,* vol. 384, pp. 84-93, 1986.

[75] G. Nikkhah, J. Eberhard, Olsson, M and A. Björklund , "Preservation of fetal ventral mesencephalic cells by cool storage: in-vitro viability and TH-positive neuron survival after microtransplantation to the striatum," *Brain Research,* vol. 687, pp. 22-34, 1995.

[76] R. F. Castilho, O. Hansson and P. Brundin, "FK506 and Cyclosporin A Enhance the Survival of Cultured and Grafted Rat Embryonic Dopamine Neurons," *Experimental Neurology,* vol. 164, pp. 94-101, 2000.

[77] G. J. Brewer and P. J. Price, “Viable cultured neurons in ambient carbon dioxide and hibernation storage for a month,” *NeuroReport,* vol. 7, no. 9, pp. 1509-12, 1996.

[78] W. A. Woods, F. Chowdhury, N. Tzerakis, C. F. Adams and D. M. Chari, “Developing a New Strategy for Delivery of Neural Transplant Populations Using Precursor Cell Sprays and Specialized Cell Media,” *Advanced Nanobiomedical Research,* pp. 1-10, 2021.

[79] B. M. Kivell, F. J. McDonald and J. H. Miller, “Serum-free culture of rat post-natal and fetal brainstem neurons,” *Developmental Brain Research,* vol. 120, pp. 199-210, 2000.

[80] M. Vieira, B. L. Christensen, B. C. Wheeler, A. S. Feng and R. Kollmar, “Survival and stimulation of neurite outgrowth in a serum-free culture of spiral ganglion neurons from adult mice,” *Hearing Research,* vol. 230, no. 1-2, pp. 17-23, 2007.

[81] S. N. Williams and A. S. Undieh, “Dopamine D1-like receptor activation induces brain-derived neurotrophic factor protein expression,” *Neuroreport,* vol. 20, no. 6, pp. 606-10, 2009.

[82] M. Brinn, K. O'Neill, I. Musgrave, B. J. Freeman, M. Henneberg and J. Kumaratilake, “An optimized method for obtaining adult rat spinal cord motor neurons to be used for tissue culture,” *Journal of Neuroscience Methods,* vol. 273, pp. 128-37, 2016.

[83] C. Apostolides, E. Sanford, M. Hong and I. Mendez, “GLIAL CELL LINE-DERIVED NEUROTROPHIC FACTOR IMPROVES INTRASTRIATAL GRAFT SURVIVAL OF STORED DOPAMINERGIC CELLS,” *Neuroscience,* vol. 83, no. 2, pp. 363-72, 1997.

[84] C. B. Hurelbrink, R. J. E. Armstrong, R. A. Barker, S. B. Dunnett and A. E. Rosser, "Hibernated Human Fetal Striatal Tissue: Successful Transplantation in a Rat Model of Huntington's Disease," *Cell Transplnatation,* vol. 9, pp. 743-9, 2000.

[85] Å. Petersén, O. Hansson, M. Emgård and P. Brundin, "Grafting of Nigral Tissue Hibernated with Tirilazad Mesylate and Glial Cell Line-Dervied Neurotrophic Factor," *Cell Transplantation,* vol. 9, pp. 577-84, 2000.

[86] A. O. Hebb, K. Hebb, A. C. Ramachandran and I. Mendez, "Glial cell line-derived neurotrophic factor-supplemented hibernation of fetal ventral mesencephalic neurons for transplantation in Parkinson disease: long-term storage," *Neurosurg. Focus,* vol. 13, no. 5, pp. 1-6, 2002.

[87] D. Yang, D. Bruun, D. A. Andres and P. J. Lein, "Method for Shipping Live Cultures of Dissociated Rat Hippocampal Neurons," *Current Neurobiology,* vol. 1, no. 2, pp. 95-98, 2010.

[88] J. Vellis and R. Cole, "Preparation of Mixed Glial Cultures from Postnatal Rat Brain," in *Astrocytes,* Springer Science+Business Media, 2012, pp. 49-59.

[89] K. D. McCarthy and J. de Vellis, "PREPARATION OF SEPARATE ASTROGLIAL AND OLIGODENDROGLIAL CELL CULTURES FROM RAT CEREBRAL TISSUE," *Journal of Cell Biology,* vol. 85, no. 3, pp. 890-902, 1980.

[90] C. Tsui, K. Koss, M. A. Churchward and K. G. Todd, "Biomaterials and glia: Progress on designs to modulate neuroinflammation," *Acta Biomaterialia,* vol. 83, pp. 13-28, 2019.

[91] C. J. Bohlen, F. C. Bennet, A. F. Tucker, H. Y. Collins, S. B. Mulinyawe and B. A. Barres, "Diverse Requirements for Microglial Survival, Specification, and Function Revealed by Defined- Medium Cultures," *Neuron,* vol. 94, pp. 759-73, 2017.

[92] J. Wang, C. Yang, Q. Zhao, Z. Zhu, Y. Li and P. Yang, “Microglia activation induced by serum of SLE patients,” *Journal of Neuroimmunology,* vol. 310, pp. 135-42, 2017.

[93] J. Tilman, S. Swioklo, D. Hallam, D. Clode, MacKenzie and A. Barnes, “Encapsulation for the Room Temperature Preservation of iPSC-Derived Microglia Using Novel Hydrogel Technology”.

[94] S. Grijalvo, M. Nieto-Díaz, R. M. Maza, R. Eritja and D. Diaz, “Alginate Hydrogels as Scaffolds and Delivery Systems to Repair the Damaged Spinal Cord,” *Biotechnology Journal,* vol. 14, no. 12, 2019.

[95] W. K. Abdelbasset, S. A. Jasim, S. K. Sharma, R. Margiana, D. O. Bokov, M. A. Obaid, B. A. Hussein, H. A. Lafta, S. F. Jasim and Y. F. Mustafa, “Alginate-Based Hydrogels and Tubes, as Biological Macromolecule-Based Platforms for Peripheral Nerve Tissue Engineering: A Review,” *Annals Biomedical Engineering,* vol. 50, no. 6, pp. 628-53, 2022.

[96] M. E. Spira and A. Hai, “Multi-electrode array technologies for neuroscience and cardiology,” *Nature nanotechnology,* vol. 8, pp. 83-94, 2013.

[97] P. J. Yates, W. H. Williams, A. Harris, A. Round and R. Jenkins, “An epidemiological study of head injuries in a UK population attending an emergency department,” *Journal of Neurology, Neurosurgery and Psychiatry,* vol. 77, no. 6, pp. 699-701, 2006.

[98] S. J. Schimmel, S. Acosta and D. Lozano, “Neuroinflammation in traumatic brain injury: A chronic response to an acute injury,” *Brain Circulation,* vol. 3, no. 3, pp. 135-142, 2017.

[99] C. J. Bryan, “Multiple traumatic brain injury and concussive symptoms among deployed military personnel,” *Brain Injury,* vol. 27, no. 12, pp. 1333-7, 2013.

[100] S. Riggio, “Traumatic brain injury and its neurobehavioral sequelae,” *Psychiatric Clinic of North America,* vol. 33, no. 4, pp. 807-19, 2010.

[101] H. G. Belanger, T. Kretzmer, R. D. Vanderploeg and L. M. French, “Symptom complaints following combat-related traumatic brain injury: relationship to traumatic brain injury severity and posttraumatic stress disorder,” *Journal of International Neuropsychology Society,* vol. 16, no. 1, pp. 194-9, 2010.

[102] E. Su, M. J. Bell, S. R. Wisniewski, D. P. Adelson, K. L. Janesko-Feldman, R. Salonia, R. S. B. Clark, P. M. Kochanek, V. E. Kagan and H. Bayir, “α-Synuclein levels are elevated in cerebrospinal fluid following traumatic brain injury in infants and children: the effect of therapeutic hypothermia,” *Developmental Neuroscience,* vol. 32, no. 5-6, pp. 385-95, 2010.

[103] K. Uryu, X.-H. Chen, D. Marinez, K. D. Browne, V. E. Johnson, D. I. Graham, V. M. Y. Lee, J. Q. Trojanowski and D. H. Smith, “Multiple proteins implicated in neurodegenerative diseases accumulate in axons after brain trauma in humans,” *Experimental Neurology,* vol. 208, no. 2, pp. 185-92, 2007.

[104] G. Ling, F. Bandak, R. Armonda, G. Grant and J. Ecklund, “Explosive blast neurotrauma,” *J Neurotrauma.,* vol. 26, no. 6, pp. 815-25, June 2009.

[105] A. I. R. Maas, C. W. P. M. Hukkelhoven, L. F. Marshal and E. W. Steyerberg, “Prediction of Outcome in Traumatic Brain Injry with Computed Tomographic Characteristics: A Comparison between the Computed Tomographic Classification and Combinations of Computed Tomographic Predictors,” *Neurosurgery,* vol. 57, no. 6, pp. 1173-82, December 2005.

[106] E. P. Thelin, D. W. Nelson, J. Vehviläinen, R. Kivisaari, J. Sirronen, M. Svensson, M. B. Skrifvars, B.-M. Bellander and R. Raj, “Evaluation of novel computerized

tomography scoring systems in human traumatic brain injury: An observational multicenter study," *PLoS Medicine,* vol. 14, no. 8, 3 August 2017.

[107] C. Bernick and S. Banks, "What boxing tells us about repetitive head trauma and the brain," *Alzheimer's research & therapy,* vol. 5, no. 3, p. 23, 2013.

[108] S. H. Yang, M. Gangidine, T. A. Pritts, M. D. Goodman and A. B. Lentsch, "Interleukin 6 mediates neuroinflammation and motor coordination deficits after mild traumatic brain injury and brief hypoxia in mice," *Shock,* vol. 40, no. 6, pp. 471-5, 2013.

[109] J. P. Barrett, S. M. Knoblach, S. Bhattacharya, H. Gordish-Dressman, B. A. Stoica and D. J. Loane, "Traumatic Brain Injury Induces cGAS Activation and Type I Interferon Signaling in Aged Mice," *Frontiers in Immunology,* vol. 12, 2021.

[110] Y. Zhou, R. Fan, B. O. A. Botschway, Z. Yong and X. Liu, "Infliximab Can Improve Traumatic Brain Injury by Suppressing the Tumor Necrosis Factor Alpha Pathway," *Molecular Neurobiology,* vol. 58, no. 6, pp. 2803-11, 2021.

[111] G. Lotocki, J. P. de Rivero Vaccari, O. Alonso, J. S. Molano, R. Nixon, P. Safavi, D. W. Dietrich and H. M. Bramlett, "Oligodendrocyte vulnerability following traumatic brain injury in rats," *Neuroscience Letters,* vol. 499, no. 3, pp. 143-8, 2011.

[112] C.-M. Lin, Y.-C. Tseng, H.-L. Hsu, C.-J. Chen, D. Y.-T. Chen, F.-X. Yan and W.-T. Chiu, "Arterial Spin Labeling Perfusion Study in the Patients with Subacute Mild Traumatic Brain Injury," *PLoS One,* vol. 11, no. 2, 2016.

[113] E. Park, J. D. Bell, I. P. Siddiq and A. J. Baker, "An analysis of regional microvascular loss and recovery following two grades of fluid percussion trauma: a role for hypoxia-inducible factors in traumatic brain injury," *Journal of Cerebral Blood Flow & Metabolism,* vol. 29, no. 3, pp. 575-84, 2009.